UNIVERSITY OF NAPLES FEDERICO II

DEPARTMENT OF EARTH, ENVIRONMENTAL & RESOURCES SCIENCES

PhD Thesis in

Sedimentary Geology

(XXXVI)

Testing models of dolomitization on large scale Mesozoic outcrops from the Sorrento Peninsula (Italy)

Ph.D. student

Muhammad Awais

Ph.D. coordinator

Prof. Rosa Di Maio

Tutor

Prof. Alessandro Iannace

Session 2020-2024

Testing models of dolomitization on large scale Mesozoic outcrops from the Sorrento Peninsula (Italy)

Muhammad Awais
University of Naples Federico II, Naples, Italy

Abstract

The present research work is focused on three research problems: (1) an experimental procedure has been tested for differential dissolution of calcite from mix lithologies (e.g., calcareous dolomites, partially dolomitized limestone) to acquire dolomite only for subsequent stable isotopes analysis, (2) testing reflux dolomitization in the Early Cretaceous carbonates of the Lattari mountains (southern Apennines, Italy), and (3) some late saddle dolomites were found, and their presence provided the possibility to test using U-Pb dating the previous model of single episode late stage, fracture-related dolomitization. An integrated approach has been deployed to assess the aforementioned research problems, including field work, petrography, scanning electron microscopy (SEM), energy dispersive x-ray spectroscopy (EDS), Electron Microprobe analysis (EPMA), XRD, pXRF, stable ($\delta^{13}C$ and $\delta^{18}O$) and Sr-isotopes ($^{87}Sr/^{86}Sr$) analyses, and U-Pb dating.

(1) An experimental study has been conducted to test dissolution of calcite in carbonates (mix of calcite and dolomite i.e., partially dolomitized limestones, calcareous dolomites, etc) to acquire dolomite only. The study is an integration of experimental work with X-Ray Diffraction (XRD) and stable isotopes ($\delta^{13}C$ and $\delta^{18}O$) analyses. In the present study, calcite (Carrara Marble), dolomite and synthetic mixtures (i.e., Calcite10%-Dolomite90%, Calcite30%-Dolomite70%, Calcite50%-Dolomite50% and Calcite70%-Dolomite30%) are used. These samples are experimentally tested with EDTA-acid (0.3M and 0.5M) and acetic acid buffer (1.75M and 3.5M) solutions. The experimental work and XRD analysis revealed less calcite is dissolved by 0.3M EDTA solution and more calcite is dissolved by 1.75M acetic acid buffer. The former solution is least reactive, and the latter is more aggressive and dissolved almost all the calcite of synthetic mixed samples. Similarly, the results show a gradual shift in dolomite percentage and isotopic values from calcite via mixtures towards dolomite in experiments using 0.3M EDTA to 1.75M acetic acid buffer solutions. The stable isotopes ($\delta^{13}C$ and $\delta^{18}O$) cross-plots are demonstrating no obvious effect of different chemical treatments on isotopic signatures although some exceptions exist. Among the tested different solutions, 1.75M acetic acid buffer is more effective and suitable for dissolving calcite and acquiring dolomite only for subsequent geochemical analyses.

(2) In the Cretaceous carbonates of the Lattari mountains, the intensity of dolomitization varies across the stratigraphy and is preserved as partially dolomitized limestones and completely dolomitized unit(s). The studied stratigraphic intervals include C (upper Barremian-lower Aptian) and B (lower Barremian-upper Hauterivian) intervals. The studied carbonates successions are made up of multiple stacked cycles. The C-interval consist of alternations of limestones and dolomites, and the B-interval is almost completely dolomitized unit.

All sections of the C-interval consist of medium (Mdol) and coarse (Cdol) crystalline dolomites except Castello-C which contain Mdol only. Mdol and Cdol's of the C-interval are usually Ca-rich non-stoichiometric having low degree of order (except for a couple of samples having Cdol's with moderate degree of order) and few nearly stoichiometric dolomites. Mdol's of the B-interval consist of Ca-rich stoichiometric, nearly stoichiometric and stoichiometric dolomites with low-moderate degree of order. The Cdol's of the B-interval are nearly stoichiometric to stoichiometric with low-moderate degree of order. Zoned (dolomite crystals with cloudy cores and limpid rims) and corroded dolomites (worn-out crystals) are noticed in both C- and B-intervals.

In the C2-interval the dolomite stoichiometry and degree of order varies from Faito-C through Moiano-C to Castello-C. These observations imply that the source of dolomitizing fluids was closer to the Faito-C Section with respect to the Castello-C Section. The geometry of beds/cycles, lithological variations, distribution of dolomites laterally and vertically, dolomites petrography and geochemistry indicate reflux dolomitization by downward and basinward flowing mesohaline fluids. The C-interval has experienced few episodes of refluxing brines due to limited occurrence of zoned dolomites. In the C-interval, the geological and geochemical characteristics of cycle 3 (selective partial dolomitization) indicate active reflux, and the dolomite mosaics (i.e., pervasive dolomitization) in cycles 1 and 2 might indicate latent reflux described by Jones et al. (2002).

The B-interval is not completely dolomitized unit but pervasively dolomitized unit due to presence of calcite inclusions and micritic matrix. Same is also applied for the dolomite mosaics having zoned dolomites (cycles 1 and 2) of C-interval. The overdolomitization in Cdol's (limpid rims on cloudy cores) is common in the B-interval indicating multiple episodes of refluxing brines. Consequently, there is superimposition of geochemical trends in single cycles (which can be seen in the C interval). This indicates that repeated lateral flow of dolomitizing fluids in the B interval have obscured vertical trends and the only variations are associated to type of dolomites.

(3) The U-Pb dating of sparry saddle dolomites found in veins and vugs of the Mesozoic (Upper Triassic, Lower Jurassic and Early Cretaceous) carbonates of the Lattari mountains (southern Apennines, Italy) has been conducted. Petrographically, the dolomite crystals are very coarse (sometimes typical saddle dolomites), euhedral and granular anhedral, geodic, having sweeping extinction and occupied irregular vugs and fractures and is usually followed by poikilotopic calcite precipitation. The U-Pb data provided four main clusters of dates for saddle dolomites: Late Jurassic (160 Ma), Albian-Cenomanian (100-90 Ma), Paleogene (>70, ~65, 50 and 35 Ma), and two clusters for calcite: Miocene (11.5 Ma and 10 Ma) and Pliocene (4 Ma). Each age corresponds to well established extensional phases affecting the Apennine Carbonate Platform on a regional scale: the formation of intraplatform restricted basins during the Mesozoic and the pre-orogenic extension of the platform. The U-Pb data suggest that each of these tectonic events promoted fluid flow, and related hydrothermal dolomitization. Consequently, a proposed model implies the circulation of warm (hydrothermal) dolomitising fluids through Mesozoic and Paleogene extensional faults in the Apenninic platform.

Table of contents

CHAPTER 1 1

INTRODUCTION 1

1.1 Introduction 1

1.2 Rationale of the present study 4

1.3 Previous work 6

1.3.1 Generalized geological studies on the study area 6

1.3.2 Previous work on dolomitization of study area and reflux dolomitization in general .. 7

CHAPTER 2 10

GEOLOGICAL SETTING AND STRATIGRAPHY 10

2.1 Tectonic setting of the Southern Apennines 10

2.2 Stratigraphy of the Apennine Carbonate Platform (ACP) 11

2.3 Stratigraphy of the Monte Lattari and Monte Faito 13

2.3.1 A-interval (Middle Berriasian – Lower Hauterivian) 14

2.3.2 B-interval (Upper Hauterivian – Lower Barremian) 16

2.3.3 C-interval (Upper Barremian – Lower Aptian) 16

CHAPTER 3 18

DOLOMITIZATION MODELS 18

3.1 Conceptual models of dolomitization 19

3.1.1 Evaporative dolomitization 19

3.1.2 Seepage-reflux dolomitization 21

3.1.3 Hydrothermal dolomitization 25

3.2 Numerical simulation (digital models) of dolomitization 29

CHAPTER 4 32

Materials and methods 32

4.1 Geological fieldwork and samples collection 32

4.2 Laboratory work 35

4.2.1 Microscopic studies 36

4.2.2 Dolomite crystal size distribution (CSD) analysis 37

4.2.3 Analytical methods 38

4.2.4 Geochemical analyses 40

CHAPTER 5 46

Calcite differential dissolution from carbonates (mix of calcite and dolomite) to acquire dolomite: an experimental study 46

CHAPTER 6.. 47
DOLOMITES AND DOLOMITIZATION IN THE C-INTERVAL 47

CHAPTER 7.. 48
DOLOMITES AND DOLOMITIZATION IN THE B-INTERVAL.. 48

Chapter 8 49
Synthesis of dolomites and dolomitization in the C- and B-intervals...................................... 49

CHAPTER 9.. 50
U-Pb dating of late-diagenetic dolomites and calcite 50

Conclusions 51
Acknowledgements 55
References 57
Appendices 85
- **Appendix 1** 85
- **Appendix 2** 86
- **Appendix 3** 87
- **Appendix 4** 88
- **Appendix 5** 89

CHAPTER 1
INTRODUCTION

1.1 Introduction

Dolomite is one of the two main minerals of carbonate rocks. Dolostones are more abundant than limestones, especially in the Paleozoic, even though it is recognized that it is a diagenetic rock. The dolomite has great economic significance as they are one of the largest and most productive hydrocarbon reservoirs worldwide (Fig. 1.1; Zenger et al., 1980; Sun, 1995). The mineral dolomite and the process of dolomitization is very important diagenetic process in carbonates because more than half of world carbonates are dolostones (Sun, 1995). The dolomitization processes are one of the most debated topic of carbonate sedimentology.

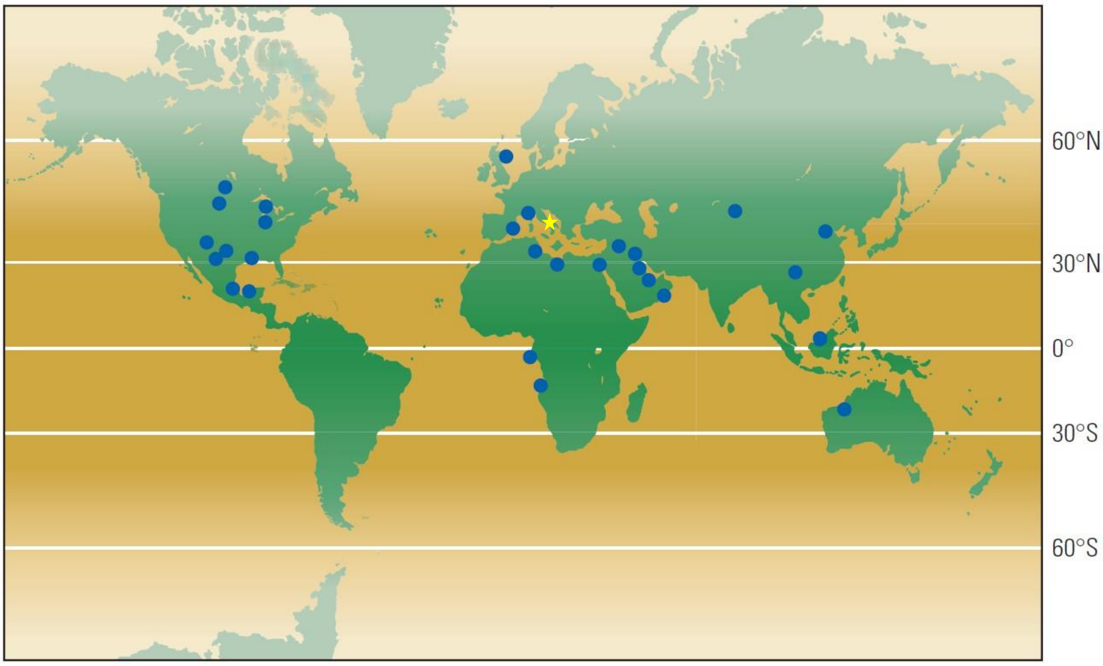

Figure 1.1. Sedimentary basins (blue circles) having production from dolomite reservoirs (Sun, 1995). The yellow star shows the present study area dolomite (Lattari mountains, southern Apennines, Italy).

In the past it was referred to as the dolomite problem. There are two important aspects about the genesis of dolomites: (1) dolomites were more abundant in the geological past but uncommon in modern environments, and (2) dolomite is not precipitated in the laboratory under near surface low temperature conditions where dolomite was usually found in nature (Fairbridge, 1957; Machel, 2004). The present-day seawater is supersaturated with respect to dolomite but there is rare formation and occurrence of dolomite in modern sedimentary environments (Warren, 2000). The modern seawater has a Mg/Ca molar value of ~5.2, which implies it should dolomitize limestone by replacement (i.e., dissolution-precipitation) (equation 1.1) and it is capable of primary precipitation (equation 1.2) of dolomite (Warren, 2000).

$$2CaCO_3 + Mg^{2+} \rightleftharpoons CaMg(CO_3)_2 + Ca^{2+} \qquad (1.1)$$

$$Ca^{2+} + Mg^{2+} + 2(CO_3^{2-}) \rightleftharpoons CaMg(CO_3)_2 \qquad (1.2)$$

Recently Kim et al. (2023) presented mechanism and kinetics of dolomite formation. Based on atomistic simulations, they concluded that repeated episodes of supersaturated and undersaturated solutions can expedite growth of dolomite by up to seven orders of magnitude (Kim et al., 2023). Initially dolomite precipitates a cation-disordered surface, which inhibits growth of crystal. Later, undersaturation causes dissolution of these disordered surfaces, thereby increases cation ordering upon reprecipitation (Kim et al., 2023). Furthermore, Kim et al. (2023) supported their idea by stating that their mechanism explains the occurrence of modern dolomite mainly in natural environments with fluctuations in pH and salinity. However, Kim et al. (2023) findings have been critically evaluated by Pina et al. (2024) and Xu et al. (2024). Pina et al. (2024) found that the newly grown material is crystalline but not an ordered dolomite. According to Pina et al. (2024), Kim et al. (2023) provided circumstantial evidence of dolomite (re)-crystallization at near ambient conditions, but further work is needed to understand mechanisms and kinetics of dolomite formation. Xu et al. (2024) concluded that dissolution-precipitation model of Kim et al. (2023) does not produce ordered dolomite in the laboratory, and it cannot explain the abundance and variation of dolomite in geological archives.

As a result of different seminal studies, now it is clear that dolomitization require some conditions i.e., carbonate matrix, dolomitizing fluid(s) and a viable mechanism to transport dolomitizing fluids through the host limestones (Morrow, 1982; Land, 1985). These conditions can be established through several mechanisms during the diagenetic history; however, the details of many of them are not clear. Most often, the debate about dolomite formation is focused about the origin of Mg, and how it is flushed through the precursor limestones (Tucker and Wright, 1990; Manche, 2021). On a local scale, dolomitized sediments can be the source of magnesium i.e., Mg^{2+} originally present in or adsorbed by Mg-calcites, biogenic silica, clay minerals, chlorophyll, organic matter and or pre-existing detrital dolomites (Lyons et al., 1984; Baker and Burns, 1985). It has been recognized that sea water is doubtlessly the most common source of Mg, and there is certainly mechanism(s) to pump seawater through the carbonates, which reduces kinetic barriers to dolomitization (Land, 1985). However, the conditions and mechanisms causing kinetics of dolomitization are debated (Machel, 2004; Gregg et al., 2015; Petrash et al., 2017 and references therein).

The abundance and occurrence of dolomite throughout the Phanerozoic has been extensively studied and multiple models have been proposed to explain the formation of dolomite e.g., evaporative, reflux, seawater and mixed marine-meteoric etc. Concerning one of the most accepted mechanisms, the early reflux dolomitization; this model had been proposed by Adams and Rhodes (1960) while studying the Permian Capitan Reef Complex (Permian Basin, West Texas, USA). The bedded dolomites in the Permian Basin were formed by replacement of limestones by hypersaline brines refluxing from evaporite lagoons (Adams and Rhodes, 1960). The reflux dolomitization model has been proposed for different age dolomites worldwide e.g., Anisian isolated carbonate platforms in Hungary (Haas et al., 2022); Jurassic-Cretaceous Adriatic Platforms in Croatia (Read et al., 2016); Upper Cretaceous Simsima Formation (Abu Dhabi, United Arab Emirates) (Morad et al., 2023); Miocene-Pliocene carbonate platform of Bonaire Island (Laya et al., 2021); Holocene reflux dolomitization in the Caicos Platform-Bahamas (Dravis and Wanless, 2018) and many others.

In the 1990's numerical simulation (reactive transport modeling, RTM) of dolomitization process was performed which considered fluids flow and rock-water interaction and consequently yielded new insights about key controls on the rate and pattern of fluid flux and the subsequent dolomitization (Wood, 1987; Whitaker et al., 2004 and references therein). The RTM of reflux dolomitization demonstrated the spatio-temporal evolution of dolomitization (Garcia-Fresca, 2009; Al-Helal et al., 2012; Whitaker et al., 2012; Gabellone and Whitaker, 2016; Gabellone et al., 2016; Lu and Cantrell, 2016).

There are some studies on outcrop-scale field test(s) of reflux dolomitization, e.g., Manche and Kaczmarek (2019) evaluated reflux dolomitization in the Cretaceous Upper Glen Rose (UGR) Formation of Central Texas (USA) using an outcrop having a thickness of ca. 17.7 m and ~ 33 m lateral transect. Earlier, it was interpreted that UGR was dolomitized by reflux dolomitization where evaporated marine fluids flowed downward from the top of each cycle into the underlying limestones (Fullmer and Lucia, 2010). Garcia-Fresca and Jones (2011) tested this reflux dolomitization process using RTM, which revealed that reflux dolomitization was feasible in UGR, provided if evaporative fluids percolated downward through multiple depositional cycles. Manche and Kaczmarek (2019) results are incompatible with reflux through a single cycle (Fullmer and Lucia, 2010) and reflux through multiple cycles (Garcia-Fresca and Jones, 2011). In this regard, studying outcrops remains a basic tool to explore the theoretical understanding of the dolomitization process in general and reflux dolomitization in particular, and to build predictive tools useful in conventional energy industry and energy transition sectors (geothermal reservoirs, underground storage of carbon and hydrogen, etc).

The Cretaceous dolomites of the Lattari mountains offer good opportunities for testing reflux dolomitization due to multiple reasons i.e., good exposure, previous detailed studies, and presence of early formation of dolomites. These Cretaceous carbonates successions are made up of alternations of limestones and dolomites. The intensity of dolomitization varies across the stratigraphy and is preserved as partially dolomitized limestones and completely dolomitized unit(s). The dolomite distribution patterns provide the possibility to assess the dolomitizing fluids flow during the process of dolomitization. The dolomite stoichiometry can be used as a proxy record for fluctuations in the dolomitizing fluids composition due to changing paleoenvironmental conditions through time (Lumsden and Chimahusky, 1980; Manche and Kaczmarek, 2019) or hydrological flow (Kaczmarek and Sibley, 2011; Ren and Jones, 2017). The present study has considered dolomite stoichiometry and degree of order together with stable isotopes ($\delta^{13}C$ and $\delta^{18}O$) to assess and interpret about the dolomitizing fluids flux and consequently spatio-temporal variations in dolomitization. The present study results are expected to further clarify the exact mechanism which formed the dolomites of Monte Faito and analogous dolomites of the same age in the peri-Adriatic carbonate platforms and provide useful constraints to assist future refinements of the reflux dolomitization model.

1.2 Rationale of the present study

The present research work considered assessing three research problems, given below.

- An experimental procedure has been tested for differential dissolution of calcite from mix lithologies (e.g., calcareous dolomites, partially dolomitized limestone) to acquire dolomite only for subsequent stable isotopes analysis.
- Detailed sampling to test vertical and lateral fluids movement during dolomitization
- Some late saddle dolomites were found, and their presence provided the possibility to test the previous model of single episode late stage, fracture-related dolomitization.

Dolomites are usually associated with limestones because most often it is the product of replacement of limestones. In a partially dolomitized limestone and calcareous dolomites, it is likely that the stable isotope (especially $\delta^{18}O$) response will be the combined effect of calcite and dolomite. To study and evaluate the dolomitization process of partially dolomitized limestone, the ideal scenario is to analyze stable isotopes of dolomite only. Therefore, it is crucial to dissolve calcite and perform subsequent analyses on dolomites only. So, it was planned to devise a mechanism to dissolve / remove calcite with some chemical treatments taking into consideration that the chemical treatment(s) will not affect the stable isotopes ($\delta^{18}O$) response of dolomites.

One of the major target of present research work is to evaluate and test the reflux model of dolomitization in the Early Cretaceous carbonates of southern Apennines (Italy). The present project is based on Lower Cretaceous carbonates outcrops at Monte Faito in the Sorrento Peninsula, Italy. At Monte Faito, a Valanginian to Albian succession of carbonates is perfectly exposed along a 5 km long transect. The study area stratigraphy is comprised of three units i.e., A, B and C in chronological order (Fig. 1.2; Vinci et al., 2017). 'A' interval (middle Berriasian – lower Hauterivian) consist of alternating limestones and dolostones. B interval (upper Hauterivian – lower Barremian) is a completely dolomitized unit. C interval (upper Barremian – lower Aptian) also consist of alternating limestones and dolostones (Vinci et al., 2017).

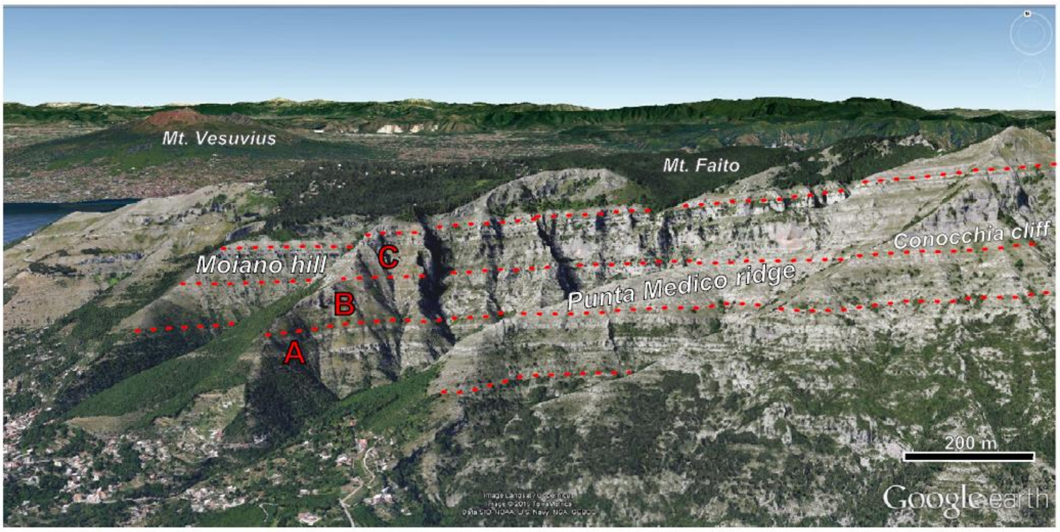

Figure 1.2. Google Earth image showing the stratigraphy of the study area (after Vinci et al. 2017).

C interval contain some distinctive stratabound dolostones i.e., at the top of the cycle is dolomite then dolomitic limestone and limestone at the bottom (Vinci et al., 2017). From available literature and outcrop observations, dolomitization trend in C-unit is visible, however, there is no such trend in dolomitized B interval. The reflux model of dolomitization is proposed for these dolostones (Vinci et al., 2017). The conceptual and numerical reflux dolomitization model(s) illustrates the quantity of dolomite decreases down and basinward away from the source of dolomitizing fluids (Whitaker et al. 2012; Gabellone et al., 2016). Considering the trends of fluids flow in reflux dolomitization, it was expected to find (in both C- and B-intervals) systematic variations in stoichiometry, degree of order and stable isotopes response (especially $\delta^{18}O$). However, there is also a possibility that the fluids might have migrated from bottom to top via capillary action (i.e., evaporative pumping dolomitization) and hence this process also needs to be considered and evaluated. An experimental study by Hsü and Siegenthaler (1969) proposed the mechanism for evaporative pumping model of dolomitization. Later McKenzie et al. (1980) demonstrated evaporative pumping dolomitization in sabkha of Abu Dhabi (UAE). In addition, Carballo et al. (1987) suggested Holocene dolomitization by tidal pumping in Sugarloaf Key (Florida, USA). However, detailed case studies focused on evaporative/tidal pumping dolomitization model(s), especially considering spatio-temporal trends of dolomite abundance, stoichiometry, degree of order and stable isotopes response are not common in literature.

In southern Apennines, the Mesozoic carbonates have experienced multiple-style and multi-stage dolomitizations at various stratigraphic levels (Iannace et al., 2011). The hydrothermal dolomitization (exemplified by saddle dolomite and poikilotopic calcite) is reported in the Mesozoic carbonates of southern Apennines (Iannace, 1991; Iannace et al., 2008; Galluccio, 2009). These late-stage hydrothermal dolomites are referred to as Neogene in age (Iannace et al., 2008 and Galluccio, 2009), may be because they are associated with Neogene faults. However, the Apennines Carbonate Platform has been affected by different tectonic episodes from Mesozoic to Neogene (e.g., studies by Catalano and D'Argenio, 1982; Shiner et al., 2004; Iannace et al., 2005a, 2005b; Caiazzo et al., 2006; Casciello et al., 2006; Tavani et al., 2013; Iannace et al., 2014; Tavani et al., 2023). There is a general agreement among the researchers with respect to these tectonic episodes, however, the precise age(s) are not well constrained. These tectonic events are preserved in the rock record, specifically in the minerals (e.g., calcite, dolomite) precipitated in the deformational structures (i.e., fractures, faults etc.), but obscured. Therefore, novel *in situ* U-Pb dating technique has been deployed to date late diagenetic dolomites and calcite present in veins and vugs of the Mesozoic (Triassic, Jurassic and Cretaceous) carbonates of the Monti Lattari (southern Apennines, Italy).

1.3 Previous work

1.3.1 Generalized geological studies on the study area

The study area has been studied by different researchers in the context of carbonate sedimentology, sequence stratigraphy, dolomitization, diagenesis and structural geology (Galluccio, 2009; Girundo, 2016; Iannace, 1991; Iannace et al., 2011, 2014; Giorgioni et al., 2016; Tavani et al., 2013, 2016, 2023; Vinci et al., 2017; Corradetti et al., 2018; Massaro et al., 2018; Vinci, 2018). In the last decade, some investigations were aimed at characterizing the area as an analogue of the Basilicata reservoirs (Iannace et al., 2014; Giorgioni et al., 2016; Vinci et al., 2017; Corradetti et al., 2018).

Galluccio (2009) worked on dolostones of Mesozoic (Early Jurassic to Early Cretaceous) carbonates succession exposed along Sorrento Peninsula (southern Apennines, Italy). Girundo (2016) studied the carbonates succession having alternations of limestone and dolostone in the context of fracture analysis and relating texture of carbonates with their mechanical behaviour and strength. Giorgioni et al. (2016) worked on dolomitization, fractures analysis and their impact on petrophysical properties of the Cretaceous carbonates of the southern Apennines. Tavani et al. (2016) worked out genesis of dolomite seams present in Jurassic – Cretaceous carbonates of the Lattari mountains (southern Apennines, Italy). Vinci (2018) carried out study on sequence stratigraphy and mechanical stratigraphy of Mesozoic carbonates of the Lattari mountains. Corradetti et al. (2018) and Massaro et al. (2018) conducted joint and fracture analysis on carbonate platform exposures along Sorrento Peninsula to better understand and demonstrate the fluid flow in carbonate platforms.

Amodio and Weissert (2017) worked on cyclostratigraphy of Early Cretaceous carbonates of the study area and concluded that the lagoonal succession stacking pattern(s) is controlled by Milankovitch-type periodicity. Bravi and De Castro (1995) reported the formation of very small intraplatform basins based on the rich fossil fish *Lagerstätten*. These basins are demonstrated by Tavani et al. (2013) and Iannace et al. (2014), who noticed breccias, soft-sediment deformation and syn-sedimentary faults in the Albian rocks. The presence of silica-replaced evaporites has also been reported in the Albian and Aptian parts of the succession (Graziano and Raspini, 2015 and references therein).

1.3.2 Previous work on dolomitization of study area and reflux dolomitization in general

The phenomena of dolomitization have been studied in detail in Mesozoic (Late Triassic to Late Cretaceous) of shallow marine carbonate platforms exposed along Sorrento Peninsula (Iannace, 1991; Galluccio, 2009; Iannace et al., 2011, 2014; Vinci et al., 2017). Middle Upper Triassic (Norian) period is dominated by near-surface early dolomitization (Iannace, 1991; Galluccio, 2009; Iannace et al., 2011). The Norian carbonates are completely dolomitized and contains fabric preserving texture. The latest Triassic (Rhaetian) to Early-Middle Jurassic successions contains late diagenetic dolomites, which are interpreted to be formed by thermal convection (Galluccio, 2009; Iannace et al., 2011). The Rhaetian and Jurassic carbonates have massive, coarse crystalline, fabric-destructive dolomites (Iannace et al., 2014).

The early-middle Cretaceous dolomites of Lattari mountains are early diagenetic and represent near-surface reflux and evaporative pumping model of dolomitization (Galluccio, 2009; Iannace et al., 2011, 2014; Vinci et al., 2017). The Cretaceous carbonates are consisting of meter-thick stratiform dolomites and shallowing upward-cycles of restricted platform carbonates topped by evaporites (silicified) and marly horizons (Iannace et al., 2014). The saddle dolomites (very late diagenetic) of hydrothermal origin (fluids inclusion temperature of 130°C) are also found in vugs, fractures and along faults within the Jurassic and Cretaceous carbonates (Galluccio, 2009).

Vinci et al. (2017) studied dolomitization in the Early Cretaceous carbonates of Monte Faito. The dolomitization was very early diagenetic and its intensity was modulated by changing salinity of marine derived fluids because of climatic changes (Vinci et al., 2017). Two groups of dolomites were identified i.e., (1) fine-medium crystalline dolomites (FMdol), and (2) coarse crystalline dolomites (Cdol) (Vinci et al., 2017). The FMdol are precipitated from concentrated brines in the early stage of reflux dolomitization, and the Cdol are precipitated from less concentrated brines during the basin-ward latent reflux process (Vinci et al., 2017). In Mesozoic (Jurassic-Cretaceous) dolomites of isolated Adriatic carbonate platform, reflux dolomitization is also interpreted to be climate-controlled (Read et al., 2016).

In the Grand Cayman Island (6.8 km wide), the Miocene Cayman Formation (~140 m thick) is incompletely dolomitized unit having dominance of dolomites in the peripheral part, and limestone still exist in the interior of island (Ren and Jones, 2017). There is a spatial trend of decreasing stoichiometry and stable isotopes ($\delta^{13}C$ and $\delta^{18}O$) towards the interior of island (Ren and Jones, 2017). These lateral variations in geochemical parameters (stoichiometry, $\delta^{13}C$ and $\delta^{18}O$) show progressive adjustment of seawater by water-rock interactions along the dolomitizing fluids flow passage from shelf edge to the center of island (Ren and Jones, 2017).

In the Trigonodus Dolomit unit of Middle Triassic Upper Muschelkalk (Switzerland), vertical trends in stable ($\delta^{18}O$) and radiogenic ($^{87}Sr/^{86}Sr$) isotopes have been reported (Adams et al., 2019). In 11 boreholes ~30 m thick unit displayed similar vertical trends with increasing depth i.e., crystal size increase, dolomite texture change from anhedral to euhedral crystals, $\delta^{18}O$ decrease from -1‰ at the top to -6.7‰ at the base, and $^{87}Sr/^{86}Sr$ increase towards the base (Adams et al., 2019). Considering water-rock interactions modeling, a single dolomitizing or recrystallization fluids cannot produce the noticed isotopic trends (Adams et al., 2019). It can be explained as a seepage-reflux dolomitization (at the top) by hypersaline brines into dense, laterally advecting groundwaters (at the base) that have negative $\delta^{18}O$ and elevated $^{87}Sr/^{86}Sr$ values (Adams et al., 2019).

In the Cretaceous UGR (USA), it has been reported that dolomite abundance, crystal size, stoichiometry and $\delta^{18}O$ response varies with sea-level fluctuations i.e., transgression and regression (Manche and Kaczmarek, 2019). The mass balance calculations and RTMs suggest that Mg/Ca in downward refluxing brines will decrease during dolomitization (Jones and Xiao, 2005; Kaczmarek and Sibley, 2011). Considering this aspect, the dolomite stoichiometry and abundance should have decreased downward from the top of each cycle (Manche and Kaczmarek, 2019). However, in UGR the dolomite stoichiometry decreases upward in the lower, transgressive part of the cycle and increases in the upper, regressive part. Similarly, absence of mineralogical and geochemical patterns in the lateral direction also suggest that dolomitizing fluids did not evolve laterally. Therefore, the cyclical oscillations with no lateral variations cannot exemplify the reflux dolomitization. Instead, Manche and Kaczmarek (2019) interpreted dolomitization in the UGR to be syndepositional whereby each facies was dolomitized prior to deposition of the overlying facies.

CHAPTER 2
GEOLOGICAL SETTING AND STRATIGRAPHY

2.1 Tectonic setting of the Southern Apennines

The Southern Apennines were produced during the Europe-Africa collision as a result of Neogene deformation of the ancient Adriatic passive margin. Adriatic post-rift sedimentary successions consist of carbonate platforms and pelagic basin that formed subsequent to rifting that emerged during the Late Triassic to Early Jurassic, which was linked to the emergence of multiple arms of the Neotethys Ocean (Robertson et al., 1991; Bosellini, 2004; Vlahovi´c et al., 2005; Santantonio and Carminati, 2011). Several paleogeographic regions, including the Latium-Abruzzi/Apennine carbonate platform, the Lagonegro and Umbro-Marchean pelagic basins, and the Apulian carbonate platform, have been incorporated into the Apennines thrust belt, where their sedimentary successions are well exposed (Fig. 2.1; Tavani et al., 2023). The current study sampled areas are specifically located in the Lattari mountains in the southern Apennines (i.e., Latium-Abruzzi/Apennine carbonate platform).

The Apennines are a northeast verging thrust belt consisting of a tectonic stack of nappes including top to bottom (1) the Liguride Complex, (2) Apennine carbonate platform, (3) Lagonegro Basin, and (4) Apulian carbonate platform (Menardi Noguera and Rea, 2000; Tavani et al., 2021). This thrust pile has been deformed since the Miocene due to crustal stretching and thinning that is connected to the formation of Tyrrhenian back-arc basin (e.g., Jolivet et al., 1998; Sartori et al., 2001).

The deformation (i.e., thrusting) has advanced eastward from the west (Menardi Noguera and Rea, 2000; Tavani et al., 2021), initially involved sedimentary succession of the Tethys Ocean and ophiolites slices (i.e., the Liguride Complex; Knott, 1987), and then sedimentary successions (carbonate platforms and pelagic basins) of the Adria passive margin since the late Oligocene. The tectonic style is characterized dominantly by thin-skinned deformation according to some authors (Fig. 2.1; Casero et al., 1988; Scrocca et al., 2005; Tavani et al., 2021); others (Mazzoli et al., 2000; Menardi Noguera and Rea, 2000) claims that thick skinned tectonics has been active in the most recent time. The burial history of Apennine carbonate platform has been established using thermal and thermochronological studies, which suggest a maximum burial of 3 km during Miocene thrusting (Aldega et al., 2005; Mazzoli et al., 2008).

2.2 Stratigraphy of the Apennine Carbonate Platform (ACP)

The Apennine Carbonate Platform (ACP) consists of Mesozoic and Cenozoic carbonates, which were deposited in shallow marine tropical/sub-tropical waters in south-western margin of the Neo-tethys Ocean (Fig. 2.2). The carbonate platform sedimentation was established over large areas and took place from Late Triassic to the Late Cretaceous with minor interruptions. There was long phase of sub-aerial exposure but in the Eocene neritic carbonate sedimentation was locally re-established with limestones (forams-rich) and marls (characean) of the Trentinara Formation (Selli, 1962). Again, during the Miocene there was deposition of limestones (containing red algae and bryozoans) of the Roccadaspide, Cerchiara and Cusano formations (Selli, 1962). In the Middle Miocene, the last phase of carbonate sedimentation was finally ceased by drowning below the photic zone and followed by the deep-water siliciclastics deposition (Lirer et al., 2005; Patacca and Scandone, 2007).

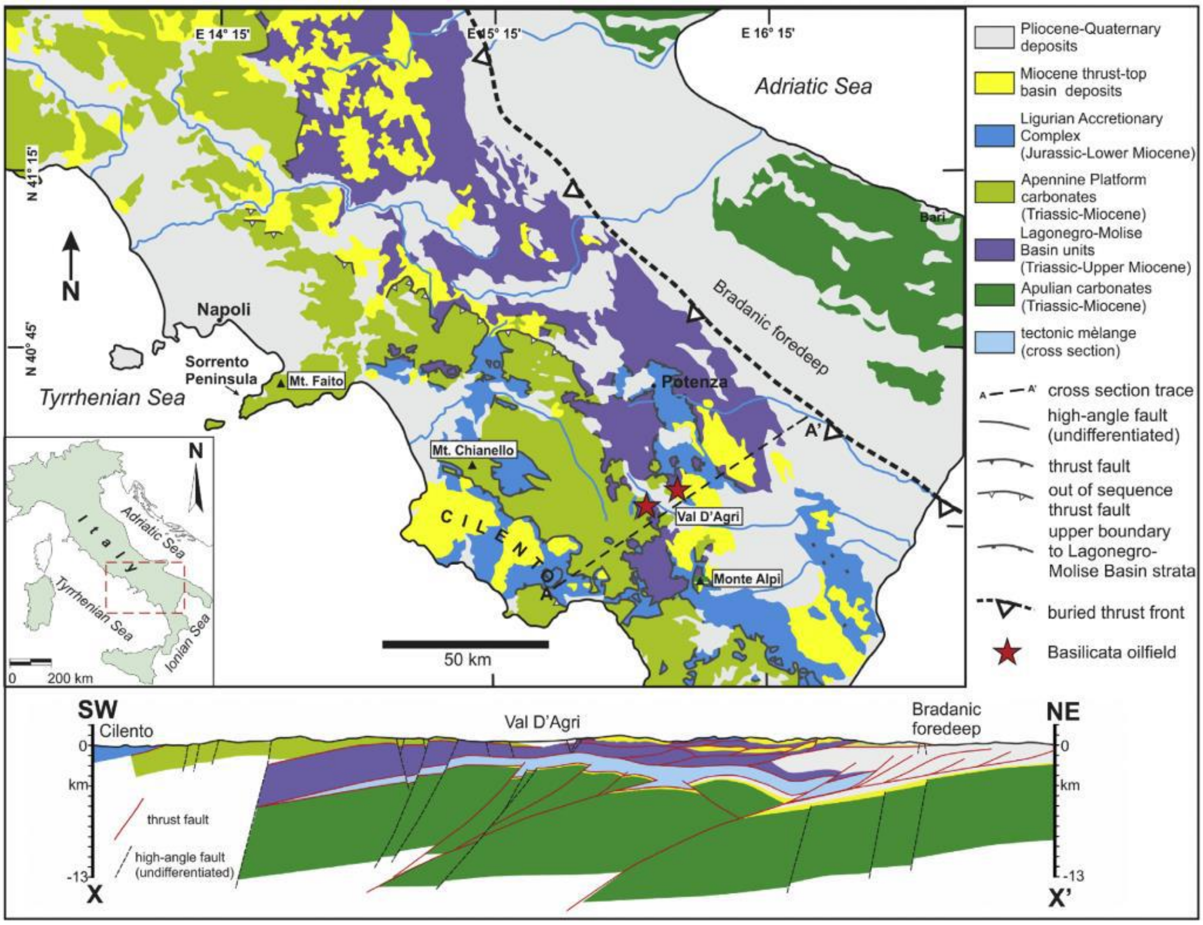

Figure 2.1. Structural framework of southern Italy and regional cross-section (from Giorgioni et al., 2016, after Vitale et al., 2012).

The oldest rocks (massive dolomites) of the ACP are exposed in the Picentini mountains (Salerno) and known as 'Dolomia massiva di base' (Basal Massive Dolomite) Formation. This Formation is overlain by Carnian 'Calcari e Marne ad Avicula e Myophoria' (Limestones and marls with Avicula and Myophoria) Formation. This unit is followed by Norian-Rhaetian 'Dolomia Superiore' (Upper Dolomite) Formation. The total thickness of Triassic units is ~1800-2000 m (Fig. 2.2; Parente et al., 2022 and references therein).

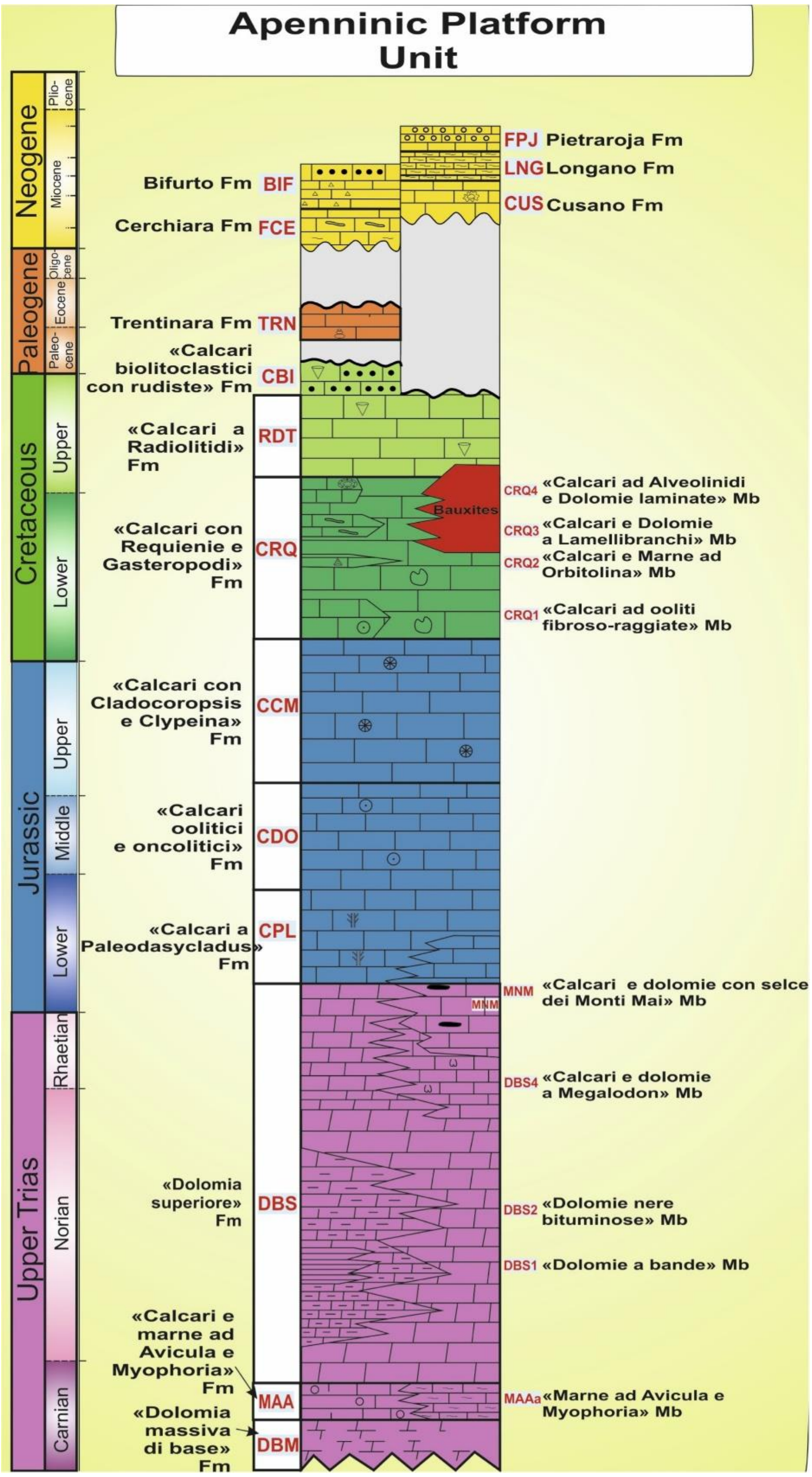

Figure 2.2. Stratigraphy of the Apenninic carbonate platform units (Parente et al., 2022).

The Jurassic succession is mainly comprised of inner platform peritidal and lagoonal facies. The Jurassic succession is divided into lower Jurassic 'Calcari a Palaedasycladus'

Formation (Palaeodasycladus Limestones), the Middle Jurassic Calcari oolitico e oncolitici Formation (Oolitic and oncolytic limestones), and the Middle-upper Jurassic ‘Calcari a Cladocoropsis e Clypeina’ Formation (Cladocotopsis and Clypeina limestones). The total thickness of Jurassic units is ~1300-1400 m (Fig. 2.2; Parente et al., 2022 and references therein).

The Cretaceous platform carbonates are mainly comprised of two lithostratigraphic units i.e., (1) Berriasian-Cenomanian ‘Calcari con Requienie e Gasteropodi’ Formation (Requienid and Gastropod Limestones), and (2) Turonian-Campanian ‘Calcari a Radiolitidi’ Formation (Radiolitid Limestones). The Requienid and Gastropod limestones are composed of inner platform peritidal and lagoonal facies having different fossils associations e.g., calcareous algae (mainly dasycladaleans), benthic foraminfera (including orbitolinids and alveolinids), gastropods and bivalves (mainly requienid rudists). The total thickness of Cretaceous units is ~1000-1200 m (Fig.2.2; Parente et al., 2022 and references therein). At relatively higher stratigraphic level within the Cretaceous, there is a meter-thick very distinctive level, known as the ‘Orbitolina level’, which consist of marly limestones dominated by flat orbitolinid shells (*Mesoorbitolina parva* and *M. texana*). The Orbitolina level is dated as Late Aptian (Gargasian) using biostratigraphy and isotope stratigraphy (Di Lucia et al., 2012 and references therein). It serves as a key level for the chronostratigraphic calibration of the biostratigraphic schemes of the ACP (Parente et al., 2022).

2.3 Stratigraphy of the Monte Lattari and Monte Faito

The carbonates succession exposed at Monte Faito (the highest area of Monte Lattari culminating at 1444 m at Monte Sant’Angelo a Tre Pizzi) was part of the western sector of the ACP. It is present as an ENE-WSW ridge (i.e., Lattari mountains of the Sorrento Peninsula; Fig. 2.3). Stratigraphically, Lattari mountains are comprised of Late Triassic Dolomia Superiore Formation to Late Cretaceous shallow water limestones and dolomites, unconformably overlain by Miocene carbonates and siliciclastics of foredeep and wedge-top (Fig. 2.3; De Castro, 1962; Robson, 1987; Iannace, 1993; Carannante et al., 2000; Iannace et al., 2011). The complete stratigraphic unit is locally covered by Quaternary pyroclastics (Fig. 2.3; Vinci et al., 2017). The current study sampled areas are in the Lattari mountains in the southern Apennines (i.e., Apennine carbonate platform).

The stratigraphy of highest part of Monte Faito is comprised of early Cretaceous Requienid and Gastropod limestones Formation (Fig. 2.3). Vinci et al. (2017) conducted a detailed study focused on stratigraphy, facies and dolomitization of Lower Cretaceous platform carbonates of Monte Faito area. The Monte Faito sedimentary succession is comprised of middle Berriasian to lower Aptian shallow water carbonates with a thickness of 466 m (Fig. 2.4; Vinci et al., 2017). Based on dolomitization intensity, the succession has been informally subdivided into three intervals i.e., A, B and C in chronological order (Fig. 2.4; Vinci et al., 2017). A is older and at lowest stratigraphic position and C is the uppermost relatively younger unit and both contains alternating limestones and dolomites. B-interval is a completely dolomitized unit (Vinci et al., 2017). The general features of these three units are described briefly below.

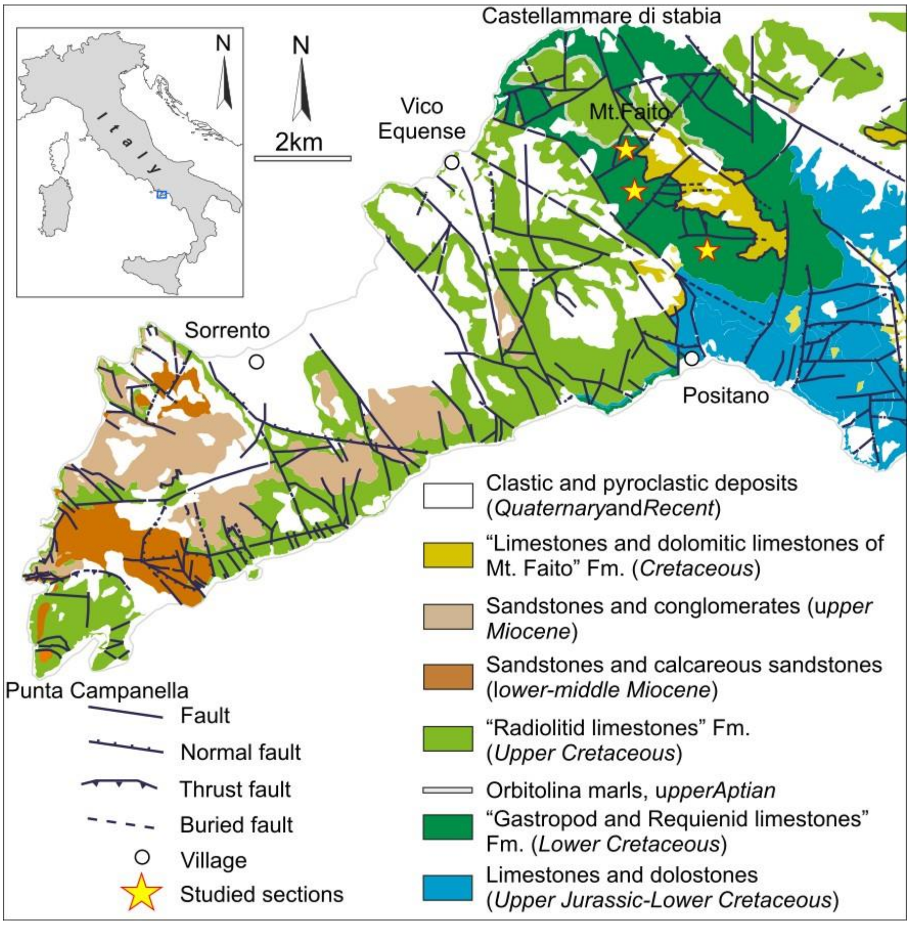

Figure 2.3. Geological map of the Sorrento Peninsula (modified after ISPRA, 2016). The studied sections are marked by yellow stars.

2.3.1 A-interval (Middle Berriasian – Lower Hauterivian)

A-interval is dominated by limestones but gradually becomes dolomitized from middle part to the top, where dolomite is more dominant. It has a total thickness of 203 m and the average bed thickness is ~ 54 cm. The sedimentary facies architecture is dominated by single-bed elementary cycles. The cycle generally starts with thin basal interval of peloidal intraclastic packstone-grainstone (reworked transgressive lag deposit) followed by ostracodal mudstone-wackestone (restricted lagoonal facies, occasionally with charophyte remains indicating more brackish conditions). The cycle top is usually occupied by thin reddened / brownish dolomitic interval capped by wavy and or nodular surface, related to an emersion surface. This facies association i.e., subtidal facies overlain by a subaerial exposure surface and lacking intertidal facies, is interpreted as a diagenetic cycle (sensu Hardie et al., 1986) produced in an inner-platform depositional setting (Vinci et al., 2017).

The dolomites are usually restricted to the upper parts of beds, making dolomite caps, and diffusing downward into the limestones. In the mudstones, dolomite usually occurs as scattered crystals (Vinci et al., 2017). At the top of elementary cycles, mm to cm-thick silicified crusts are noticed, either related to dolomite caps or as a distinct layer at the top of limestone strata. They are considered diagenetic replacement of former evaporites (Vinci et al., 2017).

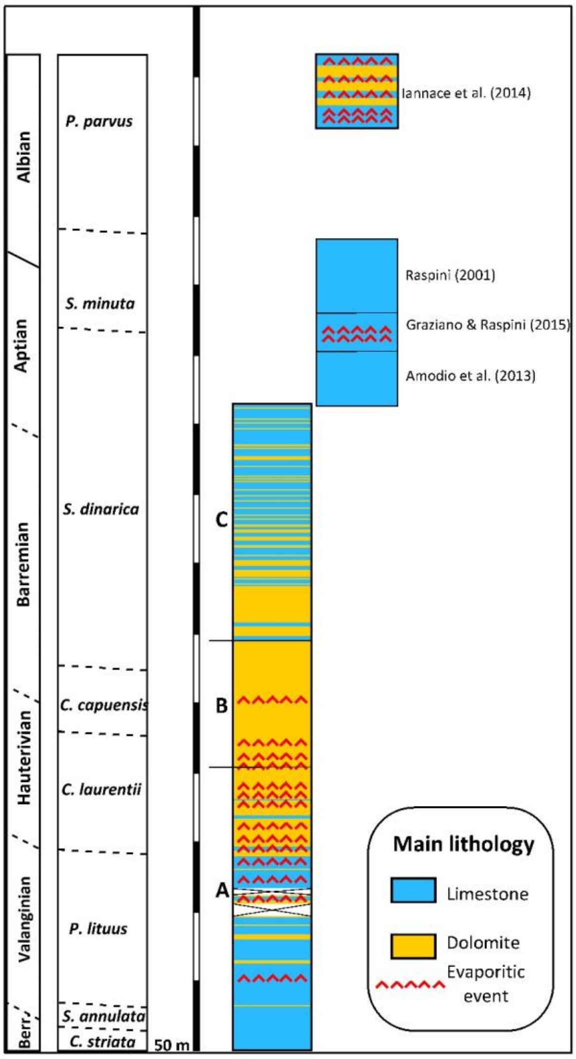

Figure 2.4. Stratigraphic column of the Lower Cretaceous shallow-water carbonates of Mt. Faito (Vinci et al., 2017 and references therein).

2.3.2 B-interval (Upper Hauterivian – Lower Barremian)

B-interval is a completely dolomitized unit and composed of alternations of yellow and greyish dolomites strata and at some levels mm-scale thin marly interlayers are present. It has a total thickness of 91 m and the average bed thickness is ~ 51 cm. Dolomites are stratabound (i.e., laterally continuous and are both massive and thinly subdivided in cm-thick levels by bed-parallel stylolites. Usually in a bed, coarse dolomites are present at the base and dark fine-medium dolomites are present at the top making dolomite caps. The later dolomites are often found in association with plane-parallel to wavy laminations of probably microbial origin, fenestrae and sheet cracks. The carbonates deposition is suggested to occurred in intertidal to supratidal environments due to the occurrence of microbial laminae and fenestrae in association with sheet cracks (Vinci et al., 2017 and references therein). The coarse dolomites preserved ghosts of precursor carbonate allochems, which may indicate a basal transgressive lag at the base of a shallowing-upward peritidal cycle (Vinci et al., 2017).

2.3.3 C-interval (Upper Barremian – Lower Aptian)

C-interval is dominated by limestones with some alternations of dolomites. The intensity of dolomitization is moderately high in the lower half, but it progressively reduces upwards. It has a total thickness of 172 m and the average bed thickness is ~ 41 cm. C-interval is comprised of shallowing-upward peritidal cycles. A cycle usually begins with a basal interval of thick limestones (foraminiferal wackestone to packstone-grainstone or intrabioclastic floatstone-rudstone; subtidal lagoon facies), grading upward into a laminated fine-medium dolomites interval (tidal flat facies), which is capped by a slightly argillaceous brownish dolomite (formed due to subaerial exposure). It is commonly noticed that the dolomitization intensity decreases progressively from the bed top towards the base (Vinci et al., 2017). At some stratigraphic levels, dolomites are concentrated in bed-parallel dolomite seams, due to pressure solution (Tavani et al., 2016).

C-interval was further divided into 07 units i.e., C1, C2, C3, C4, C5, C6 and C7 (Girundo, 2016) which were instrumental for a mechanical stratigraphy study (Corradetti et al., 2018). C1 and C2 are dominated by dolomites with some limestones/dolomitic limestones. The C3 and C4 cycles have a decrease in the presence of completely dolomitized units, even in the presence of dolomite caps. The C5, C6 and C7 cycles are characterized by almost complete absence of dolomites and dominated by limestones, which have greater thicknesses than the lower cycles and contains more fossils (Girundo, 2016).

The Cretaceous shallow water carbonates of Mt. Faito (being from different paleogeographic domain i.e., Apennine Platform) are very similar in the context of lithology, texture and facies to the contemporaneous Apulian Platform carbonates, which make up the thick reservoir interval(s) of the Basilicata oil fields i.e., Val d'Agri and Tempa Rossa (Fig. 2.5; Shiner et al., 2004; Bertello et al., 2010). The reservoir upper part is composed of Late Cretaceous rudist limestones and the lower part is comprised of interlayered Barremian – Cenomanian limestones and dolomites (Fig. 2.5; Bertello et al., 2010).

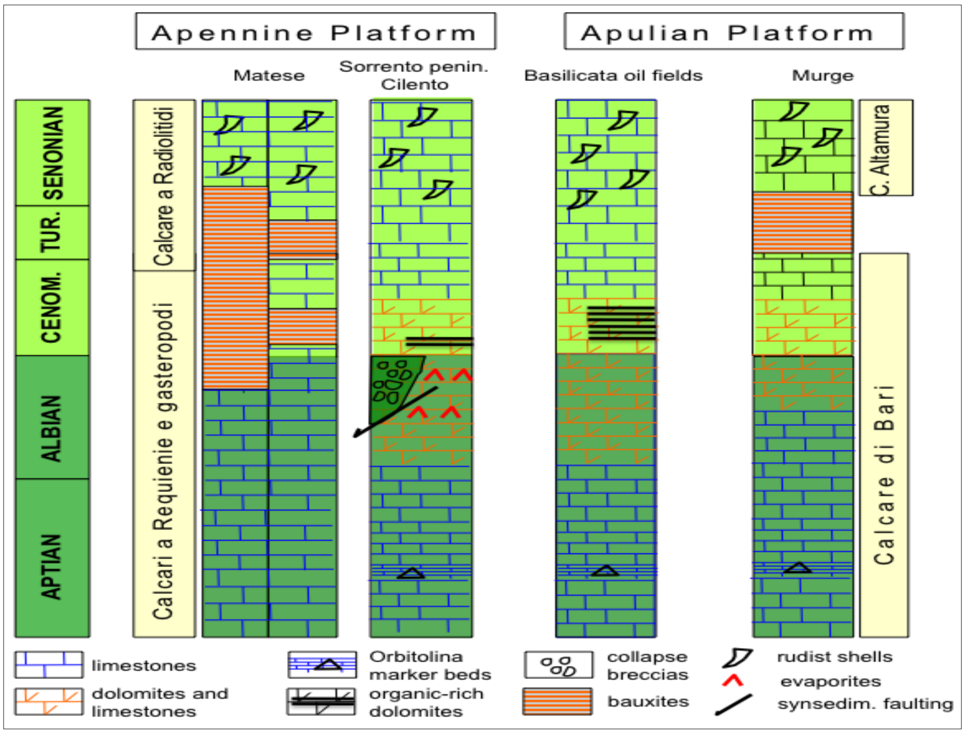

Figure 2.5. Stratigraphic columns showing correlation of Aptian to Senonian stratigraphy of the Apennine and Apulian carbonate platforms (Iannace et al., 2014).

CHAPTER 3
DOLOMITIZATION MODELS

Dolomites are almost exclusively replacement product(s) of a precursor carbonates. No organism is known to precipitate a dolomitic shell and the formation of dolomite sediment is unknown in any modern sedimentary environment. This is in agreement with the long-time known fact that dolomite do not precipitate spontaneously in the laboratory at low temperature, despite its supersaturation in marine fluids, because of kinetic problems. The role of microbes in the precipitation of dolomite at low temperature has been long suspected and found great support especially in the 1990's, following the experiments of Vasconcelos et al. (1995), Burns et al. (2000), Sánchez-Román et al. (2008), Bontognali et al. (2014) and some findings in a coastal lagoon in Brazil (Vasconcelos and McKenzie, 1997). However, also these evidences have been recently questioned (Gregg et al., 2015).

As a consequence, the origin of dolomite rocks involves the understanding of a replacement process, dolomitization, which usually involve three components:

(1) a calcareous matrix,

(2) a dolomitizing fluid

(3) a possible mechanism to transport dolomitizing fluids across the host rock (Fig. 3.1; Morrow, 1982)

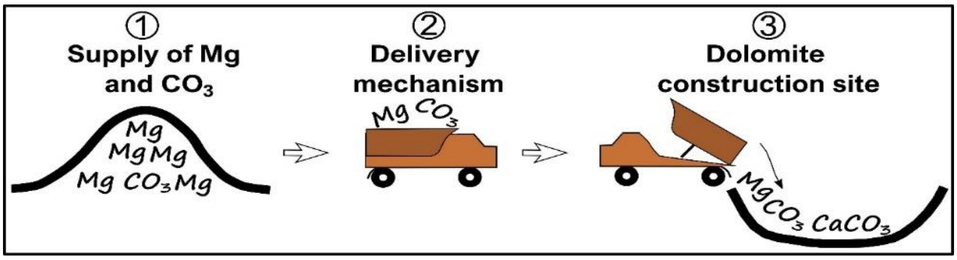

Figure 3.1. Essential elements for any dolomitization model. (1) Mg supply, (2) Delivery mechanism (fluid flow), and (3) favourable chemical conditions for dolomite precipitation (dolomite construction site) (modified after Morrow, 1982).

There is still disagreement in all dolomitization models about the source of Mg^{2+} and the mechanism through which dolomitizing fluids are pumped through the carbonate sediments (Tucker and Wright, 1990; Manche, 2021). Different models of dolomitization have been proposed demonstrating that the replacement process may occur in many different depositional and diagenetic settings and in any moment from the early to late and post diagenetic history of a carbonate succession (Fig. 3.2). The most accepted models of dolomitization, and their characteristics (sedimentology/petrography and geochemistry) with respective examples are given in Table 3.1. Early diagenetic dolomitization models include evaporation (sabkha and coorong-type) and seepage-reflux; mixed marine-meteoric dolomitization, proposed in the 1970's (Badiozamani, 1973; Land, 1985) has been progressively found unsuitable. Late diagenetic process includes tectonic squeezed burial (Dong et al., 2017) and fault related hydrothermal dolomitization (Machel and Lonnee, 2002). However, fault related dolomitization can be also a relatively early diagenetic process (Hollis et al., 2017; Rustichelli et al., 2017).

In the following section, the main models of early dolomitization, and the fracture related, hydrothermal dolomitization have been described because they are more relevant to the present research. The models have been referred to as conceptual models in contrast to some numerical models which have been developed in the last 20 years, which are reviewed in the next section.

3.1 Conceptual models of dolomitization

3.1.1 Evaporative dolomitization

Sabkha dolomitization

According to McKenzie et al. (1980), hydrological model causing sabkha dolomitization consists of three steps i.e. flood recharge, capillary-evaporation and evaporative pumping (Fig. 3.2A). Initially, recharge takes place but intense heat over the sabkha regime led to evaporation from capillary-zone above the water table. Consequently, groundwater ascends into the capillary zone (evaporative pumping) until the water table falls below a level where capillary evaporation is not active (McKenzie et al., 1980). The areas of capillary evaporation and evaporative pumping and where there is seasonal or scarce recharge are important sites for dolomitization (McKenzie et al., 1980). The sabkha dolomitization model is somewhat similar to reflux model in terms of hydrology and geochemistry but still there are some differences between them (Machel, 2005).

In sabkha, dolomitization is restricted to upper 1-2 meters of sediments and is more intense in areas where pore waters become chemically reducing causing enhanced carbonate alkalinity through sulphate reduction and or microbial methanogenesis. This is how sabkha dolomitization is linked to microbial / organogenic dolomitization (McKenzie et al., 1980). That is why sabkha dolomites are texturally and geochemically somewhat like microbial / organogenic dolomites (McKenzie et al., 1980).

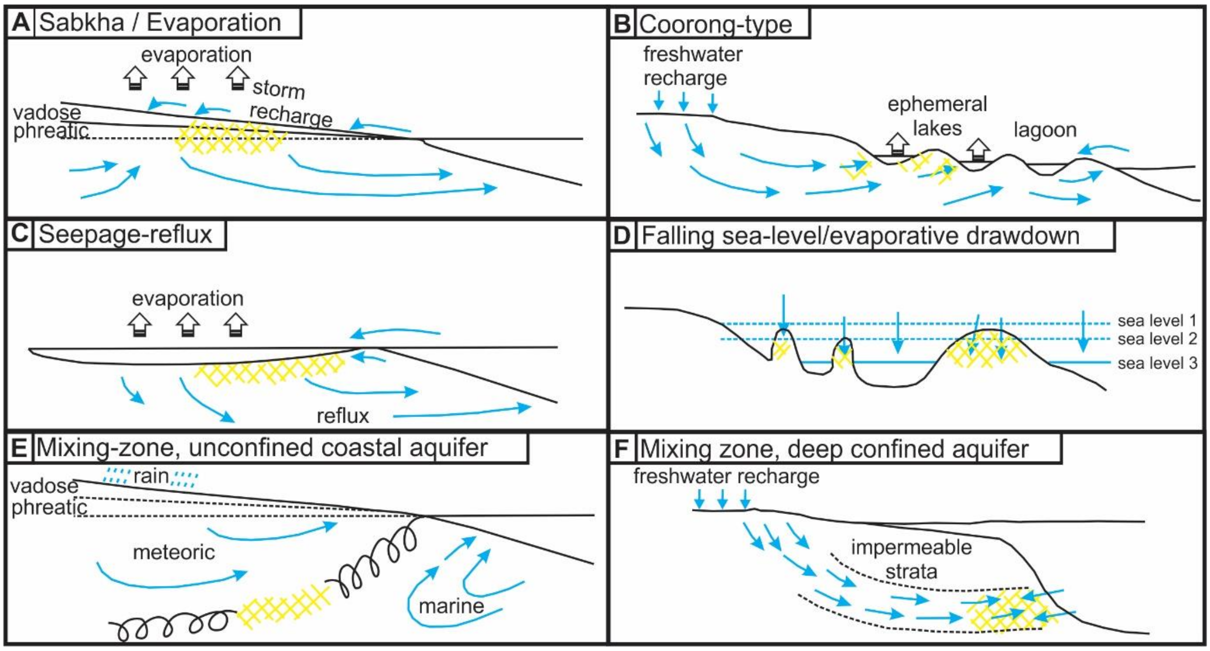

Figure 3.2. Dolomitization models illustrating various mechanisms for moving dolomitizing fluids through the sediments (modified after Land, 1985 and Tucker and Wright, 1990). The dolomite geobodies are shown by yellow hatched areas.

The sabkha dolomites are commonly associated with evaporites (gypsum and anhydrite) (Table 3.1; Morrow, 1982). Sabkha style dolomitization demonstrates shallowing upward cycles i.e., shallow marine or lagoonal limestone overlain by dolomitized intertidal algal mats which is, in turn, overlain by dolomitized supratidal sediments containing sulphates (McKenzie et al., 1980).

Coorong-type dolomitization

The penecontemporaneous dolomites are usually considered that of sabkha where arid climatic conditions prevail, for example, Abu Dhabi (UAE) sabkha. However, penecontemporaneous dolomites can also be formed in relatively humid climatic conditions such as ephemeral (alkaline) lakes of the Coorong region in southern Australia (Table 3.1; Fig. 3.2B; Muir et al., 1980). Coorong is seasonally relatively humid climatic realm and dolomites formed in this region are called as Coorong-type dolomites (Muir et al., 1980). In Coorong system, carbonates distribution is mainly controlled by depositional setting(s) hydrology (Muir et al., 1980).

The Coorong dolomites can be differentiated from arid sabkha dolomites using whole suite of sedimentary structures (desiccation features such as mud / polygonal cracks, tepee structures, breccias and stromatolites), lack of evaporites and their pseudomorphs / casts (Muir et al., 1980). Lack of evaporites does not mean that hypersaline conditions never prevailed, however, they existed and precipitated some little amount of evaporites during dry summer season but are flushed-out by reflux-mechanism during winter (Muir et al., 1980).

Table 3.1. Different dolomitization models sedimentological and geochemical attributes with respective examples.

S #	Dolomitization Model		Outcrop and Sedimentary Structures	Petrography	Stoichiometry & degree of order	Geochemistry	Examples	References
1	Evaporative	Sabkha	Distinctive cyclic lithologies and structures – dolomite culminating in displacive anhydrite. Microbial laminae, fenestrae, evaporite minerals pseudomorphs or relicts	Finely crystalline (1-5μm) euhedral dolomites	Protodolomite (poorly ordered dolomite having 50-60 % Ca)	Reduced carbon isotope ratios and mostly enriched oxygen isotopes (most probably due to evaporation)	Arabian Gulf Sabkhas, West side of Andros Island, Coorong (S. Australia)	(Shinn et al., 1965; McKenzie et al., 1980; Morrow 1982; Hardie, 1987; Tucker and Wright, 1990; Bouch, 2003
		Coorong- type		Finely crystalline /amorphous dolomites.	Higher Ca/Mg		Middle Proterozoic Yalco Formation (Australia)	Muir et al., 1980
2	Seepage-reflux		Cyclic succession. Dolomite association with evaporites, microbial laminae, fenestrae	Fine to medium crystalline, matrix-selective and usually with good to excellent preserved fabric	Relatively low Ca/Mg	Enriched in trace elements and high δ18O as they are formed by evaporated sea water	Permian Capitan reef complex, West Texas, Zechstein (Upper Permian) of Northwest Europe, Lower Cretaceous dolomites (southern Apennines), Cretaceous Upper Glen Rose Formation (USA)	Adams and Rhodes, 1960; Smith, 1981; Vinci et al., 2017; Manche and Kaczmarek, 2019
3	Mixed marine-meteoric		Associated with unconformity, might be representing karstification. Lack of evaporites.	Fine crystalline dolomites	Stoichiometric and well-ordered. Some can be non-stoichiometric and poorly ordered.	Low Trace element content (Na, Sr), light δ18O and positive correlation of δ18O and δ13C due to mixing of two different fluids.	Middle Ordovician Platteville Formation of Wisconsin (USA), Pliocene Hopegate and Pleistocene Falmouth formations of Jamaica	Badiozamani, (1973), Morrow (1982), Tucker and Wright (1990), Bouch (2003)
4	Seawater		Homogeneous bodies that cross-cut formation boundaries		Relatively high Ca/Mg (non-stoichiometirc), poorly ordered	Similar δ18O to the seawater of the respective age	Eocene Enewetak Atoll in the Pacific Ocean, Bahamas Platform, Ambergris Cay (Belize), Permian San Andres Formation	Bein and Land (1983), Saller (1984), Simms (1984), Mazzullo et al. (1987)
5	Organogenic or microbial		Microbialites (algal laminations), fenestrae and birdseye texture	Dolomite crystal size is <10 μm	Ca-rich, poorly ordered protodolomites	Negative δ13C	Coastal lagoon Lagoa Vermelha, Rio de Janeiro, Brazil, lakes of Coorong region, South Australia, microbial dolomite in Norian carbonate platform and Triassic stromatolites, Calabria, Italy	Vasconcelos and McKenzie, 1997; Wright, 1999; Mastandrea et al., 2006
6	Burial		Zebroid (bands of matrix dolomite alternating with white sparry dolomite), healed-microfractures, dolomite tongues and dolomite fronts cutting across bedding in limestone.	Coarse crystals (several millimetres in diameter)	Stoichiometric and well-ordered.	light δ18O	Cambrian carbonates of Missouri and Ordovician carbonates of southern Canadian Rocky mountains.	Gregg (1985), Yao and Demicco (1995)
7	Hydrothermal		Present along faults, in veins, vugs and hydro-brecciated fabric.	Coarse-very coarse crystals; saddle crystal habit and undulatory extinction. Associated with hydrothermal minerals, e.g., fluorite, apatite, etc.	Stoichiometric and well-ordered.	light δ18O	Mesozoic carbonates of Monti Lattari (southern Apennines, Italy) and Cantabarian zone (Spain)	Gasparrini et al. (2006) and Galluccio (2009)

3.1.2 Seepage-reflux dolomitization

The seepage-reflux model of dolomitization was proposed by Adams and Rhodes (1960). The model is postulated while studying lagoonal and reefal carbonates associated with platform evaporites (Permian Capitan Reef Complex) of Permian Basin of West Texas, USA. The conceptual model of reflux dolomitization assumes that during sedimentation marine waters in shallow water lagoon become denser because of evaporation and start to percolate through the underlying beds (Table 3.1; Figs. 3.2 and 3.3; Adams and Rhodes, 1960). The carbonate platform experiences flooding due to sea level rise. The salinity increases from platform edge towards the shoreline. Under such circumstances, carbonate platforms are penetrated by mesohaline active reflux for depths in hundreds of meters. Later, the recharge for active reflux is cut-off but still at greater depths there is reflux dolomitization considered to be caused by latent reflux (Jones et al., 2002).

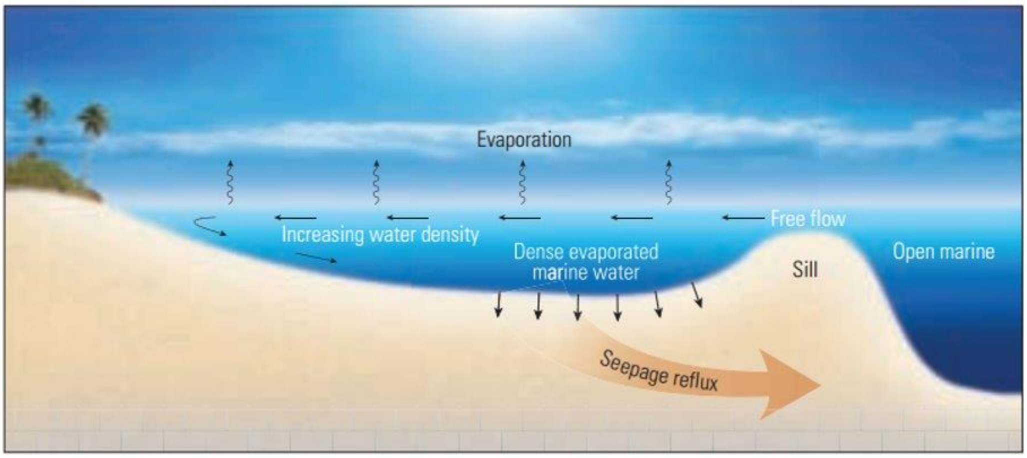

Figure 3.3. Reflux model of dolomitization (from Al-Awadi et al., 2009 who cited Allan and Wiggins, 1993).

It has been documented that reflux dolomitization can possibly pervasively dolomitize entire carbonate platforms under favourable conditions only. It is because the degree of dolomitization varies intensely with the amount and duration of evaporation and flooding, and with the sub-surface permeability distribution (Machel, 2004).

According to Fullmer and Lucia (2010), the peritidal carbonates of Lower Cretaceous (early Albian) Upper Glen Rose (UGR) Formation (central Texas, USA) were dolomitized by downward refluxing brines. Recently, Manche and Kaczmarek (2019) evaluated reflux dolomitization in the UGR (Fig. 3.4).

The UGR consists of high frequency cycles of variably dolomitized limestones demonstrating periodic deepening and shallowing in a peritidal setting. The dolomites of UGR are fine crystalline to mimetic, non-stoichiometric, moderately ordered and lacks compositional zoning (Manche and Kaczmarek, 2019). It has been demonstrated that transgressive and regressive facies have distinctive trends of dolomite crystal sizes, dolomite abundance, dolomite stoichiometry and $\delta^{18}O$ (Fig. 3.4; Manche and Kaczmarek, 2019). Transgressive facies have upward trend of increasing dolomite crystal sizes and decreasing dolomite percent, stoichiometry and $\delta^{18}O$ (Fig. 3.4; Manche and Kaczmarek, 2019). On the contrary, regressive facies have upward trend of decreasing dolomite crystal sizes and increasing dolomite percent, stoichiometry and $\delta^{18}O$ (for samples with >60% dolomite) (Fig. 3.4; Manche and Kaczmarek, 2019). Such variations in mineralogical, textural and geochemical parameters are noticed temporally with no variations laterally (spatially) (Manche and Kaczmarek, 2019). A syn-depositional dolomitization model is interpreted for UGR instead of reflux dolomitization. It is concluded that each depositional facies was dolomitized preceding the deposition of overlying facies (Manche and Kaczmarek, 2019).

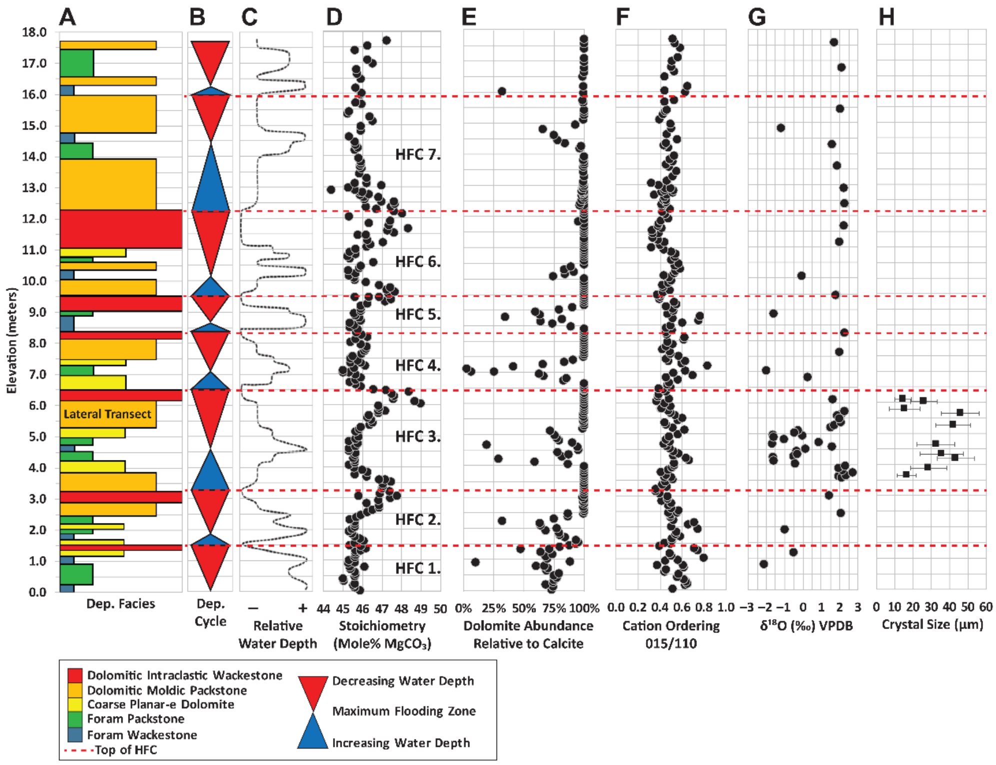

Figure 3.4. Composite section (~17.7 m vertically), showing (A) lithofacies, (B) high-frequency cycles (HFCs), (C) water depth, (D) dolomite stoichiometry, (E) dolomite abundance, (F) cation ordering, (G) $\delta^{18}O_{VPDB}$ (‰), and (H) average dolomite crystal size. Red dashed line represents top of each HFC. From Manche and Kaczmarek (2019).

The Miocene-Pliocene Seru Grandi outcrop in the Bonaire Island has well-developed tongues of dolomites that are distributed along the clinoforms underneath a sub-horizontal erosional unconformity, which is overlain by Pleistocene limestones (Fig. 3.5; Laya et al., 2021). The dolomites are non-stoichiometric, low $\delta^{18}O$ enrichment and low trace elements concentrations. Each clinoform has a distinctive dolomite stoichiometry. There are no lateral trends in the dolomite stoichiometry within individual clinoform(s). The differences in stoichiometry among the clinoform(s) is consistent with temporal variations in the chemistry of seawater derived dolomitizing fluids. It suggests that dolomitizing fluids did not evolve laterally downdip within clinoforms. The fluids might have been fluxed along the sigmoidal pattern of clinoforms, which might acted as a permeable path. However, there is no explicit evidence to interpret fluids pathways (Laya et al., 2021). It is interpreted that each clinoform is dolomitized by an episode of refluxing mesohaline brines soon after the deposition of clinoform. The dolomitizing fluids fluxed downdip along the clinoform(s) through a succession of subtidal carbonates and dolomitized them (Laya et al., 2021).

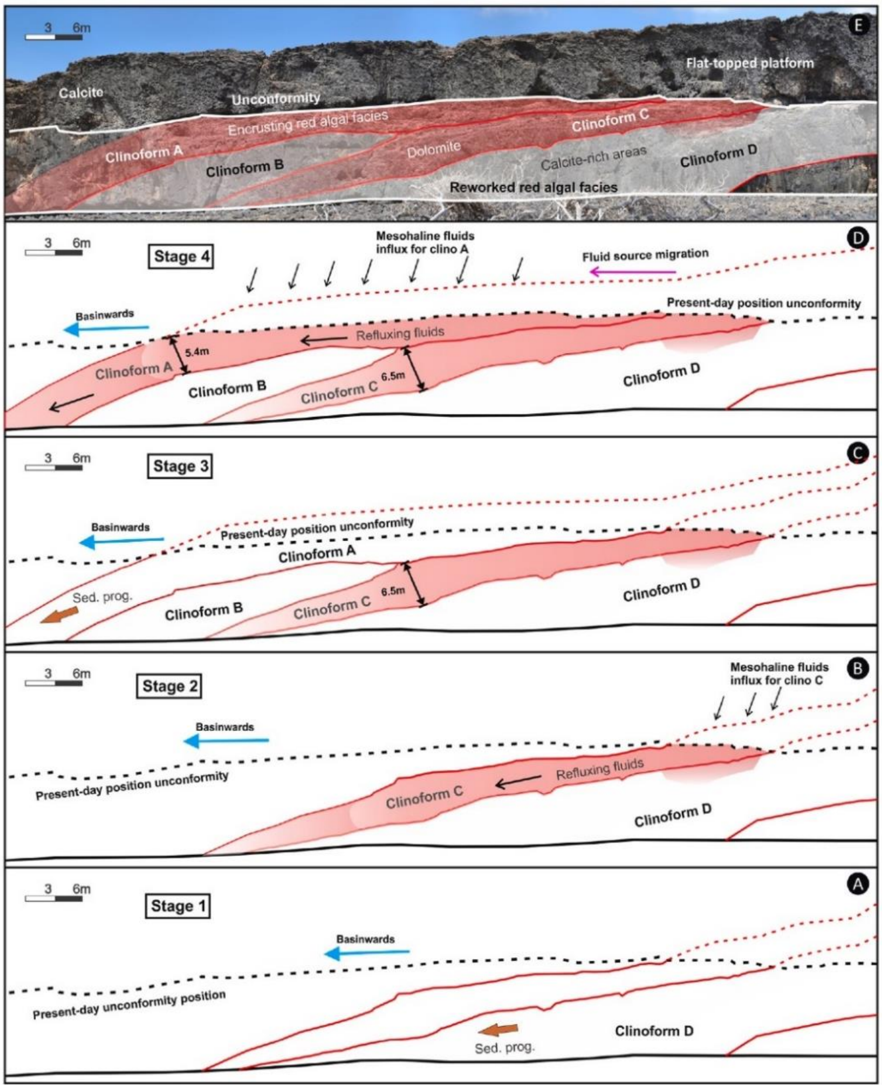

Figure 3.5. Seru Grandi reflux dolomitization model. Red shadow represents dolomite concentration within the clinoforms. A) Basinward shedding of reworked red algal facies during the formation of clinoform C; B) A pulse of refluxing mesohaline fluid dolomitizing clinoform C and partially clinoform D, prior to, or, as shown, before deposition of clinoform B; C) Additional progradation, with deposition of clinoform B at low sea level with no evidence of reflux, followed by deposition of clinoform A. D) Dolomitization of clinoform A via reflux across a wider area. E) Present day outcrop with dolomite distribution and clinoform architecture, and the erosional unconformity that separates the clinoform units from the overlying flat-topped platform. From Laya et al. (2021).

In the Caicos Platform (Bahamas), Holocene reflux dolomitization occurred beneath an evaporitic coastal salina (Fig. 3.6; Dravis and Wanless, 2018). In the Holocene sequence, evaporites (i.e., gypsum) is present at a higher stratigraphic level and dolomite is noticed at lower stratigraphic level. The dolomites are finely crystalline, Ca-rich protodolomites and poorly ordered. It is interpreted that gypsum precipitation produced Mg-rich brines. There is a downward increase of replacement dolomitization with most intensity at the contact with calcrete (a diagenetic layer). The calcrete inhibited further downward movement of the fluids. Below the calcrete, the Pleistocene limestones have no dolomitization (neither replacement nor cements). These observations implies that the calcrete served as an effective permeability barrier (aquitard), which forced downward refluxing dolomitizing fluids to initially pond at the lower most part of Holocene sequence and then move seaward and caused reflux dolomitization (Dravis and Wanless, 2018).

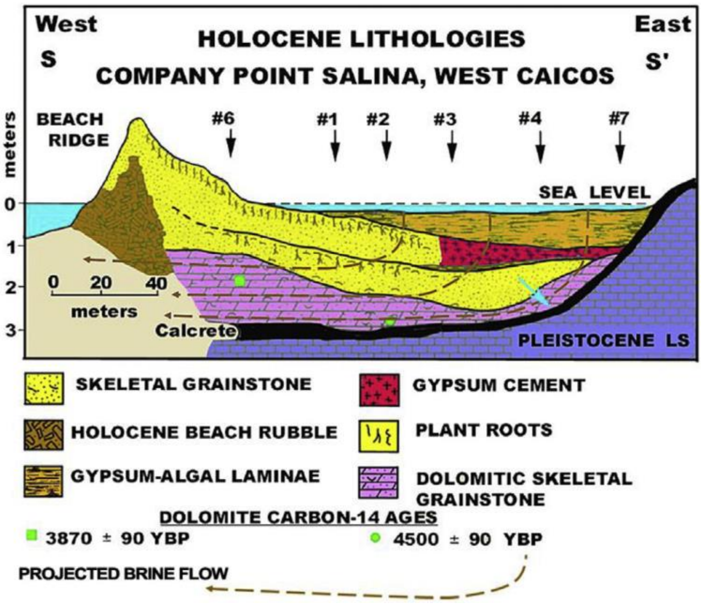

Figure 3.6. Lithostratigraphic cross section of the Holocene sequence beneath Company Point Salina (Bahamas). Coring/drilling locations are numbered. From Dravis and Wanless (2018).

3.1.3 Hydrothermal dolomitization

The hydrothermal dolomitization occurs usually at shallow depths under burial conditions by very saline fluids having higher temperature and pressure than the ambient temperature and pressure of the host formation (commonly limestone) (Davies and Smith, 2006). The hydrothermal dolomitization display a strong structural control by extensional and or strike-slip tectonics, with fluids flow usually centred at transtensional and dilational structural sites and in the hanging wall of the fault(s) (Fig. 3.7; Davies and Smith, 2006).

According to Boni et al. (2000), hydrothermal dolomitization occur in circulation cells, which are driven by heat flow. The fluids are originated in the underlying rocks and circulate upward to affect the overlying rocks (Boni et al., 2000). The assessment of genesis of hydrothermal dolomites includes integration of different datasets e.g., burial (thermal) history of sedimentary succession, microthermometry, and constraints on emplacement time (Davies and Smith, 2006).

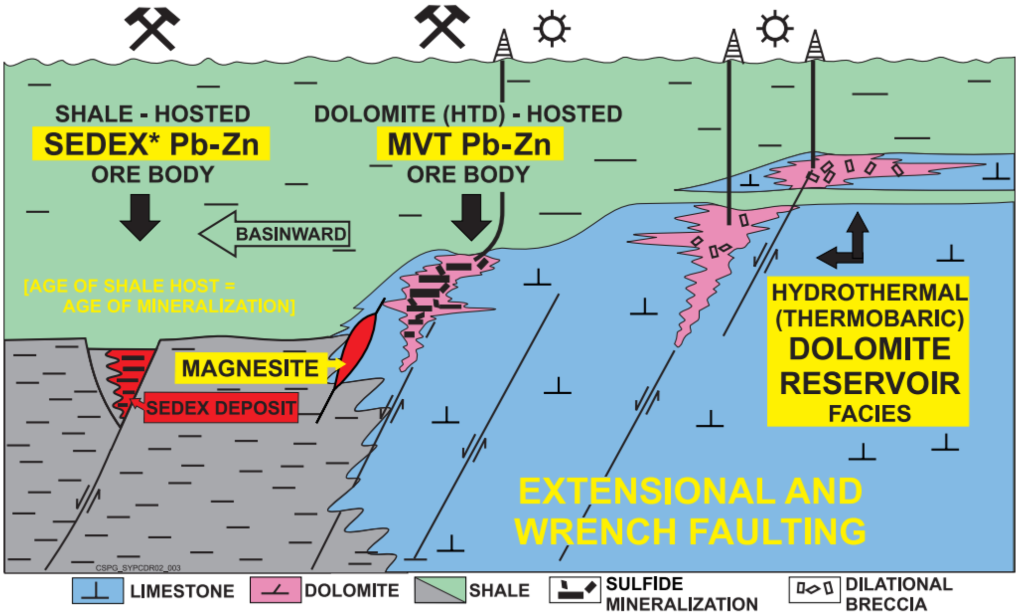

Figure 3.7. Fault related hydrothermal dolomitization. The three hydrothermal minerals associations/deposits are represented: SEDEX Pb-Zn, MVT Pb-Zn and hydrothermal dolomite reservoir facies. The common relationship is focused flow along faults in an extensional (transtentional?) to early compressional tectonic setting (Davies and Smith, 2006).

The hydrothermal dolomites are part of hydrothermal mineral deposits, which also include Mississippi Valley-type (MVT) sulfide deposits and sedimentary-exhalative (SEDEX) lead-zinc ore bodies (Fig. 3.7; Davies and Smith, 2006). The fault-driven hydrothermal dolomitization has been explored in the context of control on petrophysical properties of subsurface hydrocarbons carbonate reservoirs (Davies and Smith, 2006; Sharp et al., 2010; Mozafari et al., 2019). They are reported as proven or potential hydrocarbon reservoirs (Fig. 3.7; Davies and Smith, 2006). The hydrothermal dolomites reservoirs facies have been identified in the world's largest oil (Ghawar, Saudi Arabia) and gas (North Field, Arabian Gulf) fields hosted within the Permian-Triassic and Jurassic-Cretaceous succession of the Arabian Gulf (Davies and Smith, 2006).

The hydrothermal dolomites are generally emplaced under elevated pore fluids pressure and shear stress conditions (Davies and Smith, 2006 and references cited therein). Consequently, the characteristic features of hydrothermal dolomites include breccias (hydrobreccias), zebra fabrics and shear microfractures, specifically proximal to faults (Davies and Smith, 2006). Under the microscope, the hydrothermal (saddle) dolomites are usually coarse-very coarse crystalline, have a characteristic crystal habit (i.e., curved crystal boundaries) and sweeping extinction (Gregg and Sibley, 1984). Geochemically, the hydrothermal dolomites are commonly depleted in $\delta^{18}O$ and enriched in $^{87}Sr/^{86}Sr$ relative to strontium isotopic composition of seawater of the contemporaneous age. The enrichment in radiogenic strontium isotope (^{87}Sr) in hydrothermal dolomites is usually caused by two mechanisms i.e., interaction of dolomitizing fluids with siliciclastic sediments consisting of argillaceous and or feldspathic minerals and or with basement rocks (Davies and Smith, 2006 and references cited therein). However, recently it has been noticed in the Norian dolomites of Matese Massif (southern Apennines, Italy) that the saddle dolomites are depleted in $^{87}Sr/^{86}Sr$ relative to the host rock and Norian seawater $^{87}Sr/^{86}Sr$ values (Diamanti et al., *in progress*). It has been proposed that the hydrothermal dolomitizing fluids interacted with magmatic fluids/rocks (e.g., basaltic rocks) (Diamanti et al., *in progress*).

Some Mesozoic (Triassic, Jurassic and Cretaceous) carbonates in the Alps have been affected by hydrothermal dolomitization (Barale et al., 2013; 2016, 2021a, 2021b). In the Jurassic carbonates, hydrothermal dolomites have been noticed, which are suggested to be formed during the Cretaceous, due to hot (>200°C) dolomitizing fluids circulations along faults and fractures (Barale et al., 2013). This hydrothermal dolomitization recorded a Cretaceous faulting in the Maritime Alps segment of the European Tethyan passive margin (Barale et al., 2013). In the Maritime Alps (NW Italy-SE France), hydrothermal dolomitization is reported to be associated with hydrofracturing events, which is caused by expulsion of overpressured hot (170 to 260°C), highly saline, $\delta^{18}O$-enriched dolomitizing fluids, most probably along faults and fractures (Barale et al., 2016). The dolomitization occurred during earlier Cretaceous at shallow depth (i.e., <500 m) and hence the high temperature fluids indirectly indicate hydrothermal dolomitizing fluids circulation related to deep-rooted faults (Barale et al., 2016).

It is usually assumed that hydrothermal and or high-temperature fluids are required for fault related dolomitization, however, fault and fracture related, low temperature dolomites are also noticed in nature (Hollis et al., 2017; Rustichelli et al., 2017). In the Hammam Faraun Fault (HFF) Block (Suez Rift, Egypt), both massive and stratabound dolostones are reported in a Cenozoic succession (Fig. 3.8; Hollis et al., 2017). At the initial stages of rifting, dolomitizing fluids flux is largely controlled by geothermal convection, resulted in mimetic stratabound dolomites in discrete beds (Fig. 3.8A). At the climax of rifting, intense structural deformation caused repeated, transitory pulses of dolomitizing fluids within the fault damage zone (Fig. 3.8B). Consequently, brecciated, non-mimetic massive (non-stratabound) dolomite geobodies are formed (Fig. 3.8B). It is important to mention that some characteristic textural attributes (i.e., saddle dolomites, zebra dolomite and hydrobreccia) of hydrothermal dolomites are not noticed in HFF block (Hollis et al., 2017). These common features of hydrothermal dolomites probably form when fluids pressure is higher and cooling is more rapid during fault reactivation under transpression, however, the HFF block has undergone a short and simple history of burial and exhumation (Hollis et al., 2017).

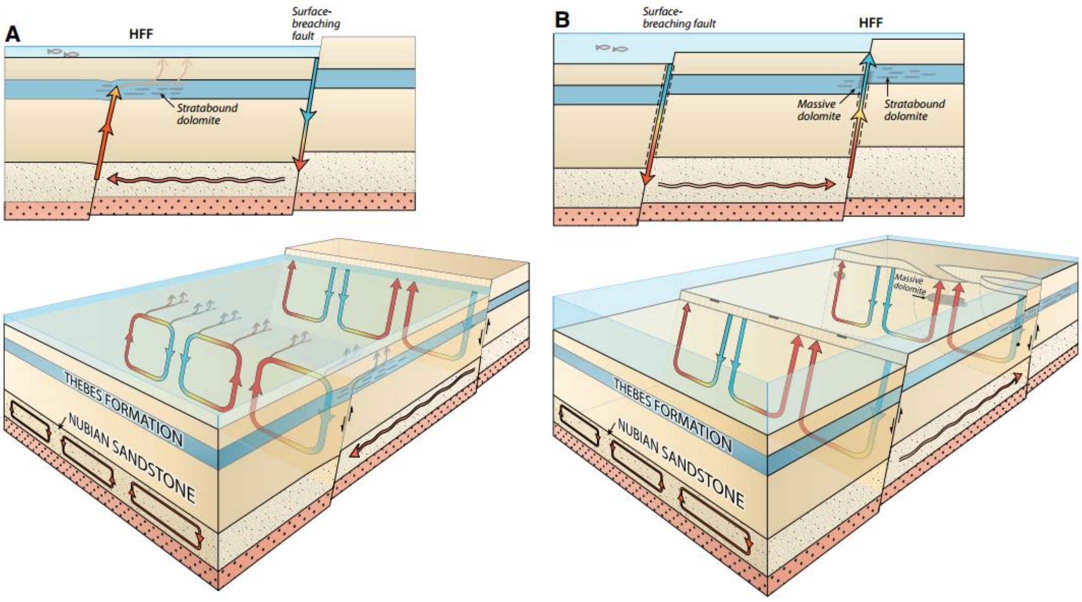

Figure 3.8. Schematic model showing the fluids circulation and fault-related dolomitization in response to progressive rifting and development of faults. (A) Rift initiation: cool seawater is migrated downward along open faults on proto-footwall, heated and convected in the Nubian Sandstone. The buoyant, hot fluids circulated up proto-HFF into lower Thebes Foramtion and reacted to form stratabound dolomites, and (B) Rift climax: Deformation is relocated to HFF and breached the surface. Cold seawater is migrated into convection cells along faults, and hot, rising fluids formed the massive dolomites in the damage zone. From Hollis et al. (2017).

In Gargano Promontory (Apulian foreland of the Apennine thrust belt), fault and fracture related, low temperature (<50°C) dolomites are noticed, which are characterized by normal to strike-slip kinematics (Rustichelli et al., 2017). These dolomites are at the scale of meters to kilometers and are formed at burial depths of <500 m (Rustichelli et al., 2017). It is anticipated that the Early Cretaceous seawater migrated downward and then flowed upward, along faults and fractures, and has experienced variations in its isotopic composition due to interactions with Triassic and Jurassic strata underlying the studied dolomitized rocks (Rustichelli et al., 2017).

The hydrothermal dolomites serve as a mean of direct dating of active faulting and hydrothermal fluids flow in the basin (Davies and Smith, 2006). Recently, some researchers conducted U-Pb dating of hydrothermal dolomites in Alps and southern Apennines (Barale et al., 2021a, 2021b; Diamanti et al., *in progress*). Within the syn-rift sediments, the U-Pb dating of dolomitized clasts indicate that the hydrothermal dolomitizing fluids circulated through sediments from the Late Triassic to Toarcian, corresponding to the entire syn-rift evolution of the western part of the Adriatic palaeomargin (Barale et al., 2021b). Similarly, in the Matese Massif (southern Apennines, Italy) U-Pb dating of saddle dolomites revealed Late Triassic fault-driven hydrothermal dolomitization (Diamanti et al., *in progress*).

3.2 Numerical simulation (digital models) of dolomitization

The study of outcrop analogues is a way to understand distribution and connectivity of dolomite geobodies (Machel, 2004 and references therein). The study and assessment of the conceptual model of dolomitization usually considers integration of outcrop (field), petrography and geochemical analysis. The source of dolomitizing fluids and mechanisms of dolomitization are usually interpreted using petrography, stable and radiogenic isotopes (C, O, Sr), and major and trace elements geochemistry. But there is substantial uncertainty in field scale prediction and spatial-temporal variations of dolomitization (Xiao and Jones, 2007; Lu and Cantrell, 2016).

To better understand the process of dolomitization, different conceptual models of dolomitization are reproduced digitally using reactive transport modeling (RTM) (Jones et al., 2002, 2003; Garcia-Fresca, 2009; Whitaker and Xiao, 2010; Al-Helal et al., 2012; Whitaker et al., 2004; 2012; Gabellone and Whitaker, 2016; Gabellone et al., 2016; Lu and Cantrell, 2016; Yappaarova et al., 2017). The present study is mainly focused on reflux dolomitization, so digital modeling aspects of reflux dolomitization are discussed only. In dolomitized carbonates, the contact between limestone and dolomite is generally at the scale of several meters to tens of meters, which is intractable to demarcate in the subsurface without sufficient seismic and or wireline logging data (Zhang et al., 2021). So, RTM, which deploys combination of basic hydrodynamic (numerical model) and geochemical processes (i.e., geochemical parameters), is used to simulate spatio-temporal variations of dolomitization at the basin and geological time scales (Zhang et al., 2021 and references therein).

Field evidence and digital models are used to study fluids flux and dolomitization, e.g., 2D reactive transport modeling of Arab-D reservoir (Ghawar Field, Saudi Arabia) attests the predicted patterns of dolomite geobodies. The RTM result corresponds to both the noticed vertical and lateral distribution of dolomites (Lu and Cantrell, 2016).

The conceptual and numerical reflux dolomitization model(s) illustrates the quantity of dolomite decreases down and basinward away from the source of dolomitizing fluids (Fig. 3.9; Whitaker et al., 2012; Gabellone et al., 2016). In the reflux dolomitization, the fluids seepage can be shallow, actively linked to the source of dolomitizing fluids and or deep, inactive not linked to the primary source of dolomitizing fluids but secondary source. The former one is called as active reflux and the latter one is called as latent reflux (Jones et al., 2002). In the latter case, brine-producing conditions stop, but brines continue to sink through the carbonate platform, entraining seawater (Jones et al., 2002). The circulation of latent reflux can deliver considerable dissolved reactants to platform carbonates (even Mg^{2+} for dolomitization) (Jones et al., 2002). The integrated interplay of active and latent refluxes can completely and or partially dolomitizes thick carbonate platforms (Jones et al., 2002). According to Jones et al. (2003, 2004), complete dolomitization requires very high permeability in carbonate platform(s) / precursor limestones, lack of effective aquitard (evaporites and shale) and relatively longer time duration for refluxion. The RTM demonstrated that platform-wide reflux circulation cannot pervasively dolomitize carbonate platform (e.g., epeiric scale ramp), which is commonly invoked (Gabellone et al., 2016). Instead, dolomitization of such carbonate systems requires local-scale fluid flow system such as topographically influenced variations in restriction of platform-top seawater circulation (Gabellone et al., 2016). Dolomitization of regional-scale carbonate platforms occurs due to overprinting and amalgamation of successive reflux events (Fig. 3.9; Gabellone et al., 2016; Lu and Cantrell, 2016). However, Saller and Handerson (1998, 2001) hypothesized a single reflux dolomitization event for platform dolomites of the Permian of West Texas.

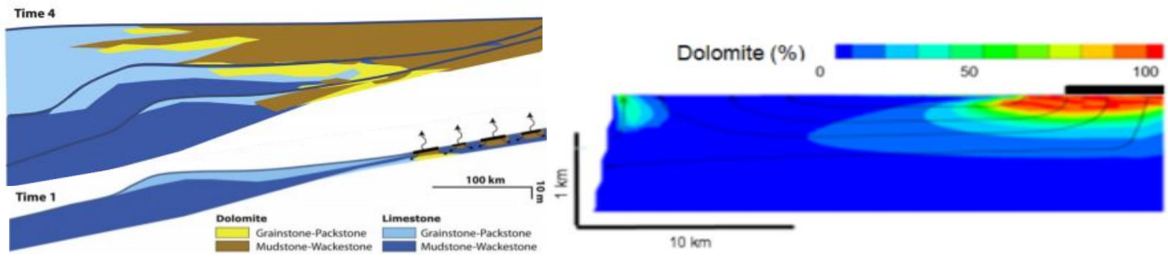

Figure 3.9. Dolomite distribution in a conceptual model to the left (Gabellone et al. 2016) and a numerical model to the right (Whitaker et al. 2012).

The RTMs demonstrate different aspects of overall diagenetic evolution and dolomitization of the carbonates. The main findings of RTM studies are given below.

- Dolomite grows at the expense of calcite (i.e., mole per mole calcite to dolomite replacement is the dominant process) (Lu and Cantrell, 2016). There is a reaction network between the reaction rates of calcite dissolution and dolomite precipitation (Lu and Cantrell, 2016).
- RTMs demonstrate the dolomitizing fluid flow pathways and patterns through the carbonates and the spatio-temporal distribution and variation of porosity-permeability and dolomitization (Al-Helal et al., 2012; Zhang et al., 2021).

- First more reactive fine-grained sediments (i.e., mudstone) are dolomitized and as flow declines so reactions are focused in less reactive more permeable (coarse grained grainstone and packstone) carbonates (Al-Helal et al., 2012). The greater fluid flux takes place in higher porosity sediments i.e., mudstones (Zhang et al., 2021). However, thicker successions of fine-grained sediments dolomitize more slowly, constrained by magnesium supply rate (Gabellone et al., 2016).
- RTMs demonstrate the mechanisms of partial and complete dolomitization (Al-Helal et al., 2012). For example, pervasive (complete) dolomitization can occur immediately below the brine pool (source of dolomitizing fluids) where fluid flow is vertical to bedding and is more rapid at high brine fluxes (Gabellone et al., 2016).
- Sediment permeability and reactive surface area are key intrinsic controls on diagenesis (Al-Helal et al., 2012). It has been documented that high permeability promotes dolomitization in the earlier stages only (Zhang et al., 2021). Intense dolomitization takes place in low permeability sediments (i.e., mudstones) because of longer fluid stagnation time (Zhang et al., 2021 and references therein). Bedding-parallel flow (stratigraphically controlled permeability) usually occurs in relatively permeable coarse-grained beds (Gabellone et al., 2016).
- Dolomites are usually genetically associated with evaporites, however, a numerical model by Garcia-Fresca (2009) illustrates that dolomites are concentrated in upper part of the succession without evaporites (anhydrite). Such decoupling of dolomites and evaporites precipitation is also reported in southern Apennines by Vinci et al. (2017).

CHAPTER 4
Materials and methods

4.1 Geological fieldwork and samples collection

The present study sampling strategy is focused on collecting samples of replacive dolomites of Cretaceous age carbonates, and collection of samples from Triassic, Jurassic and Cretaceous carbonates having late-diagenetic dolomites and calcite in veins and vugs.

Extensive geological fieldworks have been conducted in Monte Faito area of Monte Lattari (southern Apennines, Italy). Different softwares (i.e., Google Earth, Google Maps, GeoVIS3D) and available data are used to select different sections for sampling. Total of seven sites (04 from C-interval and 03 from B-interval) have been studied along three main outcrop sections i.e., Faito, Moiano and Santa Maria Del'Castello (herein used as Castello only). The available stratigraphic logs of Castello and Moiano by Girundo (2016) and Vinci et al. (2017) are used. The stratigraphic log of B-interval at Castello Section is slightly modified, and logging of Faito Road Section is done in the present study (Figs. 4.1 and 4.2). In the C-interval, samples are collected from C2 (Faito-C, Moiano-C, Castello-C sections) and C4 (Moiano-C4) units. The studied sites of B-interval include Faito-B, Moiano-B and Castello-B. The studied sites are shown in Figure 4.3.

Considering the trend of movement of dolomitizing fluids in reflux dolomitization i.e, from top of the cycle downward and basinward, the present study sampling strategy is devised. Samples are collected on cm-scale from different sites of B and C intervals in lateral and vertical directions to test the reflux model of dolomitization in these Lower Cretaceous dolostones in Monte Faito, southern Apennines. For the replacive dolomites, very high-resolution sampling (especially powder samples) has been done using portable driller on the field directly (Fig. 4.3). Total of 192 powder samples are collected from C- and B-intervals respectively (Table 4.1). 116 samples are collected from C-interval (Faito-C 29, Moiano-C 21, Castello-C 32 and Moiano-C4 34) and 76 samples are collected from B-interval (Faito-B 26, Moiano-B 26 and Castello-B 24). Total of 67 rock samples (35 from C-interval and 32 from B-interval) are collected for thin section preparation and petrographic studies (Table 4.1).

Furthermore, the rock samples having veins and cements of sparry dolomites and calcite are collected from Triassic (FS 1058 and FS 1059 samples from Maiori), Jurassic (AT11 from Atrani and N14 from Nocelle) and Cretaceous (KA-1, KA-2, KA-3 and KA-4 Castello-B) stratigraphic intervals (Fig. 4.4). In this connection, already available samples/thin sections in the repository of Sedimentary Geology Research Group of Department of Earth, Environmental and Resources Sciences (DiSTAR), University of Naples Federico II (UNINA), Naples, Italy are also consulted, restudied, and photographed. The Upper Triassic (N = 2 from Cetara area) samples belong to Iannace (1991), and Early Jurassic (N = 15 from Atrani beach, Marina di Praia, Nocelle and Positano beach) – Early Cretaceous (N = 4 from Monte Faito) samples belong to Galluccio (2009) (Fig. 4.4).

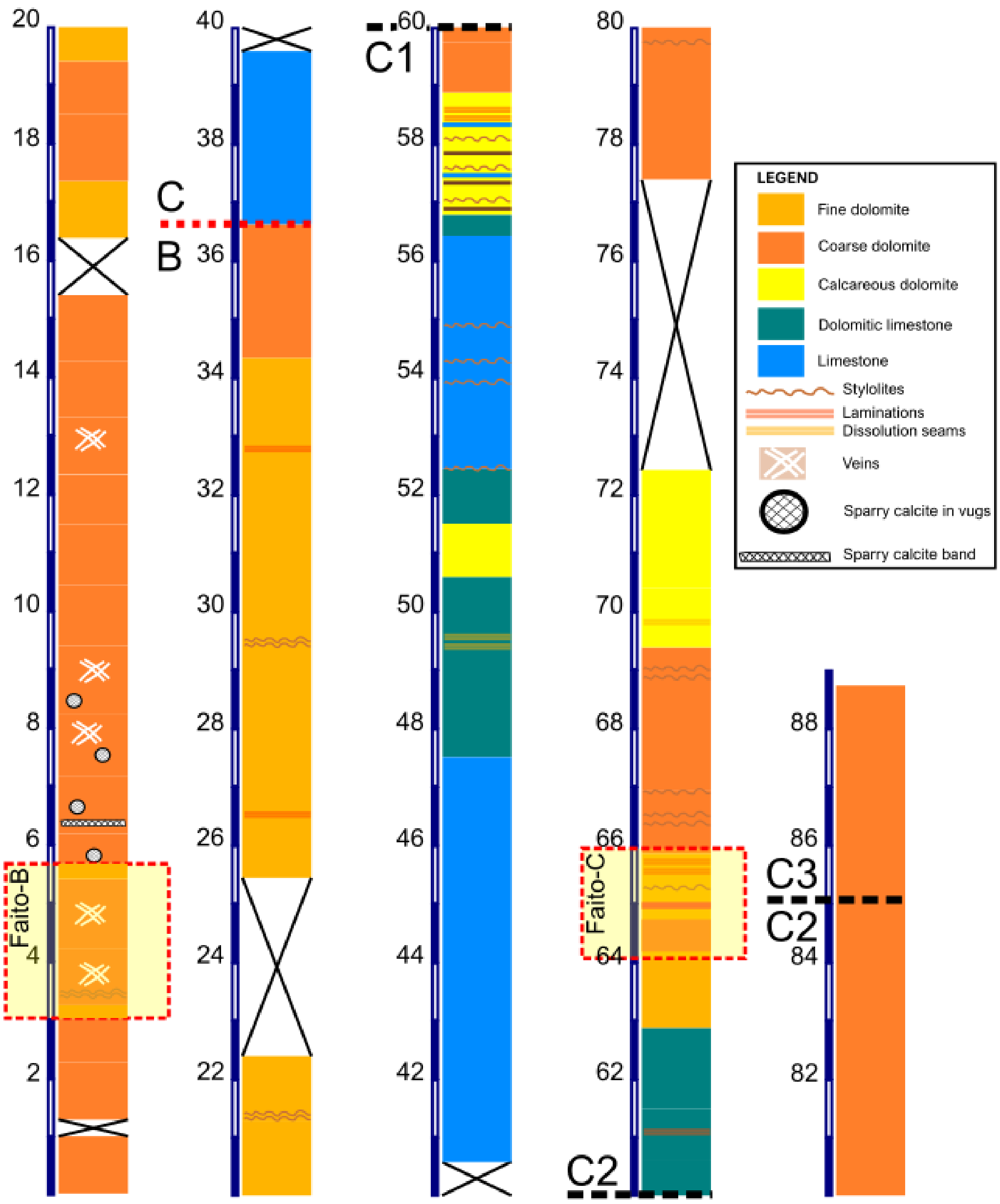

Figure 4.1. Stratigraphic column of the Faito Section. Faito-C and Faito-B sites are demarcated.

Table 4.1. Details about the studied outcrop sections and different samples collected and analyzed.

Stratigraphic intervals	Outcrop sections	Latitude	Longitude	Thicknesses (cm / m)	Powder samples	Rock samples	Polished slabs	Thin sections
C-interval	Faito-C	40° 39' 44.58" N	14° 27' 59.48" E	191 cm / 1.91 m	29	12	0	25
	Moiano-C	40° 39' 27.23" N	14° 28' 12.89" E	155 cm / 1.55 m	21	6	6	13
	Castello-C	40° 39' 27.23" N	14° 28' 12.89" E	210 cm / 2.10 m	32	10	0	27
	Moiano C4	40° 39' 25.26" N	14° 28' 17.91" E	225 cm / 2.25 m	34	7	7	21
B-interval	Faito-B	40° 39' 39.40" N	14° 27' 53.90" E	277 cm / 2.77 m	26	13	0	14
	Moiano-B	40° 39' 27.72" N	14° 28' 21.37" E	425 cm / 4.25 m	26	10	9	20
	Castello-B	40° 38' 50.74" N	14° 29' 9.67" E	246 cm / 2.246 m	24	09	0	22
				C-interval	**116**	**35**	**13**	**86**
				B-interval	**76**	**32**	**09**	**56**
				Total	**192**	**67**	**21**	**142**

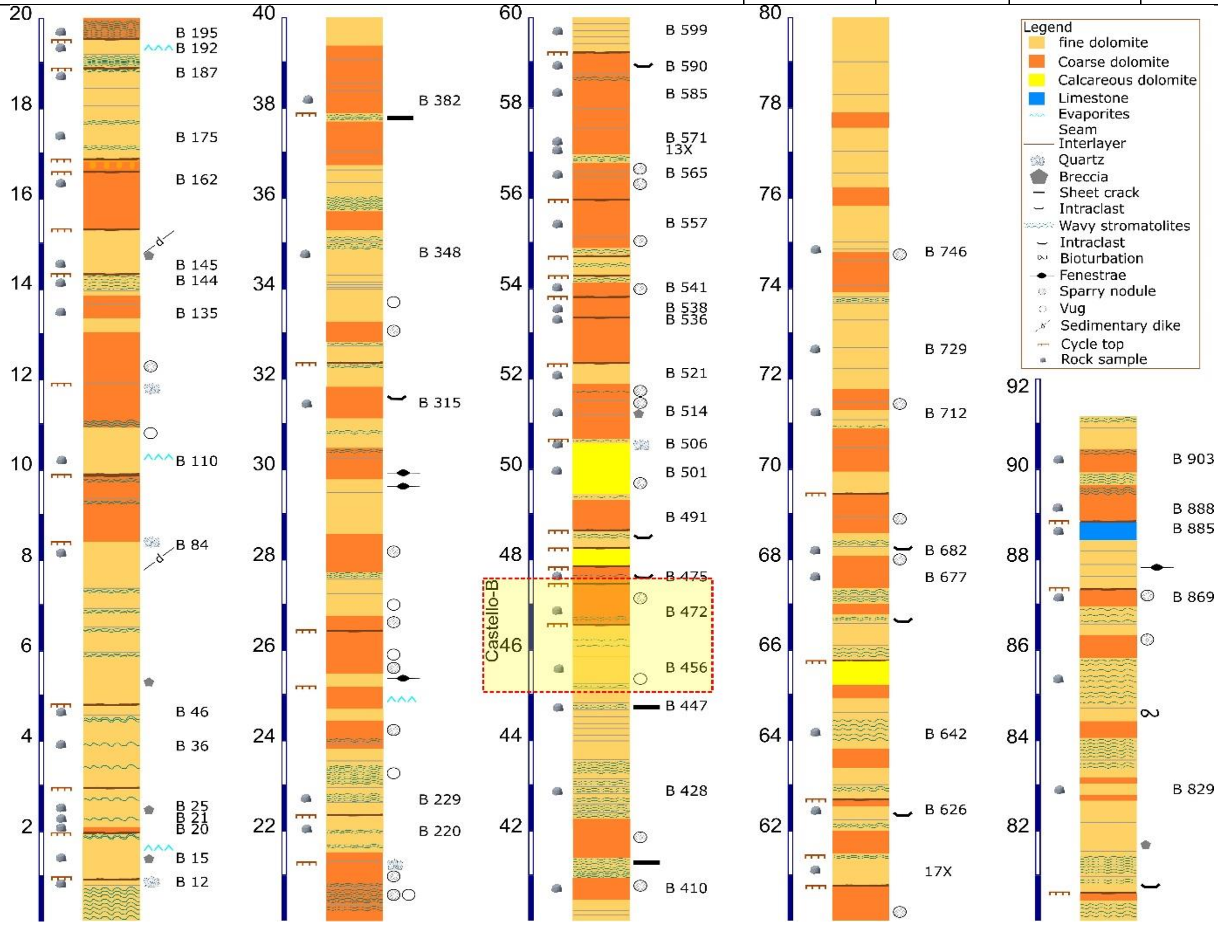

Figure 4.2. Stratigraphic column of the B-interval, Castello Section (modified after Girundo, 2016). The red box (highlighted in yellow) in third column is the present studied level named as Castello-B.

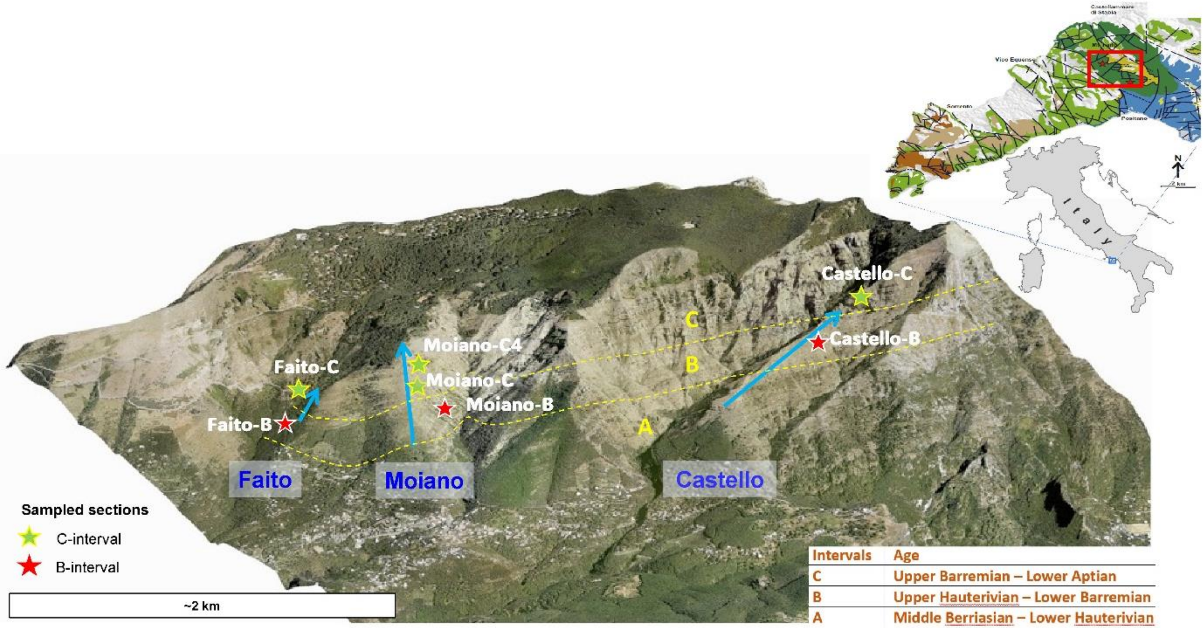

Figure 4.3. 3D model of the study area showing the location(s) of studied sections/sites. In the upper right corner, the geological map of Sorrento Peninsula is after ISPRA 2016.

Figure 4.4. Google earth image of the Sorrento Peninsula with marked locations of Mesozoic (Triassic, Jurassic and Cretaceous) carbonates. The saddle dolomites are studied and dated from these locations. Cetara samples from Iannace (1991) and other samples except Maiori, Atrani and Santa Maria Del'Castello from Galluccio (2009). The area of 3D model shown in Fig. 4.3 is marked by white outlined polygon.

4.2 Laboratory work

Initially polished rock slabs for some samples are produced for preliminary investigations (Table 4.1). Thin sections are prepared using ordinary method(s) at the thin section preparation laboratory of DiSTAR (UNINA). Total of 142 thin sections are prepared and studied for both

C- (N = 86: Faito-C 25, Moiano-C 13, Castello-C 27, and Moiano-C4 21) and B- (N = 56: Faito-B 14, Moiano-B 20, and Castello-B 22) intervals. All the diagrammatic illustrations, which are part of this dissertation, are produced/annotated/modified using Inkscape software.

4.2.1 Microscopic studies

Petrographic, scanning electron microscopy (SEM), electron microprobe analysis (EPMA) and cathodoluminescence (CL) investigations are conducted in the present research.

4.2.1.1 Polarizing / petrographic microscopy

Detailed petrography of 142 carbonate samples (86 from C-interval and 56 from B-interval) has been conducted using Leica DMEP and Leica Wild M420 petrographic microscopes with an attached camera in the Sedimentary Microscopy Laboratory of the DiSTAR, UNINA. The dolomite texture is described using classification of Sibley and Gregg (1987). The carbonates microfacies are defined and described using Dunham (1962) classification of carbonates.

Moreover, detailed petrography of samples having dolomites and calcite in veins and vugs are also studied. The saddle dolomites and poikilotopic calcite in the older collected samples of Iannace (1991) and Galluccio (2009) are also studied to better establish paragenetic sequence at the scale of Mesozoic carbonates of the Lattari mountains.

For some thin sections, photomosaics are also prepared. Photomicrographs are captured at low resolution objective lens using Leica Wild M420 petrographic microscope with attached Zeiss camera and then all photomicrographs are merged to form a complete scan of thin section using Image Composite Editor (ICE) software of Microsoft.

Few thin sections (e.g., MUC-3T, 3B, 5a, 5b, 5c, 5e, 6a, 6d and 7T) are treated with alizarin red solution to differentiate dolomite from calcite. The alizarin red solution was prepared using the methods of Evamy (1963) and Dickson (1965).

4.2.1.2 Scanning Electron Microscopy (SEM) and Energy Dispersive X-ray Spectroscopy (EDS)

The Scanning electron microscopy and energy dispersive x-ray spectroscopy (SEM-EDS) analyses are conducted for total of 48 samples (27 samples from C-interval and 21 samples from B-interval). The SEM-EDS studies are performed on carbon-coated polished thin sections (N_T = 15: N_B = 04 and N_C = 11) and fresh-broken gold and few carbon coated rock pieces (N_T = 33: N_B = 17 and N_C = 16) using ZEISS Merlin VP Compact in the SEM Lab of DiSTAR (UNINA). Few samples (rock pieces) are etched with 0.2% HCL to remove surficial materials.

4.2.1.3 Electron Microprobe analysis (EPMA)

The Electron Microprobe analysis (EPMA) analysis on 12 polished thin sections (N = 09 of C-interval and N = 03 from B-interval) has been done using Field-emission gun electron probe microanalyzer (FEG-EPMA) at the facility CAM-ES, Department of Earth Sciences, University of Cambridge, Cambridge, U.K. 06 elements including 02 major (Ca, Mg), and 04 trace elements (Ba, Sr, Fe, and Mn) with total of 874 points have been analyzed using EPMA.

4.2.1.4 Cathodoluminescence (CL) microscopy

The cathodoluminescence (CL) microscopy has been conducted, using Citl Cold Cathode Luminescence 8200 mk3 with the attached microscope Leitz Laborlux 12 POL S, in the Sedimentary Microscopy Laboratory of DiSTAR (UNINA).

4.2.2 Dolomite crystal size distribution (CSD) analysis

There are different methods of dolomite crystal size distribution (CSD) analysis including linear traverse method and random or grid/point counting method (Sibley et al., 1993). The known approach(es) for measurements of dolomite crystal size is measuring longer dimension/axis of crystals using ordinary thin section and or SEM photomicrographs (Gregg et al., 1992; Sibley et al., 1993; Jones, 2005; Manche and Kaczmarek, 2019).

The dolomite CSD analysis are done using ordinary petrographic microscope photomicrographs for a total of 115 thin sections of both C- and B-intervals (i.e., C-interval N = 77: Faito-C 22, Moiano-C 13, Castello-C 21, and Moiano-C4 21; and B-interval (N = 38; Faito-B 13, Moiano-B 11, and Castello-B 14). Mostly five photomicrographs (representative of the sample) captured using 5x magnification are used. The scheme of dolomite CSD analysis conducted in present research is shown in Figure 4.5. The scale of investigation is selected based on the overall texture (i.e., fine dolomite crystals, dolomite-scattered and floating crystals in micritic matrix, etc) of the rock. The dolomite crystals longer dimensions are measured using ImageJ software. After crystal size measurements, different statistical parameters (average crystal size, minimum-maximum crystal sizes, median and mode) are calculated using MS Excel. For the B-interval, CSD analysis are done using traverse / intercept line method using the standard of ASTM for grain size analysis, equation given below (ASTM International, 2021) (Fig. 4.5).

Grain (crystal) size = number of crystal boundary intersections / total line length

The B-interval is completely dolomitized unit having mostly cloudy (brownish) dolomite crystals and mosaic dolomites with negligible micritic matrix, thus, samples from B-interval were very inconvenient for CSD analysis. The dolomite crystal size classes (i.e., medium and coarse) are defined using Lucia (1995) classes. The appendix 1 contains data about dolomite crystal size distribution analysis of the C- and B-intervals.

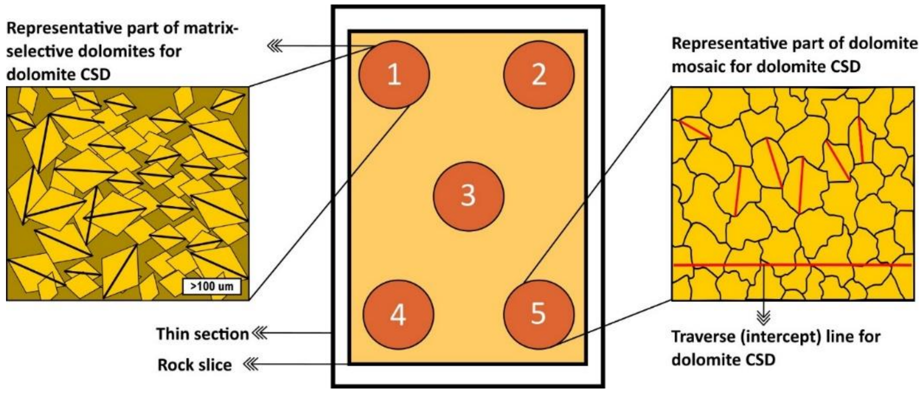

Figure 4.5. Site selection in a thin section for dolomite CSD analysis. Scheme(s) of CSD for matrix-selective dolomites (left) and dolomite mosaic (right) has been demonstrated.

4.2.3 Analytical methods

4.2.3.1 X-ray Diffraction (XRD) ANALYSIS

The X-ray diffraction (XRD) analysis of 135 samples (N = 114 in DiSTAR, UNINA and N = 21, Moiano-C Section, in Department of Earth Sciences, Sapienza University of Rome) are conducted. 77 samples of C-interval (Faito-C 18, Moiano-C 21, Castello-C 15, Moiano-C4: 23) and 58 samples of B-interval (Faito-B: 19; Moiano-B: 20; Castello-B: 19) are selected using the integration of outcrop lithology and petrographic observations. Those samples are selected for XRD analysis which contain adequate percentage of dolomite. In case of B-interval, which is a completely dolomitized unit, samples are selected by considering the texture (e.g., coarse, medium and fine crystalline dolomites).

XRD analysis at DiSTAR, University of Naples Federico II, Naples, Italy

A Panalytical X'Pert Pro Diffractometer, equipped with a RTMS X'Celerator detector with Cu-Kα radiation, operating at 40 kV and 40 mA, was used to acquire datasets. Scans were collected in the range 4–70 ◦2θ using a step interval of 0.017 ◦2θ, with a step counting time of 120 s. Every sample was added with a 20 wt% of internal standard (Buehler a alumina – 1mm). The mineral phases were identified by the Panalytical Highscore Plus 3.0e software and PDF-2/ICSD mineral databases.

The powder samples collected directly on field are further grinded manually using pestle and agate mortar for few minutes. Then the powder sample is placed in an XRD-sample holder for XRD analysis. In this case, there was a rack which can accommodate 20 sample holders at one time. The samples are run usually overnight.

XRD analysis at the Department of Earth Sciences, Sapienza University of Rome

The XRD analysis of 21 samples (Moiano-C Section) are conducted in the Department of Earth Sciences, Sapienza University of Rome, Rome, Italy. The semi-quantitative analysis was conducted using a Bruker D8 Advance X-ray system equipped with Lynxeye XE-T silicon-strip detector at the Department of Earth Sciences, Sapienza University of Rome, Rome, Italy. The instrument was operated at 40 kV and 30 mA using CuKα radiation (λ=1.5406 Å). Samples were run between 2–70° 2θ with step sizes of 0.02° 2θ while spinning the sample. Data were collected with variable slit mode to keep the irradiated area on the sample surface constant and converted to fixed slit mode for semiquantitative analysis. Semiquantitative estimation of mineral phases was performed by calculating peak areas and using mineral intensity factors as calibration constants (Moore and Reynolds, 1997). The mineral composition of the solids was determined by comparing the powder XRD diffraction pattern to the COD crystal diffractogram database in the Bruker Eva software package.

In this lab, the powder samples are further grinded manually using pestle and agate mortar for few minutes and then they were placed in a sample holder for subsequent XRD analysis. In this case, one sample is run at one time to avoid contamination. One sample took approximately 1 hr and 30 mins.

In DiSTAR (UNINA), the abundance of dolomite relative to calcite (i.e., dolomite percentage) is determined using the peak-height ratio of the dolomite (104) peak divided by the dolomite (104) peak plus the calcite (104) peak (Royse et al., 1971). In Sapienza University (Rome), dolomite percentage was determined using full width at half maximum intensity (FWHM) of dolomite d (104) peak at 30.8 2Theta. FWHM refers to the width of the XRD peak (peak) measured at half of the maximum intensity and is reported as a ratio of the width to the maximum intensity of the peak.

Dolomite stoichiometry (mole % $MgCO_3$) was calculated using the calibrated position of the dolomite (104) reflection (Lumsden, 1979). Actually, dolomite stoichiometry was determined using the relation between mole % $CaCO_3$ and d (104) spacing (Goldsmith and Graf, 1958). The following formula is used for calculating dolomite stoichiometry (Lumsden, 1979).

$$N_{CaCO_3} = Md + B$$

where N is the mole percent $CaCO_3$ in the dolomite lattice, *d* is the observed *d* spacing in Angstrom units, M is 333.33, and B is -911.99 (Lumsden, 1979). Then from mole % $CaCO_3$, mole % $MgCO_3$ is calculated. Otherwise, following equation can be used to calculate mole % $MgCO_3$.

$$\text{Mole fraction of } MgCO_3 (\%) = -333.33 * d (104) + 1011.99$$

The degree of cation ordering was determined using the ratio of the intensities of the dolomite (015) and (110) reflections (Goldsmith and Graf, 1958).

4.2.3.2 X-Ray Fluorescence (XRF) analysis

The X-ray fluorescence (XRF) analysis of 169 samples are conducted at DiSTAR, UNINA. 93 powder samples of C-interval (Faito-C: 20, Moiano-C: 21; Castello-C: 25; Moiano-C4: 27) and 76 powder samples of B-interval (Faito-B: 26; Moiano-B: 26; Castello-B: 24) are selected for XRF analysis.

The XRF analysis are conducted using portable (handheld) Bruker (tracer) X-Ray fluorescence (pXRF). The powder sample is placed in Chemplex® XRF sample cup (comprised of a cell, vented cap and collar) and sealed by prolene thin-films and analyzed using pXRF. The working conditions of pXRF used in present study are 40 kV voltage, 10 um current and 120 sec of acquisition time. All measurements were performed in dry air mode (i.e., normal conditions without any specific gas flow). The spot size (i.e., collimator) is 8 mm and sample thickness is 0.5 – 1 cm. Artax software is used to acquire the spectra of all analyzed samples.

4.2.4 Geochemical analyses

4.2.4.1 Dissolution (removal) of calcite from mixed lithologies

An experimental work has been done to dissolve (remove) calcite from mixed lithologies. The experimental work is carried out using calcite (Carrara Marble) and dolomite samples (collected from samples repository of Sedimentary Geology research group of DiSTAR, UNINA). The rock samples are grinded and powdered using Retsch Planetary Ball Mill PM 100 in sample preparation laboratory of DiSTAR (UNINA). The samples are categorized as natural samples (i.e., Calcite100% (C100) and Dolomite100% (D100)) and synthetic mixtures. Four synthetic mixtures are prepared, i.e., Calcite10%-Dolomite90% (C10-D90), Calcite30%-Dolomite70% (C30-D70), Calcite50%-Dolomite50% (C50-D50) and Calcite70%-Dolomite30% (C70-D30), by mixing defined quantities (%) of calcite and dolomite powders. The calcite (C100) and dolomite (D100) powder samples sieve analysis are performed using sieve shaker to know about the distribution of particle size in both samples. The sieve analysis data is processed using GRADISTAT (Version 9.1) software (Blott and Pye, 2001). The sieve analysis is performed in a lab at DiSTAR, UNINA.

For every sample 1 gram (g) of powder is used in the experiment and mixtures are produced considering the calcite-dolomite ratios (e.g., in sample Calcite10%-Dolomite90%, 0.1 g calcite and 0.90 g dolomite are mixed). All the samples are treated with 0.3 and 0.5 molar (M) concentrations of Ethylenediaminetetraacetic Acid (EDTA) and 3.5M and 1.75M concentrations of acetic acid buffers. Using stoichiometry, the volume of different solutions for every sample is determined (Appendix 2). The calcite and dolomite are also experimentally processed with distilled water to check the sample (powder) loss during the experiment. The treatment of samples with different solutions are carried out in the Department of Chemical Sciences, UNINA, Italy.

Different solutions preparation procedures are given below.

Preparation of 0.3 M EDTA solution

Weigh 33.50 g EDTA and put in 500 ml beaker filled up to 300 ml of distilled water. The solution was stirred while heating to about 50 $^{\circ}$C. 6.6 g of sodium hydroxide was added to the solution to dissolve EDTA at the pH value of 8. Then the pH was reduced to 6.3 using hydrochloric acid (HCL).

Preparation of 0.5 M EDTA solution

Weigh 55.8 g EDTA and put in 500 ml beaker filled up to 300 ml of distilled water. The solution was stirred while heating to about 50 $^{\circ}$C. 6.6 g of sodium hydroxide was added to the solution to dissolve EDTA at the pH value of 8. Then the pH was reduced to 6.3 using hydrochloric acid (HCL).

Preparation of Acetic Acid / Sodium Acetate buffers

Weigh 182.4 g of sodium acetate trihydrate into the 1l beaker. Add about 400 ml of ultrapure water and stir to dissolve the salt a little and make it easier to pour into the 1l flask; wash the walls of the beaker with ultrapure water to facilitate the quantitative transfer of the salt into the flask. Then go under a chemical hood and add 100 ml of acetic acid, taken with a graduated cylinder, add ultrapure water almost to the mark and stir to complete the homogenization of the solution. Remove the magnetic stir bar and bring to volume. Take an aliquot of the solution thus obtained and measure the pH using a previously calibrated pH-meter. The pH of the prepared acetic acid buffers was ~4.6.

The EDTA solution(s) are prepared at pH 6.3 using the observations reported by Glover (1961). Likewise, the pH of the prepared acetic acid buffers was ~4.6. In case of EDTA, samples are stirred for 20 minutes (Fig. 4.6). For acetic acid buffers, different stirring times are used for different samples, e.g., 1 hour for dolomite and 4 hours for calcite (Fig. 4.6). For both EDTA and acetic acid buffers, stirring is done using magnetic stirrer at room temperature.

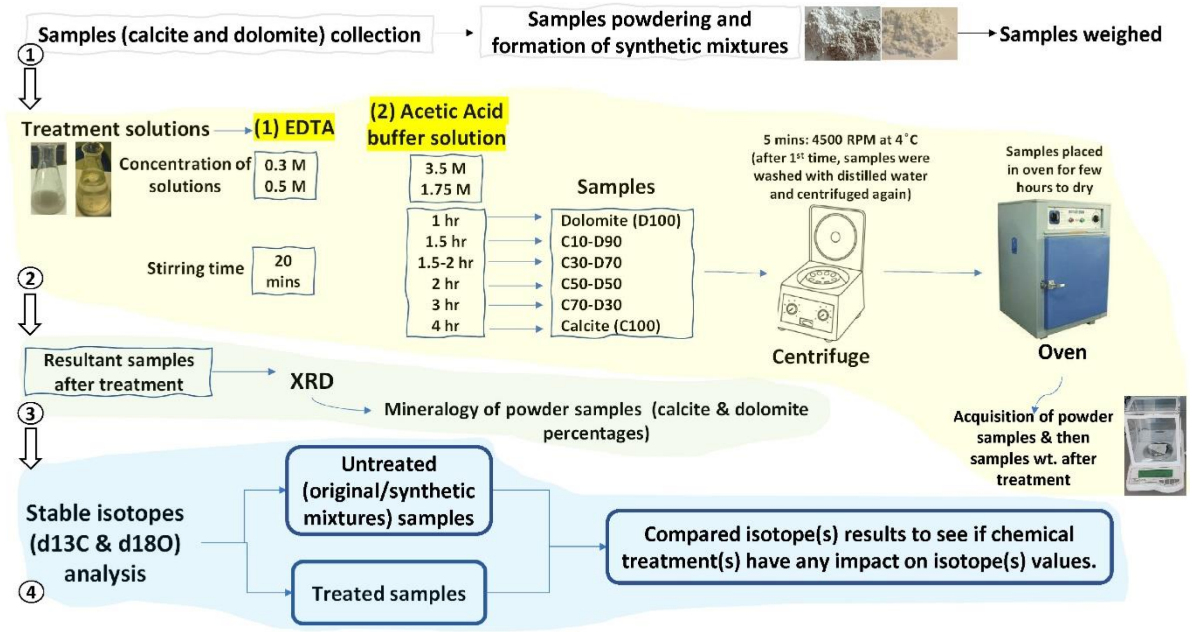

Figure 4.6. Detailed workflow of the present study. (1) Samples collection, powdering and weighing, (2) Experimental work, (3) XRD analysis, and (4) Stable isotopes analysis.

After the chemical treatments, the samples were centrifuged (using Beckman Coulter Avanti J-20 XPI centrifuge) at 4500 rpm at 4°C for 5 minutes. After centrifugation, the solution is poured out and the settled sample is washed with distilled water. Afterwards, the samples were again centrifuged with the same conditions and then put in oven at 70°C for few hours to dry. After desiccation, the acquired powder samples X-Ray Diffraction (XRD) and stable isotopes ($\delta^{13}C$ and $\delta^{18}O$) analyses are performed at the Department of Physics and Earth Sciences, University of Ferrara, Ferrara, Italy. The XRD and stable isotopes analyses of all untreated samples are also performed. The workflow of this experimental part of the work is shown in Figure 4.6.

4.2.4.2 Dissolution of calcite from mixed lithologies of the C-interval

In the C-interval, some mixed lithologies i.e., calcareous dolomite and dolomitic limestones are present. To perform stable isotopes analysis of dolomite only, calcite needs to be removed / reduced (dissolved) from mixed lithologies. Therefore, total of 40 mixed lithologies of C-interval (Faito-C 06, Moiano-C 08, Castello-C 15, and Moiano-C4 11) are treated with 1.75 M acetic acid buffer solution for 30 minutes to dissolve calcite and acquired dolomite only.

4.2.4.3 Stable isotopes ($\delta^{13}C$ and $\delta^{18}O$) analysis

The stable isotopes ($\delta^{13}C$ and $\delta^{18}O$) analysis is performed in two laboratories i.e., the University of Ferrara and the University of Padova (Italy).

Stable isotopes analysis at the University of Ferrara (Italy)

The isotopic analyses of C and O for the samples of Moiano-B, Castello-B and few samples of Moiano-C (samples MAC-1P to MAC-1U) were performed at the Laboratory of Paleoclimatology and Isotopic Stratigraphy of the Department of Physics and Earth Sciences of the University of Ferrara, using isoFLOW (Elementar©) operating in continuous flow with a PrecisION Isotopic Ratio Mass Spectrometer (IRMS; Elementar©). For each analysis, approximately 150 µg of homogenous powder of sample was weighted and put into vials. Each vial was flushed with pure He through a needle located in the autosampler in order to replace the atmospheric air in the glass tube. In each vial the powder reacted with hot viscous water-free orthophosphoric acid for 3 h at 50 °C and 7 h at 50 °C, triggering the release of CO_2 from the limestones and dolomitic samples, respectively. Using the same needle, which has flushed the vial before, the released CO_2 sample gas was extracted and transferred to the IRMS for the simultaneous analysis of C and O. In the mass spectrometer the molecules of the sample gas are ionized by the source (*i.e.*, a thorium oxide filament), and the ions pass through a magnet, which deflects and sorts them into beams with distinctive mass/charge ratios (m/z). Then ion beams arrive at the collector where three Faraday cups detect the ions of the masses 44, 45 and 46 of CO_2 simultaneously. The detection of the distinct isotopic masses of the sample is bracketed between those of reference gas (CO_2, 4.5 grade purity), which has been calibrated using reference materials. In the cups, the impact of the ions is translated into a recordable electrical signal, forming peaks, whose areas are proportional to the number of incident ions. The isotope ratio is calculated through peak definition and integration through the ionOS software. The signal intensity is amplified by an integrated Amplifier and is expressed in nano-ampere (nA). The signal intensity is referred as "peak height", and the minimum acceptable signal is 1 nA (optimum between 2 and 10 nA) in amplitude and at least 5 seconds in duration. The $^{13}C/^{12}C$ and $^{18}O/^{16}O$ isotopic ratios were expressed with the δ notation (in ‰ units) relative to V-PDB. The in-house MAQ-1 standard was used for the single-point calibration and two control standards (IAEA 603 and Carrara Marble) were measured to monitor the quality of the analysis. Analytical uncertainties (1σ) for the isotope analyses were in the order of ± 0.1‰ for $\delta^{13}C$ and $\delta^{18}O$.

Stable isotopes analysis at the University of Padova (Italy)

The isotopic analyses of C and O for the samples of C-interval (Faito-C, Moiano-C (MAC-1A to MAC-1O), Castello-C)) and Faito-B were performed at the Laboratory of the University of Padova (Italy).

The runs were done at 70°C with two internal standards for calibration. For the $\delta^{13}C$, a calibration line has been interpolated between the average of the measured and nominal values of the standards. For $\delta^{18}O$, the formulae of Kim et al. (2015) have been used. The choice of the CO_2-acid fractionation coefficient (Kim et al., 2015 proposes two difference ones) affects ~0.1‰.

As stable isotopes analysis is conducted in two laboratories so interlab correction has been applied following Kim et al. (2015). As per the correction, 1.28‰ (VPDB) is subtracted from the $\delta^{18}O$ values obtained in laboratory of the University of Ferrara.

4.2.4.4 Radiogenic ($^{87}Sr/^{86}Sr$) isotopes analysis

The Strontium (Sr) isotope ($^{87}Sr/^{86}Sr$) analyses of 36 samples (24 from C-interval and 12 from B-interval) are performed in an ISO 6 class clean room at DiSTAR (UNINA). With respect to studied sites, the analyzed samples include Faito-C 05, Moiano- 04, Castello-C 05, Moiano-C4 06, Faito-B 04, Moiano-B 04 and Castello-B 04. 0.025 g of powder samples were dissolved with high purity HCl solution(s). Sr is separated from the matrix through conventional ion-exchange procedures, explained in Arienzo et al. (2013). Sr isotopic compositions were determined by thermal ionization mass spectrometry (TIMS), using a Thermo Scientific Triton Plus mass spectrometer equipped with one fixed and eight adjustable Faraday cups. 2 s.e. (i.e., the double of standard error) with N = 150, was better than ± 0.000006, ± 0.000007 and ± 0.000009 for Sr measurement. The determined Sr isotope ratios were normalized to the recommended values of NIST-SRM 987 ($^{87}Sr/^{86}Sr$ = 0.710248 ± 0.000012) international standard, as reported by Zhang and Hu (2020). The other details of the Sr isotope analysis can be found in Arienzo et al. (2013) and Nayebi et al. (2023).

4.2.4.5 U-Pb Geochronology

The U-Pb dating of saddle dolomites in veins, poikilotopic calcite in vugs and calcite veins are performed for Triassic, Jurassic and Cretaceous rocks (Table 4.2). The U-Pb dating is performed using well-polished 50-100 µm thick, thin sections. The U-Pb dating is performed at the Department of Earth Science, University of California, Santa Barbara, United States of America (USA). These analyses were performed using LA-MC-ICPMS following the methodology described in Kylander-Clark (2020). The laser conditions for the present analyzed samples were 65–110 um, 15 Hz, and 12 seconds (180 shots or ~15 µm), following two cleaning shots and 20 seconds of baseline. The analyzed samples contain enough U-Pb ratios and U content for dating. For all samples, $^{238}U/^{206}Pb$ versus $^{207}Pb/^{206}Pb$ graphs show a considerable scatter. Reference materials (RMs) consisted of NIST614 and WC-1 (Roberts et al., 2017) as the primary RMs, and ASH 15D (2.965 Ma; Nuriel et al., 2021) and AUGB6 (43 Ma; Pagel et al., 2018) as secondary RMs; secondary RMs yielded ages within uncertainty of their accepted values, and uncertainties less than those of the unknowns; as such, we find no reason to propagate additional uncertainty to the dates reported herein. U-Pb dating is performed in two runs (i.e., in first run Triassic and Jurassic saddle dolomites are analyzed and in second run Jurassic poikilotopic calcite, and Cretaceous saddle dolomites and poikilotopic calcite are analyzed). For each thin section, multiple zones are analyzed and dated. In Triassic FS-1058 sample, total of two main zones with total spots N = 104 are analyzed (zone 1 N = 60 and zone 2 N = 44). In Jurassic AT-11 sample, a total of four main zones with total spots N = 161 are analyzed (zone 1 N = 15, zone 2 N = 15, zone 3 N = 15, zone 4 N = 15, zone 5 N = 15, zone 6 N = 15, zone 7 N = 15, zone 8 N = 15, zone 9 N = 41). In Cretaceous KA-1 sample, total of five zones with total spots N = 63 are analyzed (zone 1 N = 13, zone 2 N = 14, zone 3 N = 15, zone 4 N = 07, and zone 5 N = 14). In Cretaceous KA-3 sample, total of 8 zones with total spots N = 145 are analyzed (zone 1a N = 10, zone 1b N = 11, zone 2 N = 30, zone 3 N = 15, zone 4 N = 15, zone 5 N = 30, zone 6 N = 09, zone 7 N = 15, and zone 8 N = 10).

Table 4.2. Details about the samples analyzed for U-Pb dating.

S No.	**Samples**	**Locations**	**Host rock ages**	**Dated mineralogy and texture**	**No. of dated thin sections**
1	KA-1 and KA-3	Castello	Cretaceous	Saddle dolomites in veins, poikilotopic calcite in vugs and calcite veins	2
2	AT-11	Atrani	Jurassic	Saddle dolomites in veins and poikilotopic calcite in vugs	2
3	FS 1058	Maiori	Triassic	Saddle dolomites in veins	1

CHAPTER 5

Calcite differential dissolution from carbonates (mix of calcite and dolomite) to acquire dolomite: an experimental study

CHAPTER 6

DOLOMITES AND DOLOMITIZATION IN THE C-INTERVAL

CHAPTER 7

DOLOMITES AND DOLOMITIZATION IN THE B-INTERVAL

Chapter 8

Synthesis of dolomites and dolomitization in the C- and B-intervals

CHAPTER 9

U-Pb dating of late-diagenetic dolomites and calcite

Conclusions

The main conclusions of the present PhD research work are as follows:

The experimental study to dissolve calcite from mixed lithologies (i.e., partially dolomitized limestone and calcareous dolomites) has been tested to acquire dolomite only for subsequent stable isotopes analysis. Two solutions of two different concentrations are tested i.e., 0.3M and 0.5 M EDTA, and 1.75M and 3.5M acetic acid buffers. The experimental work and XRD analysis revealed less calcite is dissolved by 0.3M EDTA solution and more calcite is dissolved by 1.75M acetic acid buffer. The latter solution dissolved almost all calcite, however, the XRD analysis revealed that not only calcite is dissolved but some quantity of dolomite is also dissolved, and enough dolomite is acquired for subsequent analysis (especially stable isotopes). The present study concluded that 0.3M EDTA is least reactive and 1.75M acetic acid buffer is relatively more aggressive to dissolve calcite from heterogenous carbonates. The isotopic response of all the samples treated with different solutions commonly demonstrated a complete spectrum from calcite-100% (C100) via different mixtures towards dolomite-100% (D100) except for clustering of mixed samples in 1.75M acetic acid buffer. This clustering depicts and justifies the dissolution of calcite from all the mixed samples treated with 1.75M acetic acid buffer. The stable isotopes ($\delta^{13}C$ and $\delta^{18}O$) results indicate different solutions (EDTA and acetic acid buffers) chemical treatments have no obvious significant impact on isotope(s) values. Among the tested different solutions, 1.75M acetic acid buffer is more effective and suitable for dissolving calcite and acquiring dolomite only for subsequent geochemical analyses. The present experimental investigation envisaged 1.75M acetic acid buffer as a geochemical tool. These results may be helpful for subsequent analyses ($\delta^{18}O$, $\delta^{26}Mg$, Δ_{47} and calculation of temperature of dolomite formation, etc) of dolomites (acquired from heterogenous carbonates) to better understand and interpret model(s) of dolomitization. Similarly, it can be useful for geoscientists (e.g., geochemists, sedimentologists, mineralogists, clay mineralogists, palaeontologists, etc.) who need to dissolve calcite from their calcite-dolomite mixed samples.

The second main research problem which is addressed is testing of reflux dolomitization. In the studied Early Cretaceous carbonates of the Lattari mountains (southern Apennines, Italy), the intensity of dolomitization varies across the stratigraphy and preserved as partially dolomitized limestones and pervasively dolomitized units. Two dolomite classes are defined i.e., Mdol and Cdol. The Mdol and Cdol's of the C-interval are usually Ca-rich non-stoichiometric having low degree of order with few nearly-stoichiometric dolomites. Some Mdol's of the B-interval are Ca-rich non-stoichiometric, while other Mdol's and Cdols are nearly stoichiometric and stoichiometric with low-moderate degree of order.

The C-interval consists of partially dolomitized and pervasively dolomitized cycles/units. The studied cycles of the C-interval usually have a decreasing downward dolomite percentage within a cycle except the cycle 2 of C2-interval, where this trend is not visible. On the contrary, in this latter cycle dolomite percentage increases downward. All the cycles of C2 and C4-intervals indicate downward flux of refluxing brines, however, in case of cycle 2 of C2-intevral it is considered that the lateral flux of refluxing brines is more dominant. There are lateral variations in dolomite average crystal size, dolomite percentage, stoichiometry, degree of order and stable isotopes (especially $\delta^{18}O$) from Faito-C through Moiano-C to Castello-C. These observations demonstrate that the source of dolomitizing fluids was closer to the Faito-C Section with respect to the Castello-C Section. The marked variations (particularly in the lateral directions) in geochemical parameters are not very distinctive, could be because studied sites are representing just a small area of a larger carbonate platform.

The geometry of beds/cycles, lithological variations, distribution of dolomites laterally and vertically, dolomites petrography and geochemistry indicate reflux dolomitization by downward and basinward flowing mesohaline fluids. In the C-interval, the geological and geochemical characteristics of cycle 3 (selective partial dolomitization) indicate active reflux, and the dolomite mosaics (i.e., pervasive dolomitization) in cycles 1 and 2 might indicate latent reflux described by Jones et al. (2002).

The B-interval is not completely dolomitized unit but pervasively dolomitized unit. It is because it contains ample calcite (especially in the form of calcite inclusions in the cloudy zoned dolomite crystals), and some micritic matrix is also noticed in few dolomite mosaics. Same is also valid for the C-interval, wherever it contains the zoned and or cloudy dolomite crystals (especially in cycles 1 and 2). Based on petrography and scanning electron microscopy, it is suggested that the calcite-inclusions are remnants of precursor limestones, which correspond to cloudy cores in the petrographic microscope. The center(s) of the zoned dolomite crystals are initially formed by incomplete replacement of calcite mud/micrite, and later the limpid rims are formed due to pure dolomite precipitation (overdolomitization). The overdolomitization is common in the B-interval as compared to the C-interval. Based on the petrographic observation, it is proposed that zoned dolomites are formed in areas which were earlier occupied by coarse grains (e.g., wackestone, packstone) and was porous and permeable, while the unzoned relatively fine crystalline dolomites in association with zoned dolomites are formed in earlier fine-grained muddy intervals with least permeability.

In the B-interval, the only significant variation seems to be related not to the position in a cycle but to type of dolomite, Mdol vs. Cdol. This is associated to stoichiometry, oxygen isotopes, possibly degree of order and carbon isotopes. The present work demonstrates that B-interval has experienced multiple fluxes of dolomitizing fluids (evident from overdolomitization in Cdol's). Consequently, there is superimposition of geochemical trends in single cycles (which can be seen in the C interval). This indicates that repeated lateral flow of dolomitizing fluids in the B interval have obscured vertical trends and the only variations are associated to type of dolomites.

In both C- and B-intervals, some corroded dolomites (porous crystals having worn-out irregular corners and peripheries) are noticed. Based on petrography and geochemistry, it is assumed that in the C-interval, the corrosion of dolomites is polygenetic in origin and caused by hydrothermal and meteoric fluids and rare microbes induced/influenced (in Moinao-C4 Section only) corrosion. In case of B-interval the mechanism of corrosion is not obvious. However, dolomite crystals are corroded whenever they are in association with features inherited from microbes. This association indirectly indicate microbially induced/influenced corrosion.

The U-Pb dating of sparry saddle dolomites found in veins and vugs of the Mesozoic carbonates of the Lattari mountains (southern Apennines, Italy) revealed that the earlier hypothesized model of single episode late stage, fracture-related dolomitization is untrue, and the saddle dolomites indicate multiple-age hydrothermal dolomitization events. The U-Pb data provided four main clusters of dates for saddle dolomites: Late Jurassic (160 Ma), Albian-Cenomanian (100-90 Ma), Paleogene (>70, ~65, 50 and 35 Ma) and two cluster of dates for calcite: Miocene (11.5 Ma and 10 Ma) and Pliocene (4 Ma). Each age corresponds to well established extensional phases affecting the Apennine Carbonate Platform on a regional scale: the formation of intraplatform restricted basins during the Mesozoic and the pre-orogenic extension of the platform. The U-Pb data suggest that each of these tectonic events promoted fluid flow, and related hydrothermal dolomitization. A local source of Mg is suggested by the fact that dolomite veins are common only when the host rock is matrix dolomite. This is especially clear in relatively small, stratabound bodies of dolomites occurring in the Lower Cretaceous. Consequently, a proposed model implies the circulation of warm (hydrothermal) dolomitising fluids through Mesozoic and Paleogene extensional faults in the Apenninic platform, which lacked external sources of Mg. From present study, U-Pb dating technique is envisaged as a significant tool, which can unravel and attest different-age tectonic events, which are preserved but obscured in compositionally and texturally homogenous dolomites.

Acknowledgements

Although words hardly enable me to express my feelings of gratitude, yet I am bound to use them. First and most thanks are due for the Almighty Allah whose countless blessings made me capable to complete this research work. Grateful acknowledgements are extended to my supervisor Prof. Alessandro Iannace, Department of Earth, Environmental and Resources Sciences (DiSTAR), University of Naples Federico II (UNINA), Naples, Italy who assisted me in countless ways from the very beginning to the end during the PhD. I am very grateful to my advisor for giving me significant amount of time for discussion and accompanying me in most of the geological fieldworks.

I am thankful to my earlier PhD Coordinator (Prof. Vincenzo Morra) who assigned me the PhD project, and present PhD coordinator (Prof. Rosa Di Maio) for being very supportive and kept me updated about all official requirements and procedures. I am thankful to the Director of DiSTAR (UNINA) for being supportive, especially regarding approval of different missions.

Thanks are extended to DiSTAR (UNINA) for providing me the opportunity to pursue PhD in one of the oldest universities of the world. DiSTAR (UNINA) is thanked for providing research facilities for the PhD research work. Special thanks are extended to Dr. Sergio Bravi (Thin Section technician, DiSTAR, UNINA), who prepared all the thin sections of the PhD research work. I am also thankful to professors and concerned people of following labs of DiSTAR: SEM (Prof. Paola Petrosino and Dr. Roberto De Gennaro, SEM operator), Sr-isotopes (Prof. Massimo D'Antonio, Dr. Valeria Di Renzo and PhD student Piergiorgio Tranfa), XRD (Prof. Cappelletti Piergiulio, Dr. Concetta Rispoli, and PhD student Giovanna Montesano), pXRF (Prof. Alberto De Bonis and Maria Verde), sample preparation (for XRD) lab (Luigi Franciosi). Prof. Valentino Di Donato (DiSTAR, UNINA) is thanked for providing facilities in his lab for powdering few samples. Prof. Carlo Donadio (DiSTAR, UNINA) is thanked for helping in conducting sieve analysis in his laboratory. Prof. Mariano Parente (DiSTAR, UNINA) is greatly thanked for permitting me to use the chemical analysis lab and always very kind in sharing latest papers focused on dolomitization and helping me in finding papers which are not available on the internet. I am also thankful to Dr. Nicola Mondillo (DiSTAR, UNINA), who was always very kind and cooperative whenever I consulted him. I am also thankful to the administration staff of DiSTAR and PhD office of UNINA for being helpful and dealing/managing my administrative tasks.

Dr. Andrea Montanaro (Ex. PhD student of DiSTAR, UNINA) is thanked for his help during my earlier days in Italy and beginning of the research (especially use of petrographic microscope). Mr. Mubashir Mehmood and Mr. Enrico (students of DiSTAR, UNINA) are thanked for assisting me during the geological fieldworks. I am also thankful to my Italian classmates and friends Roberto Manzo and Renato Diamanti for being quite supportive and friendly especially in early days of PhD.

I am thankful to the concerned laboratories and researchers of the Department of Physics and Earth Sciences, University of Ferrara (Ferrara, Italy), and Department of Geosciences, University of Padova (Padova, Italy) for conducting stable isotopes ($\delta^{13}C$ and $\delta^{18}O$) and XRD analyses. Luca Aldega (Department of Earth Sciences, Sapienza University of Rome, Rome, Italy) is acknowledged for hosting me for a week in his lab and conducting XRD analysis of some samples.

Prof. Francesco Ruffo and PhD students Massimo Melchiorre and Vincenzo Langellotti of the Department of Chemical Sciences (UNINA) are thanked for providing facilities and guidance/help in conducting the experimental work in their lab. I am also thankful to the Professor(s)/researcher(s) of Biotechnology, Biochemistry and Enzymology (BBE) research lab of the Department of Chemical Sciences (UNINA) for allowing the use of centrifuge for the experimental work.

Andrew Kylander-Clark (Lab Manager, Department of Earth Science, University of California Santa Barbara, USA) is thanked for conducting U-Pb dating. Dr. Iris Buisman (Lab Manager) is thanked for conducting EPMA analysis in the framework of the H2020 EXCITE project (Grant agreement no. 101005611) at the Department of Earth Sciences, University of Cambridge (UK).

In addition, I am grateful to my dear wife for being supportive during the duration of PhD. I would also like to thank all my family members (especially my late father, mother, late sister and elder brother) for their continuous support since childhood. I am thankful to the Department of Geology, University of Swabi, Swabi, Khyber Pakhtunkhwa, Pakistan for allowing me to pursue PhD in DiSTAR (UNINA). Finally, I also would like to thank my Pakistani teachers, friends and colleagues who encouraged and supported me for PhD and motivated me whenever I was disheartened.

References

Adams, J.E., Rhodes, M.L., 1960. Dolomitization by seepage refluxion. American Association of Petroleum Geologists Bulletin, 44, 1912–1921.

Adams, A., Diamond, L.W., Aschwanden, L., 2019. Dolomitization by hypersaline reflux into dense groundwaters as revealed by vertical trends in strontium and oxygen isotopes: Upper Muschelkalk, Switzerland. Sedimentology, 66, 362-390.

Al-Aasm, I.S., Taylor, B.E., South, B., 1990. Stable isotope analysis of multiple carbonate samples using selective acid extraction. Chem. Geol. Isot. Geosci. 80 (2), 119–125.

Aldega, L., Cello, G., Corrado, S., Cuadros, J., Dfullmeri Leo, P., Giampaolo, C., Invernizzi, C., Martino, C., Mazzoli, S., Schiattarella, M., Zattin, M., and Zuffa, G., 2005. The Southern Apennines case-history: thermal constraints and reconstruction of tectonic and sedimentary burials. Atti Ticinensi di Scienze della Terra serie speciale, 10, 45–53.

Al-Helal, A.B., Whitaker, F.F., Xiao, Y., 2012. Reactive transport modeling of brine reflux: Dolomitization, anhydrite precipitation, and porosity evolution. Journal of Sedimentary Research, 82, 196–215.

Allan, J.R., Wiggins, W.D., 1993. *Dolomite Reservoirs: Geochemical Techniques for Evaluating Origin and Distribution*. Tulsa: The American Association of Petroleum Geologists, AAPG Continuing Education Course Note Series 36.

Al-Awadi, M., Clark, W.J., Moore, W.R., Herron, M., Zhang, T., Zhao, W., Hurley, N., Kho, D., Montaron, B., Sadooni, F., 2009. Dolomite: Perspectives on a perplexing mineral. Oilfield Review, 21(3), 32-45.

Amodio, S., Ferreri, V., D'Argenio, B., 2011. The Barremian-Aptian shallow-marine carbonates of Monte Faito and of Santa Maria bore cores (central-southern Apennines, Italy). Regional correlation based on cyclostratigraphy. Rend. Online Soc. Geol. It., 17, 9-17.

Amodio, S., Weissert, H., 2017. Paleoenvironment and palaeoecology before and at the onset of Oceanic Anoxic Event (OAE) 1a: reconstructions from Central Tethyan archives. Palaeogeography, Palaeoclimatology, Palaeoeclogy, 479, 71-89. https://doi.org/10.1016/j.palaeo.2017.04.018.

Arienzo, I., Carandente, A., Renzo, V. D., Belviso, P., Civetta, L., D'Antonio, M., Orsi, G., 2013. Sr and Nd isotope analysis at the radiogenic isotope laboratory of the National Institute of Geophysics and Volcanology, Naples Section - Vesuvian Observatory. INGV Technical Report No. 260.

ASTM (American Society for Testing and Materials) International, 2021. Standard methods for determining average grain size. Desgination: E112 – 13 (reapproved 2021). 10.1520/E0112-13R21

Awais, M., Diamanti, R., Kylander-Clark, A., Vitale, S., Camanni, G., Iannace, A., 2023. U-Pb dating of dolomite veins unveil paleo-tectonic history of Apennine Carbonate Platform. Abstract volume, 17th Bathurst Meeting-International Meeting of Carbonate Sedimentologists, Naples, Italy, 5-7 September 2023, p. 6.

Babcock, R.S., Atwood, D.K., Perry, D., 1967. Separation of dolomite from fine grained recent sediments. Am. Mineral. 52, 1563–1567.

Badiozamani, K., 1973. The Dorag Dolomitization Model-Application to the Middle Ordovician of Wisconsin. SEPM Journal of Sedimentary Research, 43(4), 965–984. https://doi.org/10.1306/74d728c9-2b21-11d7-8648000102c1865d.

Baker, P.A., Burns, S.J., 1985. Occurrence and formation of dolomite in organic-rich continental margin sediments. Bulletin of American Association of Petroleum Geologists, 69, 1917-1930.

Barale, L., Bertok, C., d'Atri, A., Domini, G., Martire, L., Piana, F., 2013. Hydrothermal dolomitization of the carbonate Jurassic succession in the Provençal and Subbriançonnais domains (Maritime Alps, North-Western Italy). Comptes Rendus Geoscience, 345, 47-53.

Barale, L., Bertok, C., Talabani, N.M., d'Atri, A., Martire, L., Piana, F., Préat, A., 2016. Very hot, very shallow hydrothermal dolomitization: An example from the Maritime Alps (north-west Italy-south-east France). Sedimentology, 63, 2037-2065.

Barale, L., Bertok, C., d'Atri, A., Piana, F., Bernasconi, S.M., Czuppon, G., Palcsu, L., Gerdes, A., Birgel, D., Martire, L., 2021a. U-Pb dating and geochemical constraints to early Cretaceous hydrothermal dolomitization in the Provençal domain (Maritime Alps), NW Italy-SE France). Ofioliti, 46(2), 131-149. DOI: 10.4454/ofioliti.v46i2.543

Barale, L., Bertok, C., d'Atri, A., Mantovani, A., Martire, L., Agostini, S., Bernasconi, S.M., Gerdes, A., Ferrando, S., 2021b. Syn-rift hydrothermal circulation in the Meoszoic carbonates of the western Adriatic continental palaeomargin (Western Southalpine Domain, NW Italy). Basin Research, 33(6), 3045-3076.

Barnett, A.J., Wright, V.P., Chandra, V.S., Jain, V., 2015. Distinguishing between eogenetic, unconformity-related and mesogenetic dissolution: a case study from the Panna and Mukta fields, offshore Mumbai, India. In: Armitage, P.J., Butcher, A.R., Churchill, J.M., Csoma, A.E., Hollis, C., Lander, R.H., Omma, J.E., Worden, R.H. (eds.), Reservoir quality of clastic and carbonate rocks: analysis, modelling and prediction. Geological Society, London, Special publications, 435. http://doi.org/10.1144/SP435.12

Baudrand, M., Aloisi, G., Lécuyer, C., Martineau, F., Fourel, F., Escarguel, G., Blanc-Valleron, M. -M., Rouchy, J. -M., Grossi, V., 2012. Semi-automatic determination of the carbon and oxygen stable isotope compositions of calcite and dolomite in natural mixtures. Applied Geochemistry, 27, 257-265.

Bein, A., Land, L.S., 1983. Carbonate sedimentation and diagenesis associated with Mg-Ca-chloride brines: the Permian San Andres Formation in the Texas Panhandle. Journal of Sedimentary Petrology, v.53, p.243-260.

Bertello, F., Fantoni, R., Franciosi, R., Gatti, V., Ghielmi, M., Pugliese, A., 2010. From thrust-and-fold belt to foreland: hydrocarbon occurrences in Italy Petroleum Geology Conference series, 7, pp. 113–126.

Blott, S.J., Pye, K., 2001. GRADISTAT: a grain size distribution and statistics package for the analysis of unconsolidated sediments. *Earth Surface Processes and Landforms*, 26, 1237-1248.

Bonie, M., Parente, G., Bechstädt, T., De Vivo, B., Iannace, A. (2000). Hydrothermal dolomites in SW Sardinia (Italy): evidence for a widespread late-Variscan fluid flow event. Sedimentary Geology, 131, 181-200.

Bontognali, T.R.R., Vasconcelos, C., Warthmann, R.J., Bernasconi, S.M., Dupraz, C., Strohmenger, C.J., McKenzie, J.A., 2010. Dolomite formation within microbial mats in the coastal sabkha of Abu Dhabi (United Arab Emirates). Sedimentology, 57, 824-844.

Bontognali, T.R.R., McKenzie, J.A., Warthmann, R.J., Vasconcelos, C., 2014. Microbially influenced formation of Mg-calcite and Ca dolomite in the presence of exopolymeric substances produced by sulphate-reducing bacteria. Terra Nova, 26, 72-77.

Böttcher, M.E., Mart, Y., Brumsack, H.J., 1998. Data report: geochemistry of pliocene and miocene carbonates from the eratosthenes seamount (site 956). In: Robertson, A. H.F., Emeis, K.C., Richter, C., Camerlenghi, A. (Eds.), Proc. ODP Sci. Results, vol. 160. Ocean Drilling Program, College Station, TX, pp. 447–451.

Bosellini, A., 2004. The western passive margin of Adria and its carbonates platforms. Special Volume of the Italian Geological Society for the IGC 32. Florence 79–92.

Bosence, D., Procter, E., Aurell, M., Bel Kahla, A., Boudagher-Fadel, M., Casaglia, F., Cirilli, S., Mehdie, M., Nieto, L., Rey, J., Scherreiks, R., Soussi, M., Waltham, D., 2009. A dominant tectonic signal in high-frequency, peritidal carbonate cycles? a regional analysis of Liassic platforms from western Tethys. Journal of Sedimentary Research, 79, 389–415.

Bouch, J.E., 2003. Models of Dolomitisation - A Literature Review. *British Geological Survey Internal Report IR/03/083*.

Braithwaite, C.J.R., 1991. Dolomites, a review of origins, geometry and textures. Transactions of the Royal Society of Edinburgh: Earth Sciences, 82, 99-112.

Brauchli, M., McKenzie, J.A., Strohmenger, C.J., Sadooni, F., Vasconcelos, C., Bontognali, T.R.R., 2016. The importance of microbial mats for dolomite formation in the Dohat Faishah sabkha, Qatar. Carbonates and Evaporites, 31, 339-345.

Bravi, S., De Castro, P., 1995. The Cretaceous fossil fishes level of Capo d'Orlando, near Castellammare di Stabia (NA): biostratigraphy and depositional environment. Sciences Géologiques - Memoires 47, 45–72.

Budd, D.A., 1997. Cenozoic dolomites of carbonate islands: their attributes and origin. Earth-Science Reviews, 42(1-2), 1-47.

Budd, D.A., Park, A.J., 2018. Formation of bed-scale spatial patterns in dolomite abundance during early dolomitization: Part I. Mechanisms and feedbacks revealed by reaction-transport modelling. Sedimentology, 65, 209-234.

Burns, S.J., McKenzie, J.A., Vasconcelos, C., 2000. Dolomite formation and biogeochemical cycles in the Phanerozoic. Sedimentology, 47, 49-61.

Caiazzo, C., Ascione, A., Cinque, A., 2006. Late Tertiary–Quaternary tectonics of the southern Apennines (Italy): new evidences from the Tyrrhenian slope. Tectonophysics 421 (1–2), 23–51. https://doi.org/10.1016/j.tecto.2006.04.011.

Carannante, G., Ruberti, D., Sirna, M., 2000. Upper Cretaceous ramp limestones from the Sorrento Peninsula (southern Apennines, Italy): micro- and macrofossil associations and their significance in the depositional sequences. Sedimentary Geology 132, 89–123.

Carballo, J.D., Land, L.S., Miser, D.E., 1987. Holocene dolomitization of supratidal sediments by active tidal pumping, Sugarloaf Key, Florida. Journal of Sedimentary Petrology, 57(1), 153-165.

Carminati, E., Corda, L., Mariotti, G., Scifoni, A., Trippetta, F., 2013. Mesozoic Syn- and Postrifting Evolution of the Central Apennines, Italy: The Role of Triassic Evaporites. The Journal of Geology, 121, 327–354. DOI: 10.1086/670730.

Casero, P., Roure, F., Endignoux, L., Moretti, I., Muller, C., 1988. Neogene geodynamic evolution of the southern Apennines. Memor. Soc. Geol. Ital. 41, 109–120.

Casciello, E., Cesarano, M., Pappone, G., 2006. Extensional detachment faulting on the Tyrrhenian margin of the southern Apennines contractional belt (Italy). J. Geol. Soc. 163 (4), 617–629. https://doi.org/10.1144/0016-764905-054.

Catalano, R., D’Argenio, B., 1982. Infraliassic strike-slip tectonics in Sicily and Southern Apennines. Rend. Soc. Geol. Ital., 5, 5-10.

Cello, G., Mazzoli, S., 1999. Apennine tectonics in southern Italy: a review. Journal of Geodynamics, 27, 191-211.

Chai, L., Navrotsky, A., Reeder, R.J., 1995. Energetics of calcium-rich dolomite. Geochimica et Cosmochimica Acta, 59(5), 939-944.

Chiocchini, M., Farinacci, A., Mancinelli, A., Molinari, V., Potetti, M., 1994. Biostratigrafia a foraminiferi, dasicladali e calpionelle delle successioni carbonatiche mesozoiche dell’Appennino centrale (Italia). In A. Mancinelli (Ed.), *Biostratigrafia dell'Italia Centrale. Studi Geologici Camerti* (pp. 9–129). Università di Camerino.

Choquette, P.W., Hiatt, E.E., 2008. Shallow-burial dolomite cement: a major component of many ancient sucrosic dolomites. Sedimentology, 55, 423-460. https://doi.org/10.1111/j.1365-3091.2007.00908.x.

Ciarapica, G., Passeri, L., 1998. Evoluzione paleogeografica degli Appennini. Atti Tic. Sc. Terra, 40, 233-290.

Cohen, H.F., 2019. Evaluating the effects of sodium, potassium, magnesium, and calcium concentrations on dolomite stoichiometry, cation ordering, and reaction rate. Unpublished Masters thesis, Western Michigan University, Kalamazoo. https://scholarworks.wmich.edu/masters_theses/5096

Corradetti, A., Tavani, S., Parente, M., Iannace, A., Vinci, F., Pirmez, C., Torrieri, S., Giorgioni, M., Pignalosa, A., Mazzoli, S., 2018. Distribution and arrest of vertical through-going joints in a seismic-scale carbonate platform exposure (Sorrento peninsula, Italy): insights from integrating field survey and digital outcrop model. Journal of Structural Geology. https://doi.org/10.1016/j.jsg.2017.09.009.

D’Argenio., B., Ferreri, V., Raspini, A., Amodio, S., Buonocunto, F.P., 1999. Cyclostratigraphy of a carbonate platform as a tool for high-precision correlation. Tectonophysics, 315, 357-384.

D’Argenio., B., Ferreri, V., Weissert, H., Amodio, S., Buonocunto, F.P., Wissler, L., 2004. A multidisciplinary approach to global correlation and geochronology. The Cretaceous shallow-water carbonates of southern Apennines, Italy. In: D’Argenio., B., Fischer, A.G., Silva, I.P., Weissert, H., Ferreri, V., (eds.), Cyclostratigraphy: Approaches and case histories. SEPM special publication no. 81, p. 103-122.

Davies, G.R., Smith, L.B., 2006. Structurally controlled hydrothermal dolomite reservoir facies: An overview. AAPG bulletin, 90(11), 1641-1690.

De Castro, P., 1962. Il Giura-Lias dei Monti Lattari e dei rilievi ad ovest della Valle dell'Irno e della Piana di Montoro. Bollettino Della Societa Dei Naturalisti in Napoli 71, 3–34.

Diamanti, R., Awais, M., Camanni, G., D'Antonio, M., Della Porta, G., Di Renzo, V., Graziano, S.F., Iannace, A, Kylander-Clark, A., Vitale, E., Vitale, S., 2023. Fault-controlled saddle dolomitization during the Late Triassic – Early Jurassic Pangea breakup in the southern Adria domain.

Dickson, J.A.D., 1965. A modified technique for carbonates in thin section. Nature, 205(4971), 587.

Di Lucia, M., Trecalli, A., Mutti, M., Parente, M., 2012. Bio-chemostratigraphy of the Barremian-Aptian shallow-water carbonates of the southern Apennines (Italy): pinpointing the OAE1a in a Tethyan carbonate platform. Solid Earth 3:1–28. https://doi.org/10.5194/se-3-1-2012.

Dong, S.F., Chen, D.Z., Qing, H., Zhou, X., Wang, D., Guo, Z., Jiang, M., Qian, Y., 2013. Hydrothermal alteration of dolostones in the Lower Ordovician, Tarim Basin, NW China: multiple constraints from petrology, isotope geochemistry and fluid inclusion microthermometry. Marine and Petroleum Geology, 46, 270-286.

Dong, S., Chen, D., Zhou, X., Qian, Y., Tian, M., Qing, H., 2017. Tectonically driven dolomitization of Cambrian to Lower Ordovician carbonates of the Quruqtagh area, north-eastern flank of Tarim Basin, north-west China. Sedimentology, 64(4), 1079-1106.

Dravis, J.J., Wanless, H.R., 2018. Reflux dolomitization – A Holocene example beneath a coastal salina, West Caicos Island, Turks and Caicos Islands. Marine and Petroleum Geology, 97, 311-322.

Dunham, R.J., 1962. Classification of carbonate rocks according to depositional texture. In Ham, W.E., (ed.) Classification of carbonate rocks. Memoir of American Association of Petroleum Geologists, 1, pp. 108-121.

Dupraz, C., Reid, R.P., Braissant, O., Decho, A.W., Norman, R.S., Visscher, P.T., 2009. Processes of carbonate precipitation in modern microbial mats. Earth-Science Reviews, 96(3), 141-162.

Du, Y., Song, H., 2020. Refined protocol for $\delta^{13}C$ analysis of calcite and dolomite in carbonate mixture samples. Rapid Commun. Mass Spectrom. 34 (10), e8743.

Durocher, S., Al-Aasm, I.S., 2004. Dolomitization and neomorphism of Mississippian (Visean) Upper Debolt Formation, Blueberry Field, Northeastern British Columbia: Geologic, petrologic and chemical evidence. AAPG Bulletin, 81(6), 954-977.

El Hefnawi, M.A., Mashaly, A.O., Shalaby, B.N., 2012. Chemical fractionation of trace elements between calcite and dolomite fractions separated from their mixture in some Egyptian dolomite limestone rock. Australian Journal of Basin and Applied Sciences, 6(3), 176-184.

Epstein, S., Graf, D.L., Degens, E.T., 1964. Oxygen isotope studies on the origin of dolomites. In: Craig, H., Miller, S.L., Wasserburg, G.J. (Eds.), Isotopic and Cosmic Chemistry. North-Holland, Amsterdam, pp. 169–180.

Esteban, M., Taberner, C., 2003. Secondary porosity development during late burial in carbonate reservoirs as a result of mixing and/or cooling of brines. Journal of Geochemical Exploration, 78, 355-359.

Evamy, B.D., 1963. The application of a chemical staining technique to a study of dedolomitization. Sedimentology, 2, 164-170.

Fairbridge, R.W., 1957. The Dolomite Question. In: LeBlanc, R.J., Breeding, J.G. (eds.), Regional aspects of carbonate deposition. SEPM Special publication 5, Tulsa, Oklahoma, p. 164-170. Doi:10.2110/pec.57.01.0125

Folk, R.L., Siedlecka, A., 1974. The ‘‘schizohaline’’ environment: its sedimentary and diagenetic fabrics as exemplified by late Paleozoic rocks of Bear Island, Svalbard. Sedimentary Geology, 11, 1-15.

Frijia, G., Parente, M., Di Lucia, M., Mutti, M., 2015. Carbon and strontium isotope stratigraphy of the Upper Cretaceous (Cenomanian-Campanian) shallow-water carbonates of southern Italy: Chronostratigraphic calibration of larger foraminifera. Cretaceous Research, 53, 110-139.

Fullmer, S.M., Lucia, F.J., 2010. Rate of reflux dolomitization based on hydrodynamic modeling of a Glen Rose dolostone, Austin, Texas. Gulf Coast Association of Geological Societies Transactions, 60, 291-300.

Gabellone, T., Iannace, A., Gasparrini, M., 2014. Multiple dolomitization episodes in deepwater limestones of the Triassic Lagonegro Basin (Southern Italy): from early reflux to tectonically driven fluid flow. Journal of Sedimentary Research 84:435–456. https://doi.org/10.2110/jsr.2014.39

Gabellone, T., Whitaker, F.F., 2016. Secular variations in seawater chemistry controlling dolomitization in shallow reflux systems: insights from reactive transport modelling. Sedimentology, 63(5), 1233-1259.

Gabellone, T., Whitaker, F.F., Katz, D., Griffiths, G., Sonnenfeld, M., 2016. Controls on reflux dolomitisation of epeiric-scale ramps: Insights from reactive transport simulations of the

Mississippian Madison Formation (Montana and Wyoming). Sedimentary Geology, 345, 85-102.

Galluccio, L., 2009. Dolomites within the Mesozoic Carbonates of Sorrento Peninsula (Southern Apennines - Italy): Genetic models and reservoir implications. Unpublished PhD thesis XXII cycle. Department of Earth, Environmental and Resources Sciences (DiSTAR), University of Naples Federico II, Naples, Italy.

Garcia-Fresca, B., 2009. Outcrop-constrained flow and transport models of reflux dolomitization. Unpublished PhD thesis. The University of Texas at Austin.

Garcia-Fresca, B., Jones, G.D., Xu, T., 2009. The apparent stratigraphic concordance of reflux dolomite: new insights from synsedimentary reactive transport models. AAPG Search and Discovery article # 50208.

Garcia-Fresca, B., Jones, G.D., 2011. Apparent stratigraphic concordance of reflux dolomite: New insight from high-frequency cycle scale synsedimentary reactive transport models. Carbonates Geochemistry: Reactions and processes in aquifers and reservoirs. Karst waters Institute special publication 16, 27-30.

Garvie-Lok, S.J., Varney, T.L., Katzenberg, M.A., 2004. Preparation of bone carbonate for stable isotope analysis: the effects of treatment time and acid concentration. Journal of Archaeological Science, 31, 763-776.

Gasparrini, M., Bechstadt, T., Boni, M., 2006. Massive hydrothermal dolomites in the southwestern Cantabarian Zone (Spain) and their relation to the Late Variscan evolution. Marine and Petroleum Geology, 23, 543-568.

Geske, A., Goldstein, R.H., Mavromatis, V., Richter, D.K., Buhl, D., Kluge, T., John, C.M., Immenhauser, A., 2015a. The magnesium isotope (d26Mg) signature of dolomites. Geochimica et Cosmochimica Acta 149, 131-151.

Geske, A., Lokier, S., Dietzel, M., Richter, D.K., Buhl, D., Immenhauser, A., 2015b. Magnesium isotope composition of sabkha porewater and related (Sub-) Recent stoichiometric dolomites, Abu Dhabi (UAE). Chemical Geology 393-394, 112-124.

Giorgioni, M., Iannace, A., D'Amore, M., Dati, F., Galluccio, L., Guerriero, V., Mazzoli, S., Parente, M., Strauss, C., Vitale, S., 2016. Impact of early dolomitization on multi-scale petrophysical heterogeneities and fracture intensity of low-porosity platform carbonates (Albian-Cenomanian, southern Apennines, Italy). Marine and Petroleum Geology, 73, 462–478. https://doi.org/10.1016/j.marpetgeo.2016.03.011

Girundo, M., 2016. Multiscalar analysis of calcareous-dolomitic successions: evaluation of the quantitative relationships between fracturing state and mechanical-textural characteristics of carbonate rocks. PhD thesis XXVII cycle. DiSTAR, University of Naples Federico II, Naples, Italy.

Glover, E.D., 1961. Method of solution of calcareous materials using the complexing agent, EDTA. J. Sediment. Petrol. 31(4), 622–626.

Glover, E.D., 1963. Addition to "Method of solution of calcareous materials using the complexing agent, EDTA". Journal of Sedimentary Research, 33(1), 227.

Goldsmith, J.R., Graf, D.L., 1958. Structural and compositional variations in some natural dolomites: The Journal of Geology, 66, 678–693. https://doi.org /10.1086 /626547.

Gomez-Rivas, E., Martin-Martin, J.D., Bons, P.D., Koehn, D., Griera, A., Travé, A., Llorens, M-G., Humphrey, E., Neilson, J., 2022. Stylolites and stylolite networks as primary controls on the geometry and distribution of carbonate diagenetic alterations. Marine and Petroleum Geology, 136, 105444.

Graziano, R., Raspini, A., 2015. Long- and short-term hydroclimatic variabilities in the Aptian Tethys: clues from the orbital chronostratigraphy of evaporite-rich beds in the Apennine carbonate platform (Mt. Faito, southern Italy). Palaeogeography, Palaeoclimatology, Palaeoecology, 418, 319-343. https:// doi.org/10.1016/j.palaeo.2014.11.021.

Gregg, J.M., Sibley, D.F., 1984. Epigenetic dolomitization and the origin of xenotopic dolomite texture. Journal of Sedimentary Petrology, 54(3), 0908-0931.

Gregg, J.M., 1985. Regional epigenetic dolomitization in the Bonneterre Dolomite (Cambrian), southeastern Missouri. *Geology*, *13*(7), 503–506. https://doi.org/10.1130/0091-7613(1985)13<503:REDITB>2.0.CO;2

Gregg, J.M., Howard, S.A., Mazzullo, S.J., 1992. Early diagenetic recrystallization of Holocene (<3000 years old) peritidal dolomites, Ambergris Cay, Belize. Sedimentology, 39, 143-160.

Gregg, J.M., Bish, D.L., Kaczmarek, S.E., Machel, H.G., 2015. Mineralogy, nucleation and growth of dolomite in the laboratory and sedimentary environment: A review. Sedimentology, 62, 1749-1769. Doi.10.1111/sed.12202.

Haas, J., Demény, A., 2002. Early dolomitization of Late Triassic platform carbonates in the Transdanubian Range (Hungary). Sedimentary Geology, 151, 225-242.

Haas, J., Budai, T., Győri, O., Czuppon, G., 2022. Development and dolomitization of Anisian isolated carbonate platforms in the Transdanubian Range, Hungary. Central European Geology, 65(1), 14-25.

Hardie, L.A., Bosellini, A., Goldhammer, R.K., 1986. Repeated subaerial exposure of subtidal carbonate platforms, Triassic, Northern Italy: evidence for high frequency sea-level oscillations on a 104 year scale. Paleoceanography, 1, 447-457.

Hardie, L.A., 1987. Perspectives - Dolomitization: a critical view of some current views. Journal of Sedimentary Petrology, 57(1), 166–183. https://doi.org/10.1306/212F8AD5-2B24-11D7-8648000102C1865D.

Hollis, C., Bastesen, E., Boyce, A., Corlett, H., Gawthorpe, R., Hirani, J., Rotevatn, A., Whitaker, F., 2017. Fault-controlled dolomitization in a rift basin. Geology, 45(3), 219-222.

Hsü, K.J., Siegenthaler, C., 1969. Preliminary experiments on hydrodynamic movement induced by evaporation and their bearing on the dolomite problem. Sedimentology, 12, 11-25.

Huang, K.-J., B. Shen, X.-G. Lang, W.-B. Tang, Y. Peng, S. Ke, A. J. Kaufman, H.-R. Ma, and F.-B. Li (2015), Magnesium isotopic compositions of the Mesoproterozoic dolostones: Implications for Mg isotopic systematics of marine carbonate, Geochim. Cosmochim. Acta, 164, 333–351.

Humphrey, J.D., 1988. Late Pleistocene mixing zone dolomitization, southeastern Barbados, West Indies. Sedimentology, 35, 327-348.

Iannace, A., 1991. Depositional environment and diagenetic processes in Upper Triassic carbonate successions of Lattari and Picentini mountains (Salerno). Unpublished PhD thesis, Department of Earth, Environmental and Resources Sciences (DiSTAR), University of Naples Federico II, Naples, Italy.

Iannace, A., 1993. Caratteri diagenetici dei carbonati di Piattaforma dell'Appennino Meridionale e loro implicazioni paleogeografiche. Rivista Italiana di Paleontologia e Stratigrafia 99, 57–80.

Iannace A., Parente M. and Zamparelli V., 2005a. The Upper Triassic platform margin facies of Southern Apennines and their Jurassic fate: state of the art. Boll. Soc. Geol. It., 124, 203-214.

Iannace A., Parente M. and Zamparelli V., 2005b. An early Jurassic submarine scarp in the Western Matese Mountains. Boll. Soc. Geol. It., 124 (4), 215-221.

Iannace, A., Galluccio, L., Guerriero, V., Mazzoli, S., Parente, M., Vitale, S., 2008. Dolomites within the Mesozoic carbonates of Southern Apennines (Italy): genetic models and reservoir implications. Rendiconti Online Della Societa` Geologica Italiana, Note Brevi 2, 109–114.

Iannace, A., Capuano, M., Galluccio, L., 2011. "Dolomites and dolomites" in Mesozoic platform carbonates of the Southern Apennines: Geometric distribution, petrography and geochemistry. Palaeogeography, Palaeoclimatology, Palaeoecology, 310(3–4), 324–339. https://doi.org/10.1016/j.palaeo.2011.07.025

Iannace, A., Frijia, G., Galluccio, L., Parente, M., 2014. Facies and early dolomitization in Upper Albian shallow-water carbonates of the southern Apennines (Italy): Paleotectonic and paleoclimatic implications. Facies, 60(1), 169–194. https://doi.org/10.1007/s10347-013-0362-4.

ISPRA, 2016. Carta Geologica d'Italia alla scala 1:50.000, foglio 466 "Sorrento".

Janssen, R., 2017. Isotope records in vertebrate fossils: from Cretaceous seas to Quaternary Sundaland. Unpublished PhD thesis, Vrije Universiteit Amsterdam.

Jadoul, F., Berra, F., Frisia, S., 1992. Stratigraphic and paleogeographic evolution of a carbonate platform in an extensional tectonic regime. The example of the Dolomia Principale in Lombardy (Italy). Riv. Ital. Paleont. Strat., 98, 29-44.

Jolivet, L., Faccenna, C., Goffé, B., Mattei, M., Rossetti, F., Brunet, C., Storti, F., Funiciello, R., Cadet, J.P., d'Agostino, N., Parra, T., 1998. Midcrustal shear zones in postorogenic extension: example from the northern Tyrrhenian Sea. Journal of Geophysical Research, 103 (B6), 12123–12160. https://doi.org/10.1029/97JB03616.

Jones, C.E., Jenkyns, H.C., Coe, A.L., Hesselbo, S.P., 1994. Strontium isotopic variations in Jurassic and Cretaceous seawater. Geochimica et Cosmochimica Acta, 58(14), 3061-3074.

Jones, C.E., Jenkyns, H.C., 2001. Seawater strontium isotopes, oceanic anoxic events, and seafloor hydrothermal activity in the Jurassic and Cretaceous. American Journal of Science, 301, 112-149.

Jones, G.D., Whitaker, F.F. Smart, P.L., Sanford, W.E., 2002. Fate of reflux brines in carbonate platforms. Geology, 30(4), 371-374. https://doi.org/10.1130/0091-7613(2002)030<0371

Jones, G.D., Smart, P.L., Whitaker, F.F., Rostron, B.J., Machel, H.G., 2003. Numerical modeling of reflux dolomitization in the Grosmont platform complex (Upper Devonian), Western Canada sedimentary basin. *AAPG Bulletin, 87*(8), 1273–1298.

Jones, G., Whitaker, F.F., Smart, P.L., Sanford, W.E., 2004. Numerical analysis of seawater circulation in carbonate platforms: II. The dynamic interaction between geothermal and brine reflux circulation. Amer. J. Sci. 304, 250-284.

Jones, B., 2005. Dolomite crystal architecture: genetic implications for the origin of the tertiary dolostones of the Cayman Islands. Journal of Sedimentary Research, 75(2), 177-189.

Jones, G.D., Xiao, Y., 2005. Dolomitization, anhydrite cementation, and porosity evolution in a reflux system: Insights from reactive transport models. American Association of Petroleum Geologists Bulletin, 89, 577-601. https:// doi.org/10.1306/12010404078.

Kaczmarek, S.E., Sibley, D.F., 2011. On the evolution of dolomite stoichiometry and cation order during high-temperature synthesis experiments: An alternative model for the geochemical evolution of natural dolomites. Sedimentary Geology, 240, 30-40. Doi:10.1016/j.sedgeo.2011.07.003

Kaczmarek, S.E., Sibley, D.F., 2014. Direct physical evidence of dolomite recrystallization. Sedimentology, 61, 1862-1882.

Kaczmarek, S.E., Thornton, B.P., 2017. The effect of temperature on stoichiometry, cation ordering, and reaction rate in high-temperature dolomitization experiments. Chemical Geology, 468, 32-41.

Kaczmarek, S.E., Gregg, J.M., Bish, D.L., Machel, H.G., Fouke, B.W., 2017. Dolomite, very high-magnesium calcite, and microbes – implications for the microbial model of dolomitization. In: Macneil, A.J., Lonnee, J., Wood, R. (eds.), Characterization and modeling of carbonates-Mountjoy Symposium 1. SEPM special publication 109, p. 7-20. Doi:10.2120/sepmsp.109.01

Kaufman, J., 1994. Numerical models of fluid flow in carbonate platforms: implications for dolomitization. Journal of Sedimentary Research, A64, 128-139.

Kim, S-T., Coplen, T.B., Horita, J., 2015. Normalization of stable isotope data for carbonate minerals: Implementation of IUPAC guidelines. Geochimica et Cosmochimica Acta, 158, 276-289.

Kim, J., Kimura, Y., Puchala, B., Yamazaki, T., Becker, U., Sun, W., 2023. Dissolution enables dolomite crystal growth near ambient conditions. Science, 382, 915-920.

Knott, S.D., 1987. The Liguride complex of southern Italy-A Cretaceous to Paleogene accretionary wedge. Tectonophysics 142 (2–4), 217–226.

Krause, S., Liebetrau, V., Gorb, S.N., Sánchez-Román, M., McKenzie, J.A., Treude, T., 2012. Microbial nucleation of Mg-rich dolomites in exopolymeric substances (EPS) under anoxic modern seawater salinity: new insight into an old enigma. Geology, 40, 587-590.

Kylander-Clark, A.R.C., 2020. Expanding the limits of laser-ablation U–Pb calcite geochronology. Geochronology, 2(2), 343-354.

Kyser, T.K., James, N.P., Bone, Y., 2002. Shallow burial dolomitization and dedolomitization of Cenozoic cool-water limestones, southern Australia: geochemistry and origin. Journal Sedimentary Research, 72 (1), 146–157.

Land, L.S., Salem, M., Morrow, D., 1975. Paleohydrology of ancient dolomites: geochemical evidence. American Association of Petroleum Geologists Bulletin, 59, 1602-1625.

Land, L.S., 1985. The origin of massive dolomite. *Journal of Geological Education*, *33*(2), 112–125. https://doi.org/10.5408/0022-1368-33.2.112.

Lavoie, D., Chi, G., Urbatsch, M., Davis, W. J., 2010. Massive dolomitization of a pinnacle reef in the Lower Devonian West Point Formation (Gaspé Peninsula, Quebec): An extreme case of hydrothermal dolomitization through fault-focused circulation of magmatic fluids. AAPG bulletin, 94(4), 513-531.

Laya, J.C., Teoh, C.P., Whitaker, F., Manche, C., Kaczmarek, S., Tucker, M., Gabellone, T., Hasiuk, F., 2021. Dolomitization of a Miocene-Pliocene progradational carbonate platform by mesohaline brines: Re-examination of the reflux model on Bonaire Island. Marine and Petroleum Geology, 126, 104895.

Leighton, M.W., Pendexter, C., 1962. Carbonate rock types. In: Classification of carbonate rocks, Ham, W.E. (Ed.). American Association of Petroleum Geologists Memoir 1, 33-61.

Lirer, F., Persico, D., Vigorito, M., 2005. Calcareous plankton biostratigraphy and age of the middle Miocene deposits of Longano Formation (eastern Matese Mountains, southern Apennines). Riv. Ital. Paleontol. Stratigr., 111, 91-108.

Li, S., Schauer, A., Licht, A., Liang, J., Huntington, K., Peng, K., 2023. Clumped isotope analysis of calcite and dolomite mixtures using selective acid extraction. Journal of Earth Science, 34(3), 726-734.

Li, X., Zhu, G., Li, T., Zhou, L., Wu, Y., Shen, B., Ning, M., 2023. Conservative behavior of Mg isotopes in dolomite during diagenesis and hydrothermal alteration: A case study in the Lower Cambrian Qiulitage Formation, Gucheng area, Tarim Basin. Applied Geochemistry, 148, 105540.

Liu, X., Deng, W., Wei, G., 2019. Carbon and oxygen isotopic analyses of calcite in calcite–dolomite mixtures: optimization of selective acid extraction. Rapid Commun. Mass Spectrom. 33 (5), 411–418.

Liu, D., Xu, Y., Papineau, D., Yu, N., Fan, Q., Qiu, X., Wang, H., 2019. Experimental evidence for abiotic formation of low-temperature proto-dolomite facilitated by clay minerals. Geochimica et Cosmochimica Acta, 247, 83-95.

Lucia, J.F., 1995. Rock-fabric/petrophysical classification of carbonate pore space for reservoir characterization. Bulletin of American Association of Petroleum Geologists, 79, 1275–1300. https://doi.org/10.1306/7834D4A4-1721-11D7-8645000102C1865D

Lu, P., Cantrell, D., 2016. Reactive transport modelling of reflux dolomitization in the Arab-D reservoir, Ghawar field, Saudi Arabia. Sedimentology, 63, 865–892.

Lu, C., Swart, P.K., 2024. The application of dual clumped isotope thermometer (Δ_{47} and Δ_{48}) to the understanding of dolomite formation. Geology, 52(1), 56-60.

Lumsden, D.N., 1979. Discrepancy between thin-section and X-ray estimates of dolomite in limestone. Journal of Sedimentary Research, 49, 429–436. https://doi.org/10.1306/212F7761-2B24-11D7-8648000102C1865D.

Lumsden, D.N., Chimahusky, J.S., 1980. Relationship between dolomite nonstoichiometry and carbonate facies parameters. In: Zenger, D.H., Dunham, J.B., Ethington, R.L. (eds.), Concepts and models of dolomitization. SEPM Special publication 28, p. 123-137. Doi:10.2110/pec.80.28.0123

Lyons, W.B., Hines, M.E., Gaudette, H.E., 1984. Major and minor element pore water geochemistry of modern marine sabkhas: the influence of cyanobacterial mats. In Cohen, Y., Castenholz, R. W., and Halvorson, H. O., (eds.), Microbial mats, New York: A. R. Liss, pp. 411-423.

Machel, H.G., Burton E.A., 1994. Golden Grove Dolomite, Barbados; origin from modified seawater. Journal of Sedimentary Research, 64(4a), 741-751.

Machel, H.G., 2002. The dolomite problem – quo vadis? In: Hüssner, H., Hindered, M., Gotz, A.E., Petschick, R. (eds.), SEDIMENT 2002, 17. Sedimentologentreffen, Frankfurt a.M./Darmstadt, 29-31. Mai 2002, Kurzfassungen und Programm. Schr. Deutsch. Geol. Ges., 17, pp. 135-140.

Machel, H.G., Lonnee, J., 2002. Hydrothermal dolomite—a product of poor definition and imagination. Sedimentary Geology 152(3-4), 163-171.

Machel, H.G., 2004. Concepts and models of dolomitization: a critical reappraisal. In: The Geometry and Petrogenesis of Dolomite Hydrocarbon Reservoirs, Braithwaite CJR, Rizzi G, Darke G (eds.). Geological Society, London, Special Publications, 235, 7-63.

Machel, H.G., 2005. Sedimentary rocks / Dolomites. In I. R. P. Richard C. Selley, L. Robin M. Cocks (Ed.), *Encyclopedia of Geology* (pp. 79–94). Elsevier. https://doi.org/10.1016/B0-12-369396-9/00308-7.

Manche, C.J., Kaczmarek, S.E., 2019. Evaluating reflux dolomitization using a novel high-resolution record of dolomite stoichiometry: A case study from the Cretaceous of central Texas, USA. *Geology*, *47*(6), 586–590. https://doi.org/10.1130/G46218.1.

Manche, C.J., 2021. Dolomite stoichiometry as a proxy for fluid chemistry. Unpublished PhD thesis 3705, Western Michigan University, United States of America (USA).

Mansurbeg, H., Alsuwaidi, M., Salih, N., Shahrokhi, S., Morad, S., 2021. Integration of stable isotopes, radiometric dating and microthermometry of saddle dolomite and host dolostones (Cretaceous carbonates, Kurdistan, Iraq): New insights into hydrothermal dolomitization. Marine and Petroleum Geology, 127, 104989.

Mansurbeg, H., Alsuwaidi, M., Morad, D., Morad, S., Tiepolo, M., Shahrokhi, S., Al-Aasm, I.S., Koyi, H., 2024. Disconformity-controlled hydrothermal dolomitization and cementation during basin evolution: Upper Triassic carbonates, UAE. Geology, 52, 486-491. https://doi.org/10.1130/G51990.1

Mastandrea, A., Perri, E., Russo, F., Spadafora, A., Tucker, M., 2006. Microbial primary dolomite from a Norian carbonate platform: northern Calabria, southern Italy. Sedimentology, 53, 465-480.

Martin-Martin, J.D., Gomez-Rivas, E., Gómez-Gras, D., Travé, A., Ameneiro, R., Koehn, D., Bons, P.D., 2018. Activation of stylolites as conduits for overpressured fluid flow in dolomitized platform carbonates. Geological Society of London Special Publication, 459, 157-176.

Massaro, L., Corradetti, A., Vinci, F., Tavani, S., Iannace, A., Parente, M., Mazzoli, S., 2018. Multiscale fracture analysis in a reservoir-scale carbonate platform exposure (Sorrento Peninsula, Italy): Implications for fluid flow. Geofluids. https://doi.org/10.1155/2018/7526425

Matsumoto, R., Matsuda, H., 1988. Occurrence, chemistry and isotopic composition of carbonate concretions in the Miocene to Pliocene siliceous sediments of Aomori, northeast Japan. J. Facul. Sci. 21 (4), 351–377. University of Tokyo, Section 2: Geology, Mineralogy, Geography, Geophysics.

Mazzullo, S.J., Bischoff, W.D., Teal, C.S., 1995. Holocene shallow-subtidal dolomitization by near-normal seawater, northern Belize. Geology, 23(4), 341-344.

Mazzoli, S., Corrado, S., De Donatis, M., Scrocca, D., Butler, R., Di Bucci, D., Naso, G., Nicolai, C., Zucconi, V., 2000. Time and space variability of ‘‘thin-skinned’’ and ‘‘thick-skinned’’ thrust tectonics in the Apennines (Italy). Rend. Fis. Accad. Lincei., 11(1), 5-39.

Mazzoli, S., D'Errico, M., Aldega, L., Corrado, S., Invernizzi, C., Shiner, P., Zattin, M., 2008. Tectonic burial and "young" (<10 Ma) exhumation in the southern Apennines fold-and-thrust belt (Italy). Geology, 36, 243-246.

McArthur, J.M., Howarth, R.J., Shields, G.A., Zhou, Y., 2020. Strontium isotope stratigraphy, Chapter 7, p211 – p238. In: Gradstein F.M., Ogg J.G., Schmitz M.D. and Ogg G.M. A Geologic Time Scale, Elsevier B.V., Vol 1 of 2, 1357 pp, 2020.

McCormik, C.A., Corlett, H., Roberts, N.M.W., Johnston, P.A., Collom, C.J., Stacey, J., Koeshidayatullah, A., Hollis, C., 2024. U-Pb geochronology reveals that hydrothermal dolomitization was coeval to the deposition of the Burgess Shale lagerstätte. Communications earth and environment, 5, 318.

McKenzie, J.A., Hsü, K.J., Schneider, J.F., 1980. Movement of subsurface waters under the sabkha, Abu Dhabi, UAE, and its relation to evaporative dolomite genesis. In: Zenger, D.H., Dunham, J.B., Ethington, R.L. (eds.), Concepts and models of dolomitization. Society of Economic Paleontologists and Mineralogists Special Publication No. 28., pp. 11-30.

McKenzie, J.A., 1981. Holocene dolomitization of calcium carbonate sediments from the coastal sabkhas of Abu Dhabi, U.A.E.: a stable isotope study. Journal of Geology, 89, 185-198.

Menardi Noguera, A., Rea, G., 2000. Deep structure of the Campanian–Lucanian arc (southern Apennine, Italy). Tectonophysics 324 (4), 239–265. https://doi.org/10.1016/S0040-1951(00)00137-2.

Montañez, I.P., Read, J.F., 1992. Eustatic control on early dolomitization of cyclic peritidal carbonates: Evidence from the Early Ordovician Upper Know Group, Appalachians. Geological Society of America Bulletin, 104, 872-886.

Moore, D.M., Reynolds, R.C., 1997. X-ray Diffraction and the Identification and Analysis of Clay Minerals. Oxford Univ. Press, Oxford, New York.

Morad, S., Farooq, U., Mansurbeg, H., Alsuwaidi, M., Morad, D., Al-Aasm, I.S., Shahrokhi, S., Hozayen, M., Koyi, H., 2023. Variations in extent, distribution and impact of dolomitization on reservoir quality of Upper Cretaceous foreland-basin carbonates, Abu Dhabi, United Arab Emirates. Marine and Petroleum Geology, 155, 106357.

Morrow, D.W., 1982. Diagenesis 2. Dolomite - Part 2: Dolomitization models and ancient dolostones. Geoscience Canada, v.9(2), p.95-107.

Morse, J.W., Arvidson, R.S., 2002. The dissolution kinetics of major sedimentary carbonate minerals. Earth-Science Reviews, 58, 51-84.

Mozafari, M., Swennen, R., Balsamo, F., El Desouky, H., Storti, F., Taberner, C., 2019. Fault-controlled dolomitization in the Montagna dei Fiori Anticline (Central Apennines, Italy): record of a dominantly pre-orogenic fluid migration. Solid Earth, 10, 1355-1383.

Muir, M., Lock, D., Borch, C.V.D., 1980. The Coorong model for penecontemporaneous dolomite formation in the Middle Proterozoic McArthur Group, Northern Territory, Australia. In D. H. Zenger, J. B. Dunham, & R. L. Ethington (Eds.), *Concepts and models* *of dolomitization* (SEPM Speci, pp. 51–67). The Society of Economic Paleontologists and Mineralogists.

Müller, I.A., Rodriguez-Blanco, J.D., Storck, J.C., Santilli do Nascimento, G., Bontognali, T.R.R., Vasconcelos, C., Benning, L.G., Bernasconi, S.M., 2019. Calibration of the oxygen and clumped isotope thermometers for (proto-) dolomite based on synthetic and natural carbonates. Chemical Geology, 525, 1-17.

Muñoz-López, D., Lu, C., Li, W., Corlett, H., Hollis, C., Swart, P.K., Koeshidayatullah, A., 2024. What is the source of magnesium in hydrothermal dolomites? New insights from coupling $\delta^{26}Mg$ – Δ_{47} isotopes. Earth and Planetary Science Letters, 638, 118760.

Murray, R.C., 1964. Preservation of primary structures and fabrics in dolomite. In: Imbrie, J., Newell, N. (eds.), Approaches to paleoecology, p. 388-403. John Wiley and Sons, Inc.

Murgia, M.V., Ronchi, P., Ceriani, A., 2004. Dolomitization processes and their relationships with the evolution of an orogenic belt (central Apennines and periAdriatic foreland, Italy). In: Swennen, R., Roure, F., Granath, J.W. (Eds.), Deformation, Fluid Flow, and Reservoir Appraisal in Foreland Fold and Thrust Belts: AAPG Hedberg Series, 1, pp. 277–294.

Mutti, M., Simo, J.A., 1994. Distribution, petrography and geochemistry of early dolomite in cyclic shelf facies, Yates Formation (Guadalupian), Capitan Reef Complex, USA. International Association of Sedimentologists special publication 21, 91-107.

Nagy, Z.S.R., Gregg, J.M., Shelton, K.L., Becker, S.P., Somerville, I.D., Johnson, A.W., 2004. Early dolomitization and fluid migration through the Lower Carboniferous carbonate platform in the SE Irish Midlands: implications for reservoir attributes. In: Braithwaite, C.J.R., Rizzi, G., Darke, G. (eds.), The geometry and petrogenesis of Dolomite hydrocarbon reservoirs. Geological Society, London, Special Publications, 235, 367-392.

Nayebi, N., Esmaeily, D., D'Antonio, M., Xia, X., Renzo, V. D., Lehmann, B., Shinjo, R., Babazadeh, S., Deevsalar, R., Modabberi, S., 2023. Zircon U–Pb ages and Sr–Nd–Pb–Hf isotopic compositions constrain the tectono-magmatic evolution of the Anomaly 21-A iron ore region, Bafq metallogenic province, Central Iran. Journal of Asian Earth Sciences. 250, 105646.

Ning M, Huang K, Lang X, Ma H, Yuan H, Peng Y, Shen B (2019). Can crystal morphology indicate different generations of dolomites? Evidence from magnesium isotopes. Chemical Geology, 516, 1-17.

Nuriel, P., Wotzlaw, J.F., Ovtcharova, M., Vaks, A., Stremtan, C., Šala, M., Roberts, N.M.W., Kylander-Clark, A.R.C., 2021. The use of ASH-15 flowstone as a matrix-matched reference material for laser-ablation U-Pb geochronology of calcite, Geochronology, 3, 35-47, 10.5194/gchron-3-35-2021.

Özkan, A. M., 2019. Geochemical Features of Rare Earth Elements in the Dolomites of the Bozdağ Formation (Early Silurian–Middle Devonian) from Söğütözü-Ladik (Konya/Turkey) Area. The International Journal of Engineering and Science, 8(8), Series I, 30-46.

Pagel, M., Bonifacie, M., Schneider, D. A., Gautheron, C., Brigaud, B., Calmels, D., Cros, A., Saint-Bezar, B., Landrein, P., Sutcliffe, C., Davis, D., Chaduteau, C., 2018. Improving paleohydrological and diagenetic reconstructions in calcite veins and breccia of a sedimentary basin by combining Δ47 temperature, δ18Owater and U-Pb age. Chemical Geology, 481, 1-17, https://doi.org/10.1016/j.chemgeo.2017.12.026.

Palladino, G., Parente, M., Prosser, G., Di Staso, A., 2008. Tectonic control on the deposition of the Lower Miocene sediments of the Monti della Maddalena ridge (Southern Apennines): synsedimentary extensional deformation in a foreland setting. Italians Journal of Geosciences, 127(2), 317-335.

Parente, M., Amodio, S., Iannace, A., Sabbatino, M., 2022. Stratigraphy and facies of the Apennine Carbonate Platform (southern Italy): the record of Mesozoic OAEs and Miocene transgression. Geological Field Trips and Maps (Periodical of ISRPA and Geological Society of Italy), 14.

Perri, E., Tucker, M., 2007. Bacterial fossils and microbial dolomite in Triassic stromatolites. Geology, 35(3), 207-210.

Patacca, E., Scandone, P., 2007. Geology of Southern Apennines. Italian Journal of Geosciences, 7, 75-119.

Petersen, G.W., Chesters, G., 1966. Quantitative determination of calcite and dolomite in pure carbonates and limestones. European Journal of Soil Science, 17, 317-327.

Petrash, D.A., Bialik, O.M., Bontognali, T.R.R., Vasconcelos, C., Roberts, J.A., McKenzie, J.A., Konhauser, K.O., 2017. Microbially catalyzed dolomite formation: From near-surface to burial: Earth-Science Reviews, 171, 558-582. Doi:10.1016/j.earscirev.2017.06.015

Pierattini, D., Scandone, P., Cortini, M., 1975. Eta' di Messa in posto ed eta' di metamorfismo delle limburgiti Nord Calabresi. Boll. Soc. Geol. It., 94, 367-376.

Pina, C.M., Pimentel, C., Crespo, A., 2022. The Dolomite Problem: A matter of time. American Chemical Society (ACS) Earth and Space Chemistry, 6, 1468-1471.

Pina, C.M., Pimentel, C., Crespo, A., 2024. Comment on the article Dissolution enables dolomite crystal growth near ambient conditions by Kim et al. 2023. eLetters, Science.

Pleydell, S.M., Jones, B., Longstaffe, F.J., Baadsgaard, H., 1990. Dolomitization of the oligocene–miocene bluff formation on grand Cayman, British west Indies. Can. J. Earth Sci. 27 (8), 1098–1110.

Petro, N., 2015. Primary dolomite in the Late Triassic Travenanzes Foramtion, Dolomites, Northern Italy: Facies control and possible bacterial influence. Sedimentology, 62, 697-716.

Pollitt, D.A., Anthonissen, E., Saller, A.H., BouDagher-Fadel, M.K., Dickson, J.A.D., 2012. Abrupt early Eocene global climatic change as a control of carbonate facies and diagenesis: a new record of the Paleocene-Eocene Thermal Maximum in the Umm er Radhuma Formation, Saudi Arabia and Kuwait. Terra Nova, 24, 487-498.

Qing., H., Bosence, D.W.J., Rose, E.P.F., 2001. Dolomitization by penesaline sea water in Early Jurassic peritidal platform carbonates, Gibraltar, western Mediterranean. Sedimentology, 48, 153-163.

Rameil, N., 2008. Early diagenetic dolomitization and dedolomitization of Late Jurassic and earliest Cretaceous platform carbonates: A case study from the Jura Mountains (NW Switzerland, E France). Sedimentary Geology, 212(1-4), 70-85.

Raspini, A., 2001. Stacking pattern of cyclic carbonate platform strata: Lower Cretaceous of southern Apennines, Italy. Journal of the Geological Society, London, 158, 353-366.

Raspini, A., 2012. Shallow water carbonate platforms (Late Aptian-Early Albian, Southern Apennines) in the context of supraregional to global changes: re-appraisal of palaeoecological events as reflectors of carbonate factory response. Solid Earth, 3, 225-249.

Ray, J.S., Ramesh, R., 1998. Stable carbon and oxygen isotope analysis of natural calcite and dolomite mixtures using selective acid extraction. J. Geol. Soc. India 52 (3), 323–332.

Read, J.F., Husinec, A., Cangialosi, M., Loehn, C.W., Prtoljan, B., 2016. Climate controlled, fabric destructive, reflux dolomitization and stabilization via marine- and synorogenic mixed fluids: an example from a large Mesozoic, calcite-sea platform, Croatia. Palaeogeography, Palaeoclimatology, Palaeoecology 449:108–126. https://doi.org/10.1016/j.palaeo.2016.02.015

Ren, M., Jones, B., 2017. Spatial variations in the stoichiometry and geochemistry of Miocene dolomite from Grand Cayman: Implications for the origin of island dolostone. Sedimentary Geology, 348, 69-93. Doi:10.1016/j.sedgeo.2016.12.001

Riechelmann, S., Mavromatis, V., Buhl, D., Dietzel, M., Immenhauser, A., 2020. Controls on formation and alteration of early diagenetic dolomite: A multi-proxy δ44/40Ca, δ 26Mg, δ18O and δ13C approach. Geochimica et Cosmochimica Acta, 283, 167-183. DOI: 10.1016/j.gca.2020.06.010. hal-03373097

Rivers, J.M., Kyser, T.K., James, N.P., 2012. Salinity reflux and dolomitization of southern Australian slope sediments: the importance of low carbonate saturation levels. Sedimentology, 59. 445-465.

Robertson, A.H.F., Clift, P.D., Degnan, P.J., Jones, G., 1991. Palaeogeographic and palaeotectonic evolution of the eastern Mediterranean Neotethys. Palaeogeogr. Palaeoclimatol. Palaeoecol. 87 (1–4), 289–343. https://doi.org/10.1016/0031-0182(91)90140-M.

Roberts, N.M., Rasbury, E.T., Parrish, R.R., Smith, C.J., Horstwood, M.S., Condon, D.J., 2017. A calcite reference material for LA-ICP-MS U-Pb geochronology. Geochemistry, Geophysics, Geosystems, 18(7), 2807-2814.

Robson, J., 1987. Depositional models for some Cretaceous carbonates from the Sorrento Peninsula, Italy. Memorie Della Società Geologica Italiana 40, 251–257.

Ronchi, P., Casaglia, F., Ceriani, A., 2003. The multiphase dolomitization of the Liassic Calcare Massiccio and Corniola succession (Montagna dei Fiori, Northern Apennines, Italy). Bollettino della Societa Geologica Italiana 122, 157–172.

Ronchi, P., Jadoul, F., Ceriani, A., Di Giulio, A., Scotti, P., Ortenzi, A., Previde Massara, E., 2011. Multistage dolomitization and distribution of dolomitized bodies in Early Jurassic carbonate platforms (Southern Alps, Italy). Sedimentology 58:532–565. https://doi.org/10.1111/j.1365-3091.2010.01174.x

Rosen, M.R., Holdren G.R., 1986. Origin of dolomite cement in Chesapeake Group (Miocene) siliciclastic sediments: an alternative model to burial dolomitization. Journal of Sedimentary Petrology, 56(6), 788-798.

Rosen, M.R., Miser, D.E., Starcher, M.A., Warren, J.K., 1989. Formation of dolomite in the Coorong region, South Australia. Geochimica et Cosmochimica Acta, 53, 661-669.

Royse, C.F., Wadell, J.S., Petersen, L.E., 1971. X-ray determination of calcite-dolomite; an evaluation. Journal of Sedimentary Research, 41, 483-488. Doi: 10.1306/74D722a7-1012B21-11D7-8648000102C1865D.

Ruiz-Agudo, E., Putnis, C.V., Putnis, A., 2014. Coupled dissolution and precipitation at mineral-fluid interfaces. Chemical Geology, 383, 132–146. https://doi.org/10.1016/j.chemgeo.2014.06.007

Rustichelli, A., Iannace, A., Tondi, E., Di Celma, C., Cilona, A., Giorgioni, M., Parente, M., Girundo, M., Invernizzi, C., 2017. Fault-controlled dolomite bodies as palaeotectonic indicators and geofluid reservoirs: New insights from Gargano Promontory outcrops. Sedimentology, 64(7), 1871-1900.

Ryan, B.H., Kaczmarek, S.E., Rivers, J.M., 2019. Dolomite dissolution: An alternative diagenetic pathway for the formation of palygorskite clay. Sedimentology, 66, 1803-1824. DOI: 10.1111/sed.12559

Ryan, B.H., Kaczmarek, S.E., Rivers, J.M., 2020. Early and pervasive dolomitization by near-normal marine fluids: New lessons from an Eocene evaporative setting in Qatar. Sedimentology, 67, 2917-2944.

Ryan, B.H., Kaczmarek, S.E., Rivers, J.M., Manche, C.J., 2022. Extensive recrystallization of Cenozoic dolomite during shallow burial: A case study from the Palaeocene-Eocene Umm er Radhuma Formation and a global meta-analysis. Sedimentology, 69, 2053-2079.

Sabbatino, M., Vitale, S., Tavani, S., Consorti, L., Corradetti, A., Cipriani, A., Arienzo, I., Parente, M., 2020. Constraining the onset of flexural subsidence and peripheral bulge extension in the Miocene foreland of the southern Apennines (Italy) by Sr-isotope stratigraphy. Sedimentary Geology, 401, 105634.

Sabbatino, M., Tavani, S., Vitale, S., Ogata, K., Corradetti, A., Consorti, L., Arienzo, I., Cipriani, A., Parente, M., 2021. Forebulge migration in the foreland basin system of the central-southern Apennine fold-thrust belt (Italy): New high-resolution Sr-isotope dating constraints. Basin Research, 33, 2817-2836. DOI: 10.1111/bre.12587.

Sadooni, F.N., Howari, F., El-Saiy, A., 2010. Microbial dolomites from carbonate-evaporite sediments of the coastal sabkha of Abu Dhabi and their exploration implications. Journal of Petroleum Geology, 33(4), 289-298.

Salas, J., Taberner, C., Esteban, M., Ayora C., 2007. Hydrothermal dolomitization, mixing corrosion and deep burial porosity formation: numerical results from 1-D reactive transport models. Geofluids, 7, 99-111.

Saller, A.H., 1984. Petrologic and geochemical constraints on the origin of subsurface dolomite: Enewetak Atoll: an example of dolomitization by normal seawater. Geology, v.12, p.217-220.

Saller, A.H., Henderson, N., 1998. Distribution of porosity and permeability in platform dolomites: insight from the Permian of West Texas. Am. Assoc. Pet. Geol. Bull., 82, 1528-1550.

Saller, A.H., Henderson, N., 2001. Distribution of porosity and permeability in platform dolomites: Insight from the Permian of west Texas: Reply. AAPG Bulletin, 85(3), 530-532.

Saller, A.H., Pollitt, D.A., Dickson, J.A.D., 2014. Diagenesis and porosity development in the First Eocene reservoir at the giant Wafra Field, Partitioned Zone, Saudi Arabia and Kuwait. AAPG Bulletin, 98, 1185-1212.

Salih, N., Mansurbeg, H., Kolo, K., Gerdes, A., Préat, A., 2019. In situ U-Pb dating of hydrothermal diagenesis in tectonically controlled fracturing in the Upper Cretaceous Bekhme Formation, Kurdistan, Region-Iraq. International Geology Review, DOI: 10.1080/00206814.2019.1695151

Salomon, E., Rotevatn, A., Kristensen, T.B., Grundvåg, S.A., Henstra, G.A., Meckler, A.N., Albert, R., Gerdes, R., 2020. Fault-controlled fluid circulation and diagenesis along basin-bounding fault systems in rift – insights from the East Greenland rift system. Solid Earth, 11, 1987-2013.

Sánchez-Román, M., Vasconcelos, C., Schmid, T., Dittrich, M., McKenzie, J.A., Zenobi, R., Rivadeneyra, M.A., 2008. Aerobic microbial dolomite at the nanometer scale: Implication for the geologic record. Geology, 36(11), 879-882.

Sánchez-Román, M., McKenzie, J.A., Wagener, A.L.R., Romanek, C.S., Sánchez-Navas, A., Vasconcelos, C., 2011. Experimentally determined biomediated Sr partition coefficient for dolomite: Significance and implication for natural dolomite. Geochimica et Cosmochimica Acta, 75, 887-904.

Santantonio, M., Carminati, E., 2011. Jurassic rifting evolution of the Apennines and southern Alps (Italy): Parallels and differences. Geol. Soc. Am. Bull. 123 (3–4), 468–484. https://doi.org/10.1130/B30104.1

Sartori, R., Carrara, G., Torelli, L., Zitellini, N., 2001. Neogene evolution of the southwestern Tyrrhenian Sea (Sardinia basin and western Bathyal plain). Mar. Geol. 175, 47–66. https://doi.org/10.1016/S0025-3227(01)00116-5.

Scrocca, D., Carminati, E., Doglioni, C., 2005. Deep structure of the southern Apennines, Italy: Thin-skinned or thick-skinned? Tectonics, 24, TC3005.

Selli, R., 1962. Il Paleogene nel quadro della geologia dell'Italia Meridionale. *Memorie Della Società Geologica Italiana*, 3, 733–789.

Servizio Geologico D'Italia, 2015. Carta Geologica d'Italia alla scala 1:50,000, Fogli 466-485, Sorrento-Termini. Istituto Superiore per la Protezione e la Ricerca Ambientale (ISPRA).

Shalev, N., Bontognali, T.R.R., Vance, D., 2021. Sabkha dolomite as an archive for the magnesium isotope composition of seawater. Geology, 49, 253-257.

Sharp, I., Gillespie, P., Morsalnezhad, D., Taberner, C., Karpuz, R., Verges, J., Horboury, A., Pickard, N., Garland, J., Hunt, D., 2010. Stratigraphic architecture and fracture-controlled dolomitization of the Cretaceous Khami and Bangestan groups: an outcrop case study, Zagros mountains, Iran. Geological Society, London, Special publications, 329(1), 343-396.

Shinn, E.A., Ginsburg, R.N., Lloyd, R.M., 1965. Recent supratidal dolomite from Andros Island, Bahamas. In: Dolomitization and Limestone Diagenesis, Pray, L.C., Murray, R.C. (eds.), SEPM Special Publication 13, 112-123.

Shiner, P., Beccacinia, A., Mazzoli, S., 2004. Thin-skinned versus thick-skinned structural models for Apulian carbonate reservoirs: constraints from the Val d'Agri fields, S Apennines, Italy. Marine and Petroleum Geology, 21, 805-827.

Sibley, D.F., 1980. Climatic control of dolomitization, Seroe Domi Formation (Pliocene), Bonaire, N.A. SEPM Special Publication no. 28, 247-258.

Sibley, D.F., 1982. The origin of common dolomite fabrics: Clues from the Pliocene. Journal of Sedimentary Research, 52, 1087-1100.

Sibley, D.F., Gregg, J.M., 1987. Classification of dolomite rock textures. Journal of Sedimentary Petrology, 57(6), 967–975. https://doi.org/10.1306/212f8cba-2b24-11d7-8648000102c1865d

Sibley, D.F., Dedoes, R.E., Bartlett, T.R., 1987. Kinetics of dolomitization. Geology, 15, 1112-1114.

Sibley, D.F., 1990. Unstable to stable transformations during dolomitization. Journal of Geology, 98, 739-748.

Sibley, D.F., Gregg, J.M., Brown, R.G., Laudon, P.R., 1993. Chapter 15: Dolomite crystal size distribution. In: Carbonate Microfabrics, Rezak R et al. (eds.), Springer-Verlag New York, Inc.

Sibley, D.F., Nordeng, S.H., Borkowski, M.L., 1994. Dolomitization kinetics in hydrothermal bombs and natural settings. Journal of Sedimentary Research, A64(3), 630-637.

Simms, M.A., 1984. Dolomitization by groundwater-flow systems in carbonate platforms. Transactions of the Gulf Coast Association of Geological Societies, 34, 411-420.

Skippington, J., Veth, P., Manne, T., Slack, M., 2019. Preanalytical processing of archaeological mammal enamel apatite carbonates for stable isotope investigations: A comparative analysis of the effect of acid treatment on samples from Northwest Australia. International Journal of Osteoarchaeology, 29, 760-771.

Smith, D.B., 1981. Bryozoan-algal patch reefs in the Upper Permian Magnesian limestones of Yorkshire, Northeast England. in: TOOMEY, D.F. (ed) European Fossil Reef Models. Society of Economic Paleontologists and Mineralogists Special Publication, v.33, p.187-202.

Smith, L.B., Jr., Eberli, G.P., Sonnenfeld, M.D., 2004. Sequence-stratigraphic and paleogeographic distribution of reservoir-quality dolomite, Madison Formation, Wyoming and Montana. In: Grammer, G.M., Eberli, G.P., Harris, P.M. (eds.), Integration of outcrop and modern analogs in reservoir modeling: American Association of Petroleum Geologists Memoir 80, p. 94-118.

Snoek, C., Pellegrini, M., 2015. Comparing bioapatite carbonate pre-treatments for isotopic measurements: Part 1-impact on structure and chemical composition. Chemical Geology, 417, 394-403.

Sperber, C.M., Wilkinson, B.H., Peacor, D.R., 1984. Rock composition, dolomite stoichiometry, and rock/water reactions in dolomitic carbonate rocks. Journal of Geology, 92(6), 609-621.

Sreenivasan, S.P., Bera, M.K., Samanta, A., 2023. A simple but improved protocol for measuring carbon and oxygen isotope ratios of calcite in calcite-dolomite mixtures. Applied Geochemistry, 150, 105600.

Sun, S.Q., 1994. A reappraisal of dolomite abundance and occurrence in the Phanerozoic. Journal of Sedimentary Research, A64, 396-404.

Sun, S.Q., 1995. Dolomite reservoirs: Porosity evolution and reservoir characteristics. Bulletin of American Association of Petroleum Geologists, 79(2), 186-204.

Swart, P.K., Melim, L.A., 2000. The origin of dolomites in Tertiary sediments from the margin of Great Bahama Bank. Journal of Sedimentary Research, 70(3), 738-748.

Tavani, S., Iannace, A., Mazzoli, S., Vitale, S., Parente, M., 2013. Late Cretaceous extensional tectonics in Adria: Insights from soft-sediment deformation in the Sorrento Peninsula (southern Apennines). Journal of Geodynamics, 68, 49-59.

Tavani, S., Vitale, S., Grifa, C., Iannace, A., Parente, M., Mazzoli, S., 2016. Introducing dolomite seams: hybrid compaction –solution bands in dolomitic limestones. Terra Nova, 28, 195-201. https://doi.org/10.1111/ter.12210.

Tavani, S., Granado, P., Corradetti, A., Camanni, G., Vignaroli, G., Manatschal, G., Mazzoli, S., Munoz, J.A., Parente, M., 2021. Rift inheritance controls the switch from thin-to thick-skinned thrusting and basal decollement re-localization at the subduction-to-collision transition. Geol. Soc. Am. Bull. https://doi.org/10.1130/ B35800.1.

Tavani, S., Ogata, K., Vinci, F., Sabbatino, M., Kylander-Clark, A., Caterino, G., Buglione, A., Cibelli, A., Maresca, A., Iacopini, D., Parente, M., Iannace, A., 2023. Post-rift Aptian-Cenomanian extension in Adria, insight from the km-scale Positano-Vico Equense syn-sedimentary fault. Journal of Structural Geology, 168, 104820.

Taylor K.G., Gawthorpe, R.L., Curtis, C.D., Marshall, J.D., Awwiller, D.N., 2000. Carbonate cementation in a sequence-stratigraphic framework: Upper Cretaceous sandstones, Book Cliffs, Utah-Colorado. Journal of Sedimentary Research, 70(2), 360-372.

Teal, C.S., Mazzullo, S.J., Bischoff, W.D., 2000. Dolomitization of Holocene shallow-marine deposits mediated by sulfate reduction and methanogenesis in normal-salinity seawater, northern Belize. Journal of Sedimentary Research, 70(3), 649-663.

Toyama, K., Terakado, Y., 2015. Differential dissolution technique for the geochemical separation of calcite and dolomite of dolomitic limestones. Geochemical Journal, 49, 567-570.

Tucker, M.E., Wright, V.P., 1990. Carbonate sedimentology. Blackwell Science Ltd., Oxford, United Kingdom.

Vasconcelos, C., McKenzie, J.A., 1997. Microbial mediation of modern dolomite precipitation and diagenesis under anoxic conditions (Lagoa Vermelha, Rio de Janeiro, Brazil). Journal of Sedimentary Research, 67, 378–390.

Vecchio, E., Hottinger, L., 2007. Agglutinated conical foraminifera from the Lower-Middle Eocene of the Trentinara Formation (southern Italy). Facies, 53, 509-533. https://doi.org/10.1007/s10347-007-0112-6

Vecchio, E., Barattolo, F., Hottinger, L., 2007. Alveolina horizons in the Trentinara Formation (southern Apennines, Italy): Stratigraphic and paleogeographic implications. Rivista Italiana di Paleontologia e Stratigrafia, 113(1), 21-42.

Videtich, P.E., 1981. A method for analyzing dolomite for stable isotopic composition. Journal of Sedimentary Research, 51, 661-662.

Vinci, F., Iannace, A., Parente, M., Pirmez, C., Torrieri, S., Giorgioni, M., 2017. Early dolomitization in the Lower Cretaceous shallow-water carbonate of Southern Apennines (Italy): Clues about palaeoclimatic fluctuations in western Tethys. Sedimentary Geology, 362, 17-36.

Vinci, F., 2018. Sequence stratigraphic controls on reservoir-scale mechanical stratigraphy of shallow-water carbonates. Unpubslihed PhD thesis, DiSTAR, University of Naples Federico II, Naples, Italy.

Vitale, S., Dati, F., Mazzoli, S., Ciarcia, S., Guerriero, V., Iannace, A., 2012. Modes and timing of fracture network development in poly-deformed carbonate reservoir analogues, Mt. Chianello, southern Italy. J. Struct. Geol. 37, 223e235.

Vitale, S., Amore, O.F., Ciarcia, S., Fedele, L., Grifa, C., Prinzi, E.P., Tavani, S., Tramparulo, F.D., 2018. Structural, stratigraphic, and petrological clues for a Cretaceous–Paleogene abortive rift in the southern Adria domain (southern Apennines, Italy). Geological Journal, 53, 660-681. DOI: 10.1002/gj.2919

Vlahović, I., Tišljar, J., Velić, I., Matičec, D., 2005. Evolution of the Adriatic carbonate platform: palaeogeography, main events and depositional dynamics. Palaeogeography, Palaeoclimatology, Palaeoecology, 220 (3–4), 333–360. https://doi.org/10.1016/j.palaeo.2005.01.011.

Von der Borch, C.C., 1976. Stratigraphy and formation of Holocene dolomitic carbonate deposits of the Coorong area, South Australia. Journal of Sedimentary Petrology, 46, 952-966.

Wada, H., Suzuki, K., 1983. Carbon isotopic thermometry calibrated by dolomite-calcite solvus temperatures. Geochem. Cosmochim. Acta 47 (4), 697–706.

Walters Jr., L.J., Claypool, G.E., Choquette, P.W., 1972. Reaction rates and δO18 variation for the carbonate-phosphoric acid preparation method. Geochem. Cosmochim. Acta 36 (2), 129–140.

Warren, J., 2000. Dolomite: Occurence, evolution and economically important associations. *Earth Science Reviews*, *52*, 1–81. https://doi.org/10.1016/S0012-8252(00)00022-2.

Warthman, R., Lith, Y.V., Vasconcelos, C., McKenzie, J.A., Karpoff, A.M., 2000. Bacterially induced dolomite precipitation in anoxic culture experiments. Geology, 28(12), 1091-1094.

Weyl, P.K., 1960. Porosity through dolomitization: Conservation-of-mass requirements. Journal of Sedimentary Petrology, 30(1), 85-90.

Whitaker, F.F., Smart, P.L., Vahrenkamp, V.C., Nicholson, H., Wogelius, R.A., 1994. Dolomitization by near-normal seawater? Field evidence from the Bahamas. International Association of Sedimentologists (IAS) special publication no. 21, 111-132.

Whitaker, F.F., Smart, P.L., Jones, G.D., 2004. Dolomitization: from conceptual to numerical models. Geological Society, London, Special Publications, 235, 99-139. DOI: 10.1144/GSL.SP.2004.235.01.05

Whitaker, F., Xiao, Y., 2010. Reactive transport modeling of early burial dolomitization of carbonate platforms by geothermal convection. AAPG Bulletin, 94(6), 889-917. https://doi.org/10.1306/12090909075.

Whitaker, F.F., Al-Helal, A.B., Gabellone, T., Griffiths, G.L., 2012. Integrated reactive transport modelling: challenges and opportunities for improved prediction of diagenetic impact on reservoir quality. Proceedings of the TOUGH Symposium 2012.

Wilson, A.M., Sanford, W.E., Whitaker, F.A., Smart, P.L., 2001. Spatial patterns of diagenesis during geothermal circulation in carbonate platforms. American Journal of Science 301, 727–752.

Wood, J.R., 1987. A model for dolomitisation by pore fluid flow. Proceedings of the conference on Physics and Chemistry of Porous Media II, American Institute of Physics, New York, 17-36.

Wright, D.T., 1999. The role of sulphate-reducing bacteria and cyanobacteria in dolomite formation in distal ephemeral lakes of the Coorong region, South Australia. Sedimentary Geology, 126, 147–157.

Wright, D.T., 2000. Benthic microbial communities and dolomite formation in marine and lacustrine environments – a new dolomite model. In: Glenn, C.R., Prévôt-Lucas, L., Lucas, J., (eds.), Marine authigenesis from Global to Microbial. Society of Economic Mineralogists and Palaeontologists, Special publication, 60, 7-20.

Wright, V.P., Harris, P.M., 2013. Carbonate dissolution and porosity development in the burial (mesogenetic) environment. Search and Discovery Article 50860. AAPG Annual Convention and Exhibition, 19-22 May 2013, Pittsburgh, PA. https://www.searchanddiscovery.com/pdfz/documents/2013/50860wright/ndx_wright.pdf.html

Xiao, Y., Jones, G.D., 2007. Reactive transport models of limestone-dolomite transitions: Implications for reservoir connectivity. In Proceedings of the IPTC 2007: International Petroleum Technology Conference, Dubai, UAE, 4–6 December 2007; European Association of Geoscientists & Engineers: Houten, The Netherlands.

Xia, Z., Li, S., Hu, Z., Bialik, O., Chen, T., Weldeghebriel, M. F., Fan, Q., Fan, J., Wang, X., An, S., Zhang, F., Xu, H., Chen, J., Ji, Z., Shen, S., Lowenstein, T. K., Li, W., 2024. The evolution of earth's surficial Mg cycle over the past 2 billion years. Science Advances, 10, eadj5474.

Xu., H., Gregg, J., Hobbs, F., Pósfai, M., 2024. The dolomite problem is not solved: Comment on dissolution enables dolomite crystal growth near ambient conditions by Kim et al. 2023. eLetters, Science.

Yao, Q., Demicco, R.V., 1995. Paleoflow patterns of dolomitizing fluids and paleohydroogeology of the southern Canadian Rockie Mountains: evidence from dolomite geometry and numerical modeling. Geology, 23, 791–794.

Yapparova, A., Gabellone, T., Whitaker, F., Kulik, D.A., Matthäi, S.K., 2017. Reactive transport modelling of hydrothermal dolomitisation using the CSMP++GEM coupled code: Effects of temperature and geological heterogeneity. Chemical Geology, 466, 562-574.

Yui, T-F., Gong, S-Y., 2003. Stoichiometry effect on stable isotope analysis of dolomite. Chemical Geology, 201, 359-368.

Zenger, D.H., Dunham, J.B., Ethington, R.L., 1980. Concepts and models of dolomitization. SEPM Society for Sedimentary Geology Special publication no. 28.

Zhao, Y.Y., Zheng, Y.F., Chen, F.K., 2009. Trace element and strontium isotope constraints on sedimentary environment of Ediacaran carbonates in southern Anhui, South China Chemical Geology, 265, 345-362.

Zhao, H., Jones, B., 2012. Genesis of fabric-destructive dolostones: A case study of the Brac Formation (Oligocene), Cayman Brac, British West Indies. Sedimentary Geology, 267-268, 36-54.

Zhang, F, Xu, H., Konishi, H., Shelobolina, E.S., Roden, E.E., 2012. Polysaccharide-catalyzed nucleation and growth of disordered dolomite: A potential precursor of sedimentary dolomite. American Mineralogist, 97, 556-567.

Zhang, W., Hu, Z., 2020. Estimation of Isotopic Reference Values for Pure Materials and Geological Reference Materials. Atomic Spectroscopy. 41(3), 93-102. doi: 10.46770/AS.2020.03.001

Zhang, W., Wang, G., Cao, Z., 2021. Reactive Transport Modeling of Reflux Dolomitization of Carbonate Platforms: Enlightenment from Yingshan Formation in Shunnan Area, Tarim Basin. Minerals, 11, 1340. https://doi.org/10.3390/min11121340

Appendices

Appendix 1

Dolomite crystal size distribution (CSD) analysis of the C-interval. 100 µm, 200 µm and 500 µm photomicrographs are captured using 10x, 5x, and 2.5x objectives lens, respectively.

Crystal size distribution (CSD) analysis of the B-interval.

Appendix 2

Empirical determination of volume of different solutions as per stoichiometry.

Appendix 3

Dolomite textural and geochemical data of the C- and B-intervals.

Appendix 4

Elemental (counts) data of dolomites of the C- and B-intervals acquired using portable XRF (pXRF).

Appendix 5

Thin sections scans of Triassic (FS-1058) and Jurassic (AT-11) samples with marked spots of U-Pb dating and SEM-EDS analysis.

EDS based compositional data of saddle dolomite veins. All results in compound%. Processing option: Oxygen by stoichiometry.